UNIVERCITY OF CRETE
SCHOOL OF HEALTH SCIENCES
FACULTY OF MEDICINE
DEPARTMENT OF BASIC SCIENCES

A ONE DIMENSIONAL ONE DIRECTIONAL NEURAL NETWORK MODEL OF THE SUPERIOR COLLICULUS

PhD Thesis

ADONIS BOZIS

SUPERVISOR: ADONIS MOSCHOVAKIS

HERAKLION NOVEMBER 2002

CONTENTS

AKNOWLEDGMENTS

I thank my teachers at the departments of Medicine and Mathematics of the University of Crete for the help that I received from their inspiring teaching and also my father for certain discussions regarding the mathematical terminology of this manuscript. I am grateful to Drs Giannis Dalezios and Vasilis Raos for their help with computers. My thanks also go to my parents and all my good friends for their moral support and especially to Giannis Asteris for his hospitality.

INTRODUCTION

The oculomotor system

Vision is the primary sense that we use in order to move and act. Humans and other primates devote almost one third of their cerebral cortex to the sense of vision. The organs of vision, the eyes, do not act as a simple immobile camera that transmits a fixed image to the visual cortex, in order to be interpreted. On the contrary, the eyes have a sensitive, high discrimination area, the fovea, and they move so that the crucial features of an image are focused on it. The eyes also move in order to compensate for head movements and for movements of a visual target.

The oculomotor system is responsible for the movement of the eyes in general, and acts in close coordination with the visual and vestibular systems. Movements of the eyes can be classified into slow and fast; in this work we are concerned with the fast eye movements called saccades .

Reasons for studying the oculomotor system

Direct and indirect benefits have contributed to make the oculomotor system one of the best-studied systems of the brain.

direct benefit

The direct benefit from the study of the oculomotor system becomes obvious, as we understand its importance for the sense of vision. Saccades are an essential part of the visual process. When we see an object, our eyes perform a series of saccades, exploring the picture and extracting from it several features, which are crucial for its recognition by the visual cortex. When eyes are immobilised for whatever reason, visual scenes fade away, despite the fact that the visual pathway is intact. The system of attention also interacts with the oculomotor system, orienting the eyes to salient features of the word.

indirect benefit and the problem of body and limb movement

An old problem of neurophysiology is the discovery of the neural mechanisms of body movement. Apart from being important for the understanding of the main output of the neural system, it is also believed that it will become a source of inspiration for the design of artificial limbs for robots and handicapped people. With recent technology, robots are still unable to move properly and handle efficiently equipment in a real, everchanging environment. Progress at the field of robotics surprisingly lagged that in artificial intelligence. It seems to be easier to imitate human thinking than human walking, not to mention dancing.

But body and limb motion are, as will be shown by a simple example, very complicated computational problems, in comparison with the problem of eye movement. The reasons have as follows:

1) Fewer degrees of freedom. The distal phalanx of the index, assuming that the trunk remains still, has 13 degrees of freedom. The eye, as a three dimensional solid body with one fixed immobile point (its center) has three degrees of freedom by Euler' s theorem. Given that the difficulty in performing a movement is an exponential function of its degrees of freedom, it becomes obvious that the control of eye movement is a problem

much simpler for the neural system, in comparison with the control of upper limb movement.

2) Simplicity of mechanics. The viscosity, inertia and elasticity of the eye normally remain constant, in contrast with the upper limb that is challenged to move in an everchanging environment (to carry weights, move in water or against elastic resistance).

3) The number and complexity of eye muscle action. The upper limb possesses 39 muscles which control its movement, whereas the eye only 6. The action of each of these upper limb muscles depends on the position of the articulation controlled by the muscle in question. For example, the brachioradialis muscle pronates the elbow when it is at the supine position, and supines the elbow when it is at the pronate position. On the contrary, the action of the muscles of the eye depends less on the position of the eye and is much more simply related to movement.

The oculomotor system can thus serve as a comparatively simple first step, in order to hope in the future to tackle with success the harder problem of body and limb movement. We can also hope that this knowledge will enable the construction of artificial moving limbs and robots.

Eye coordinates with a head-fixed frame of reference

The eye is attached to the surrounding connective tissue with a spheroidal articulation. Being spheroidal, this articulation gives to the eye three degrees of freedom. If we imagine one axon (the axon of the eye) passing through the center of the eyeball and the center of the pupil, we need three generalised coordinates in order to specify the position of the eye, which correspond to the following three degrees of freedom (Fig. 1A,B):

1) The angle of torsion of the eye around this axis, i.e. the clockwise measured angle between a sagittal plane of the eye connected to this axis and a plane connected to the head. The sagittal plane of the eye is defined to coincide with the one connected to the head plane, when the subject looks straight ahead.

2) The angle between this axis and the median plane of the head, i.e. the horizontal position.

3) The angle between this axis and the horizontal plane of the head, i.e. the vertical position.

We define the primary position of the eye to be the position where both eyes look straight ahead to a distant object, and all three of the above angles are equal to zero (Fig. 1A).

The oculomotor range is the range of eye positions that the eye can occupy, when they start from the primary position. It differs among species. The hare can see objects almost anywhere without having to move its head, whereas the cat can move its eyes ±25 degrees in the horizontal direction, and relies mostly on head movements in order to look at objects not directly in front of it. Monkeys have an oculomotor range of ±45 degrees in the horizontal direction, and humans ±50 degrees.

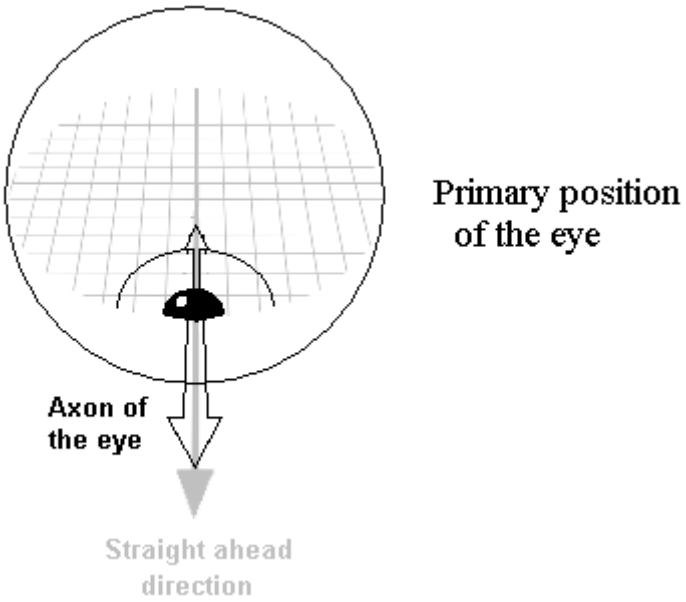

Fig. 1A. Primary position of the eye. The gray plane is fixed to the head and parallel to the horizon, when the head is immobilized. The gray arrow denotes the direction straight ahead. The big empty arrow denotes the axon of the eye. The small empty arrow starts from the center of the pupil and is connected to the eyeball; it will be used to define torsion. When eyes are at the primary position, the axon of the eye is parallel with the straight-ahead direction, and the small empty arrow lies inside the sagittal plane.

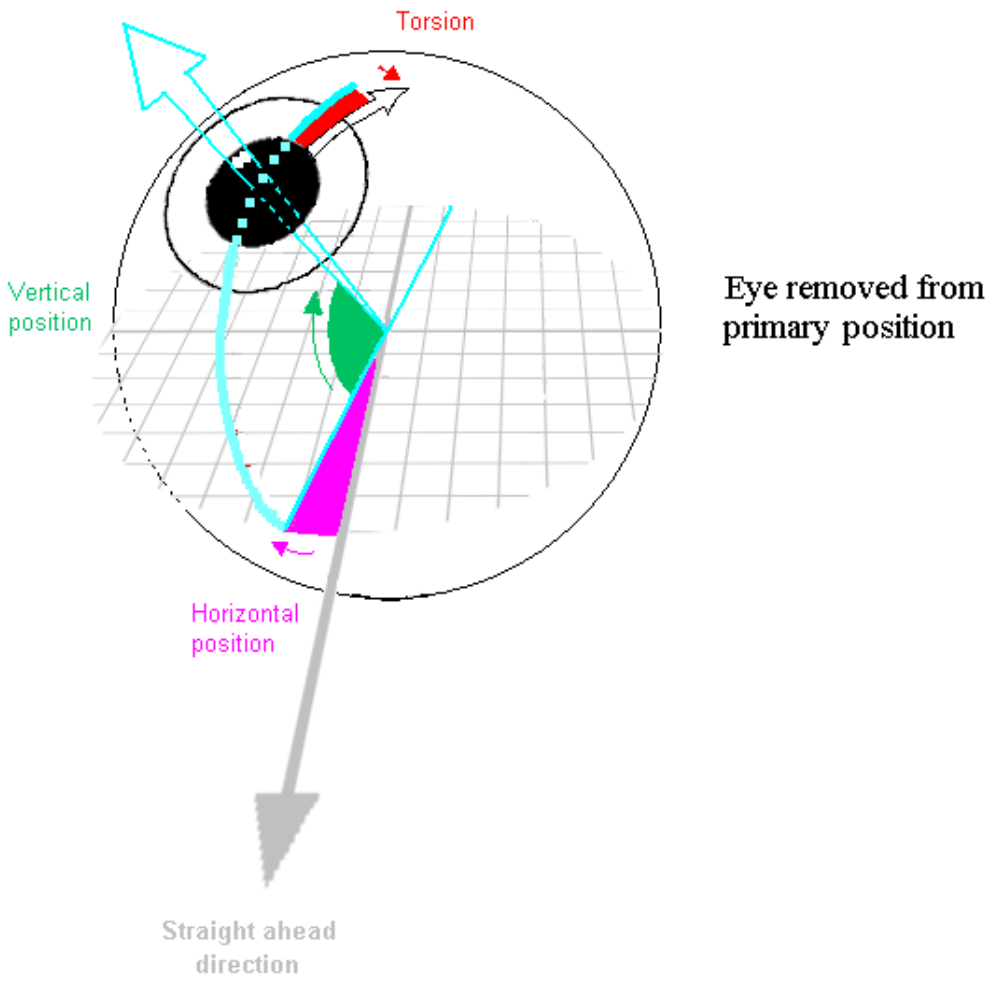

Fig. 1B. Eye removed from primary position. The blue line on the horizontal plane and the blue arc denote the meridian plane, which contains the axis of the eye and is orthogonal to the horizontal plane. The horizontal position (purple angle) is the angle between the meridian plane and the sagittal plane. The vertical position (green angle) is the angle between the horizontal plane and the axis of the eye. The torsion (red angle) is the angle between the empty arrow connected to the eyeball and the meridian.

Listing's Law

The three angles mentioned in paragraph 1.1.1, which specify eye position, do not in general vary independently. Listing's law states that we can express the torsion of the eye as a function of the horizontal and vertical position of the eye. The graph of torsion as a function of horizontal and vertical position creates Listing's plane. By expressing the state of the eye with only two free variables, the horizontal and vertical position of the eye, we end up with only two degrees of freedom.

Torsional nystagmus: a violation of Listing's Law

Listing's Law is not absolutely accurate: when a human subject looks straight ahead to an object rotating around the eye axis, the eyes exhibit a movement called torsional nystagmus. Torsional nystagmus is a periodic movement consisting of two components:

1) One slow component with the same direction and speed with the rotating object, which moves the eye away from the initial position.

2) One fast component with the opposite direction of the rotating object, which moves the eye back to the initial position.

When torsional nystagmus emerges, torsion varies independently of the horizontal and vertical position of the eye (horizontal and vertical positions remain zero). This is merely an exceptional and small movement, whereas in the majority of eye movements that we normally execute, the axes of rotation of our eyes remain on Listing's plane. It is however an indication for an independent Listing operator, which will be described in the section about SC models, (0, page 70).

Definition of saccades and saccadic subsystem

Saccades are rapid eye movements with speeds reaching 1000 degrees/sec, which reorient the eyes in various circumstances. Humans make about 3 saccades per second, when they visually explore an object of the environment. The only purely voluntary movements that we can perform with our eyes are saccades. Most of the saccades we perform, however, are involuntary A more accurate description of saccades, which serves also as a more precise definition, is given in the section about psychophysics of saccades (see 0, page 13).

The saccadic subsystem, a part of the oculomotor system, is responsible for saccade execution. The rapid eye movements (saccades) of higher mammals, and the areas which control saccades, have been the object of extensive experimental work spanning several decades. This has resulted in the functional identification of more than 30 classes of saccade related neurons distributed within at least 10 brain areas (summarized in Moschovakis et al., 1996). We will not mention all of these areas and the classes of cells that they contain, just a few to give a glimpse of the complexity of the saccadic system. These regions include:

1) The Paramedian Pontine Reticular Formation (PPRF) of the brainstem, which includes Long Lead Burst Neurons (LLBs) and Medium Lead Burst Neurons (MLBs). These cells fire shortly before and during saccades with a horizontal component.
2) The rostral interstitial nucleus of the median longitudinal fasciculus (riMLF). It contains LLBs, which fire shortly before and during oblique and vertical saccades (upward or downward saccades).

3) The central mesencephalic reticular formation (cMRF), which blends with the fields of Forel rostrally and with the interstitial nucleus of Cajal medially. It contains RTLLBs and other LLBs (Long lead burst neurons).
4) The superior colliculus (SC), which contains a multitude of functionally distinct neurons. These include Tectal Long Lead Burst neurons (TLLBs), Quasivisual cells (QVs), Predictive Visual cells (PVs) and others. As our model focuses on the SC, its cells will be described in detail in 0 - 0., p.15 - 20.
5) The nucleus raphe interpositus, which contains the Omnipause Neurons (OPNs). These cells fire tonically during fixation, and stop firing shortly before and during saccades.
6) Cortex areas like the frontal eye fields (FEF), the supplementary eye fields (SEF) and the posterior parietal cortex (PPC). FEF is essential for the execution of voluntary saccades, and destruction of area LIP seems to influence the correct execution of saccades to visual targets.
7) The thalamus
8) The basal ganglia
9) The cerebellum

Classification of saccade related neurons

The different patterns of activity of all these cells are separated with the use of complex experimental paradigms. All these neurons change their firing rate before, during or after saccades. The patterns of activity that they display distinguish them into three main classes:

a) The phasic-tonic neurons, which exhibit a high frequency burst, with intensity proportional to the amplitude of saccades in particular directions (the on-direction or preferred direction), and pauses in the opposite direction (off direction).
b) The burst neurons, which give a burst of activity for saccades of particular amplitude and direction.
c) The pause neurons, which fire at a constant rate during fixation and stop firing for saccadic movements in one or more directions.

The performance of the saccadic subsystem

Saccades, are rapid eye movements with speeds reaching 1000 degrees/sec. In this section we will mention the basic functional properties of this system.

Different kinds of saccades

The quick phase of the vestibulo-ocular and optokinetic reflexes is in fact a saccade. When the eye cannot keep up with a fast moving target during smooth pursuit, quick movements are performed in the same direction as the pursuit, called "catch up saccades", in order to keep eye contact with the target. When a sudden change happens in the extrafoveal visual field, a "foveating" or "reaction saccade" is performed in order to explore this possible danger or interesting new visual information. But most commonly, we perform 2-3 scanning saccades every second, in order to explore the interesting features of the object we observe. We can also, of course, perform conscious saccades, a function for which an intact frontal eye field (FEF) is needed. The SC, the nucleus of interest in this work, is essential for the production of reaction saccades. All categories of saccades listed above share stable common features concerning their velocity, amplitude,

time course and latencies, i.e. they share common psychophysics, which clearly distinguish them from other kinds of eye movements.

Psychophysics of saccades

Duration versus amplitude of saccades

The duration of saccades has a stable relation with their size (Yarbus, 1967; Baloh et al., 1975). In humans, saccade duration S_d increases together with movement amplitude ΔE. For ΔE ranging between 0.5 and 20^o, S_d is given by the formula

$S_d = \Delta E^{0.2}$, where ΔE is measured in degrees and S_d in ms (Yarbus, 1967).

For bigger saccades ranging between 5 and 60^o, Baloh gives a linear relationship between S_d and ΔE:

$S_d = a + 2.5\ \Delta E$, where "a" has a value between 20 and 30 ms, ΔE is measured in degrees and S_d in ms (Baloh et al., 1975).

Duration versus peak velocity of saccades (main sequence)

Saccades have a peak velocity, which reaches 800 degrees/sec and about 1000 degrees/sec in monkeys, and increases with saccade size ΔE. The relationship of peak saccadic velocity versus saccade amplitude is adequately described by a straight line for saccades ranging between 0.03 and 20 degrees. This relationship is known as the "main sequence" (Bahill et al., 1975). The range between 0.03 and 20 degrees contains the vast majority of saccades executed by humans during normal activity, although the human oculomotor range ($\pm 50^o$) is bigger.

Definition of saccades with the main sequence

The stability of the main sequence relationship, makes a clear distinction between saccades and other kinds of eye movements. We thus define as saccades all eye movements that obey the main sequence relation. In addition, we know today that this distinction between saccades and other eye movements is not based only on psychophysics, because different kinds of eye movements have been related with different brain circuits, which work in parallel.

Vector average or "global effect"

The simultaneous presentation of two targets in the visual field results in a saccade, which ends at a point between the two targets (Coren and Hoenig, 1972; Findlay, 1982) (Fig 2). The ratio between the distances from this point to the two targets equals the ratio of the luminance of the two targets. When three or more visual targets are presented simultaneously, a saccade towards their "center of gravity" is executed. This phenomenon is called "global effect", and we obtain an identical result upon simultaneous electrical stimulation of two collicular sites as will be described in 0 (page 22).

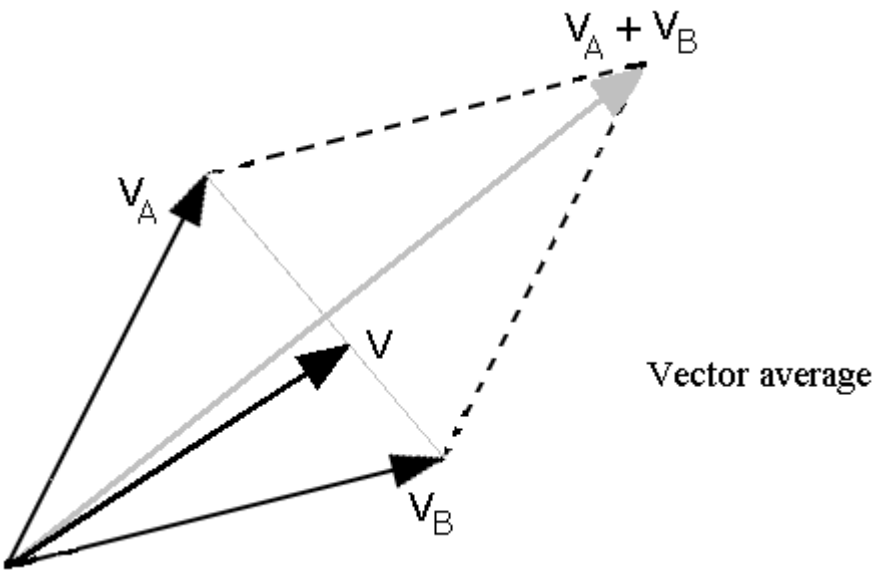

Fig. 2. The vector average (global effect). Two targets located at positions V_A and V_B are presented simultaneously. The result is a movement with vector V, whose endpoint lies at the line connecting the endpoints of vectors V_A and V_B, and not the sum V_A+V_B. In this example the target B is more luminescent, and the vector V is closer to V_B than to V_A.

Sequential saccades to two targets (double step saccade)

When two targets are presented, the result is not always a "global effect". Usually a sequence of two saccades takes place, which brings the eye initially to the first, and after a short delay to the second target (Fig.3). When there is a difference at the presentation times of the two targets, then the double step saccade is more probable than when the two targets are presented simultaneously. Humans and monkeys are able to perform accurately the second of two saccades, even when both visual targets are extinguished before the execution of the first saccade. The saccadic system is able to perform this, although the position of the second target in retinal coordinates has changed after (and due) to the first movement (Hallet and Lightstone, 1976b; Schlag et al., 1990). In another impressive experiment done by Hallet and Lightstone (Hallet and Lightstone, 1976a,b), one target was flashed (turned on for only a few ms, and turned off) during a visually elicited saccade (i.e., while the eyes were moving at fairly high speeds). After the end of this saccade, the eyes performed accurately a second saccade towards the target that was flashed. This experiment shows that during the movement, information about visual targets reaches the saccadic system, although due to visual suppression these targets are not visible.

Figure 3 shows the sequential execution of saccades to two targets. Two targets A and B with positions defined by vectors V_A and V_B, respectively, are presented sequentially. First target A is presented and after a short delay B, before the eye starts to move. If the system relied only on retinal errors at the moment of target presentation,

then the saccades with vectors V_A and V_B would be executed sequentially, and the eye would finally land at the endpoint of $V_A + V_B$. On the contrary, the eye executes first a saccade with vector V_A and after it a saccade with vector $V_B - V_A$. The eye thus finally lands at the point where target B was located before it disappeared.

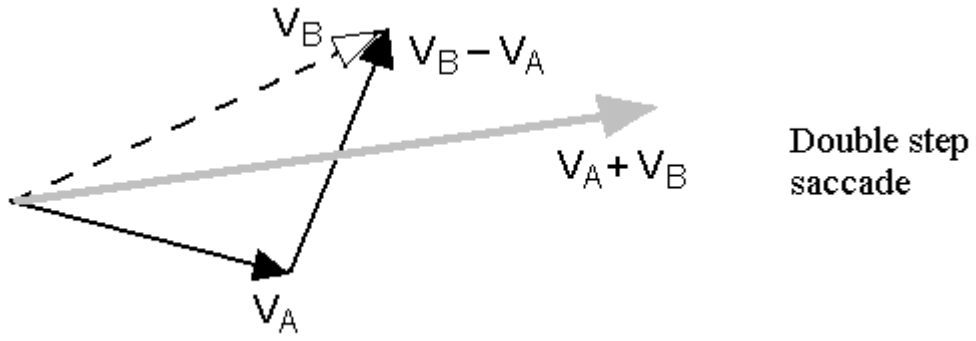

Fig.3. Double step saccade. Black arrows denote the two sequential saccades. The dashed arrow denotes the retinal error vector of the target B. The gray arrow denotes where the eye would land finally, if the system relied only on the retinal error and did not have a dynamic representation of the target B.

Superior Colliculus physiology and connections

An important part of the saccadic subsystem is confined to the superior colliculus (SC), the nucleus which is the object of this study. Electrical stimulation of the SC has been long known to evoke saccades whose size depends on the site stimulated, so that rostral sites produce small saccades and caudal sites large saccades, medial sites upward saccades and lateral sites downward saccades (Robinson, 1972). On the other hand, neither their size nor their direction changes much as the intensity of stimulation increases. When the stimulus is prolonged, several similar saccades are evoked which follow each other in quick succession to form a staircase of saccades. Finally, the movement produced in response to the simultaneous activation of two SC sites is the weighted average of the movements that are produced when the two sites are stimulated in isolation.

Cells, layers and maps

The SC is placed inside the midbrain and contains a multitude of functionally and anatomically distinct neurons (Moschovakis and Karabelas 1985; Moschovakis et al. 1988a,b), which receive input from a multitude of sources, (Huerta and Harting 1984) and establish connections with a multitude of targets (Harting 1977; Harting et al., 1980). The superficial layers of the SC, which are located at the frontal wall of the fourth ventricle, receive input from the Y-ganglion cells of the retina, which are sensitive to fast moving targets or swift local changes of lighting. The deeper layers give the main output to the reticular formation, where the midbrain cellular circuit of the Burst Generator is thought to reside. The Burst Generator drives properly the brainstem oculomotor nuclei, which contain the motoneurons that move the eye.

Visual receptive fields of collicular cells

Many cells of the SC have visual responses, which depend on the retinal error R_e of the visual stimulus. The retinal error R_e is defined as a two-dimensional vector, with horizontal and vertical components the horizontal and vertical distance (in degrees) respectively between the image of the visual stimulus on the retina and the center of the fovea. The cells that exhibit visual responses are transiently activated when a target with amplitude and direction close to an optimal vector in retinotopic coordinates is presented to them. The set of all endpoints of vectors R_e that excite a particular cell form the visual receptive field of that cell. A collicular cell with a visual response does not respond for stimuli with R_e outside its receptive field.

The superficial layers of the SC contain many cells with visual responses, and as a recording electrode proceeds deeper inside the SC, it encounters more cells with mixed visual and motor responses and at the deeper layers cells with pure motor responses.

The visual map of the SC

Visual cells responding to target images formed near the fovea are located in the rostral SC, while cells responding to target images formed near the periphery of the retina are located more caudally. Also cells that respond to targets located in the upper visual hemi-field are located in the medial SC, while targets that respond to targets located in the lower hemi-field are located in the lateral SC. In general, the visual receptive fields of superficial tectal cells are in register with the movement fields of the deeper tectal cells (PVs, QVs and TLLBs) (for a review cf. Sparks, 1986). Similarly with the motor map of the SC (0) of the SC.), in the visual map of the superficial layers the amplitude of the horizontal component of the optimal vector of an L-cell is an exponential function of the distance of this cell from the rostral pole of the SC.

Some of the visual cells found in the superficial layers, send their axon toward the parabigeminal nucleus and emit collaterals which deploy terminal fields in the superficial layers (close to the soma they originate from) and in the deeper layers (in a region underlying the dendritic tree of the soma they originate from). These cells are called L-neurons and play a prominent role in our model.

Movement fields of collicular cells

Of particular importance is the fact that the deeper layers of the SC contain neurons, which emit bursts of discharge prior to all saccades of the appropriate amplitude and direction (collectively defining a cell's "movement field"). In other words every cell having a movement field, gives a maximal response for movements of specific amplitude and direction. The set of the endpoints of all vectors of the saccades that evoke a motor response in a particular cell, form the movement field of this cell. The collicular cells which have movement fields and are used in our model are the TLLBs. Oculomotor cells outside the SC which have movement fields include the FEF LLBs, the V-bursters of the PPRF (Hepp K. and Henn V., 1983) and the RTLLBs.

The non-linear movement map of the SC

By reconstruction of the movement fields of anatomically located TLLBs, we can get a map of the SC, to any small region of which corresponds the vector of the preferred saccadic displacement for this region. This map is called the movement map of the SC.

We get a similar map if we use instead of movement fields, the vector of the saccade that is elicited by electrical stimulation of this area. In fact, this second map came chronologically first (Robinson, 1972). The important feature of this map is that it is non-linear. As the electrode is displaced from the rostral pole towards the caudal one, the size of evoked saccades increases faster than the distance between sites. Small saccades are represented in a region of the SC that is bigger than the region representing bigger saccades. The amplitude of electrically elicited saccades is an exponential function of the distance from the rostral pole (Robinson, 1972). Because of the correspondence between all layers of cells in the SC including TLLBs, L-cells, QVs and PVs, the same nonlinearity holds also for the superficial visual layers and generally all classes of cells in all layers. Some models of the SC simulate this nonlinearity, and others do not as it is not essential for exploring their performance.

The space code of the SC

Both visual and movement responses in the SC have a common characteristic: Neurons in both cases respond with a maximal response for visual stimuli or saccades respectively, with an optimal vector. If the stimulus or the saccade falls far from this optimal vector, the neuron does not respond. In addition, as we will see in the following paragraphs concerning the TLLBs and the Ls, collicular cells corresponding to different optimal vectors are not randomly intermixed inside the SC (as for example in the PPRF region). On the contrary, the optimal vector of every kind of cell is an increasing function of its position inside the SC. We express this fact by saying that the SC uses a space code for saccade metrics. Synonyms of space code are place code, topographical code and labeled-line code.

The collicular neurons of interest for this model include the TLLB, QV, PV and V populations. All of them give responses related to saccades or to important features of targets.

TLLBS

Responses of TLLBs

The best-studied collicular cells are the Tectal Long Lead Burst neurons (TLLBs). They form the main output of the SC to the reticular burst generator. TLLBs are known also as “SRBNs” (Saccade Related Burst Neurons) and are located in the deeper layers of the primate SC. TLLBs increase their firing rate immediately before and during a saccade, which lies inside their movement field. When the eyes are still, TLLBs are rather silent. Other researchers distinguish between “unclipped” and “clipped” cells as those which still fire and those that do not after saccade offset, respectively, and treat them as separate cell groups (Waitzman et al., 1991).

TLLBs are topographically arranged over a horizontal map of the SC so that cells preferring small saccades are located in the rostral SC while cells preferring big saccades are located more caudally. Also, cells that discharge before upward saccades are located medially in the SC whereas cells that discharge before downward saccades are located laterally (Moschovakis et al., 1988b). The movement fields of TLLBs and their location in the SC are consistent with the metrics of saccades evoked in response to electrical stimuli delivered in the same region of the SC (Schiller and Stryker 1972). It is for this reason that the SC is said to use a “place code” to specify movement parameters. We may say that TLLBs code for the “ static motor error Me”, which is the distance between

present eye position and the eye position that must be occupied for the target to be foveated. Every region of the TLLB layer corresponds to movements of specific amplitude, and when a saccade is about to happen, this and only this region is going to be activated, giving a "mountain" of activity. This activity increases and then decreases, lasting for about 80 ms in total, regardless of movement amplitude and direction. When two targets are presented simultaneously, the ensuing movement usually sends the eye somewhere between the two targets, the so-called "global effect". According to some researchers, the TLLB layer responds with a "mountain" of activity which lies between the sites that would be activated if each target was presented alone (Glimcher and Sparks, 1993). According to other researchers, the TLLB layer will give two mountains of activity, each of which corresponds to the response of superficial neurons to one of the targets (Edelman and Keller, 1998).

Connections of TLLBs

The axonal system of TLLBs has been studied light-microscopically, almost in its entirety, following the functional identification of their axons in alert monkeys and their injection with tracers (Moschovakis et al, 1988b; Scudder et al., 1996a). The TLLBs give connections mostly:

a) To the reticular formation, at areas that are known to house the vertical and horizontal burst generators (Moschovakis et al, 1988b; Scudder et al., 1996a,b). This connection is the main output of the SC. We assume that the so called "statiotemporal transformation" is accomplished by a graded output to the burst generators. The statiotemporal transformation takes place between the SC, where the amplitude of the saccade is coded in a space code, and the burst generators, where the horizontal and vertical components of the saccade depend only from the duration (and intensity) of the firing, in all cells of the burst generators. This was believed to be the result of a higher density of TLLBs at the caudal areas of the SC, which give saccades of big amplitude. This gradient of density would result in a stronger output from these areas to the burst generator (Edwards and Henkel, 1978). Later studies, (Kawamura and Hashikawa, 1978; Stanton and Greene, 1981; Olivier et al., 1991) did not confirm this gradient of density; a more recent study (Grantyn et al., 2002) found such a gradient of density, but it is not good enough to explain the spatiotemporal transformation alone. A gradient at the strength of projections was found, however, which may explain the spatiotemporal transformation. The caudal areas of the deeper SC (at the TLLB layer) that are responsible for bigger movements give a stronger output (more boutons) to the burst generator, whereas the output from rostral areas, which are responsible for smaller movements, is weaker (Moschovakis et al., 1998b).

b) To the contralateral SC, by SC commissure fibers. These connections exist between both corresponding superficial and deeper layers of the two colliculi (Olivier et al, 1998), and are stronger between the deeper layers of the superior colliculus in the cat (Edwards, 1977) and humans (Tardif and Clarke, 2002). In cats (Behan, Kime, 1996) and humans (Tardif and Clarke, 2002), these connections have been shown to connect the mirror-symmetric locations of the two colliculi. We think that these connections may participate at the formation of a functionally unified region, which encompasses both right and left superior colliculi.

c) To the ipsilateral SC, by recurrent collaterals, which terminate in the neighborhood of the soma they originate from (Moschovakis, 1988a,b). Because of the functional

significance of these connections for our model, we evaluated their spread quantitatively. As will be described later, the number of boutons (synaptic terminals) that a TLLB cell deployes is a symmetric function of the distance from its soma, and resembles a bi-lobal curve with two local maxima (peaks), and a local minimum at zero distance (see Fig.2). The number of boutons is not necessarily directly proportional to the functional strength of a connection; but one would need to be too much of a sceptic to believe that the two are entirely unrelated. In our model, we used the number of these boutons counted in our laboratory, as a measure of the weight between TLLB units (see Fig. 7).

L-cells

Responses of L-cells

Cells of all tectal layers respond to visual stimuli. In general, as an electrode progresses from the superficial layers to the deep layers, cells respond in relation more with a motor command for the execution of the saccade, and less with the visual stimulus. Most cells of the intermediate layers, however, have a mixed response. The motor and visual response of a cell can be easily separated, by varying the delay in delayed saccade paradigm. Visual cells receive input from the Y-ganglion cells of the retina, and give a transient response of 10-20ms duration after the presentation of a new visual stimulus. Accordingly, Visual neurons can be thought to code the retinal error (Re) of targets (the distance of their image from the fovea). Our model relies on superficial layer visual cells that project to the deeper collicular layers and are called L-cells. This connection could mediate the execution of saccades with very short latencies, called express saccades (par. 1.2.2) (Moschovakis et al. 1988a).

Visual receptive fields of L-cells

When a target with amplitude and direction close to an optimal vector is presented in the visual field, a small area of neighbouring L-cells will be transiently activated. The total spike count of a L-cell as a function of the retinal error R_e of the visual stimulus, forms the visual receptive field of the particular L-cell. An L-cell does not respond for stimuli with R_e outside its receptive field.

Correspondence between the visual and motor maps

The connection from L-cells to the deep collicular layers is also used in our model. If a saccade to a target is executed immediately after its presentation and no other eye movements intervene, then the receptive fields of L-cells are in register with the movement fields of the TLLBs and QVs of the deeper layers beneath them. When other eye movements intervene, these must be taken into account if the target is to be foveated. This correspondence between the topographical maps at the input and at the output of the SC is very interesting and unique at the neurous system. Due to this fact, the motor deeper layers can use directly the visual information of the superficial layers.

Connections of L-cells

L-cells of the superficial layers give projections to neurons of the deep layers from collaterals of the tectoparabigeminal pathway that they give rise to (Mooney et al., 1988; Moschovakis et al, 1988a). This connection from the superficial visual layers to the deeper motor layers seems to be gated by γ-aminobutyric acid A ($GABA_A$), but when it is disinhibited (Isa and Saito, 2001) reveals its functional significance. When it is not actively disinhibited in rat collicular slices, it seems to be weak (Özen et al., 2000).

QVs

Responses of QVs

The deeper layers of the SC also contain neurons that respond to visual stimuli. Some of them demonstrate long stretches of low frequency discharge that commences soon after the presentation of a visual target, and ends soon after the end of a saccade to it. These cells are called quasivisual (Qv) and they are thought to store the location of visual targets in a spatial register in the SC (Mays and Sparks 1980). This means that the receptive fields of the QVs are in register with the motor fields of the neighbouring TLLBs. The activation of QVs shows that a movement with a particular amplitude and direction has been programmed. Their most interesting feature is that QVs fire not only for targets presented inside their visual field. QVs also start to fire for a target, which was flashed outside their visual field and was moved inside it after a movement of the eyes, even if this movement takes place after the target was turned off. In other words, the QV cell starts a low frequency firing when a future target selected for a saccade is moved inside its receptive field, and stops soon after the execution of the saccade to it. This movement will take place after a variable time interval, i.e. each specific QV codes for a particular value of eye position error and keeps it in a memory register (Mays and Sparks, 1980).

PVs.

Responses of PVs

Other cells of the deeper collicular layers are known to be predictive visual neurons (Pv cells), in the sense that they discharge for visual stimuli that lie outside their receptive field but are brought inside their receptive field by saccades executed soon thereafter (Walker et al., 1995). Actually, the neuron's response can precede the movement by more than 50 ms whereas the visual stimulus enters the cell's receptive field after the saccade is over (Walker et al., 1995).

SNR

The substantia nigra (SN) contains two parts, the pars compacta and the pars reticulata. Of the multitude of inputs reaching the SC, those originating in the substantia nigra pars reticulata (SNR) and the mesencephalic reticular formation are of particular relevance to the present study. The former is known to contain a multitude of functionally distinguishable cell classes (Hikosaka and Wurtz 1983a,b). Whatever their differences, these cells display tonic discharges (Hikosaka and Wurtz 1983a,b), inhibit their targets (Karabelas and Moschovakis, 1985; Moschovakis et al., 1988a), and project to the SC ([Jayaraman et al., 1977; Anderson and Yoshida, 1980; Hikosaka and Wurtz, 1983c; Karabelas and Moschovakis, 1985; Harting et al., 1988; Moschovakis et al., 1988a; Harting and van Lieshout, 1991). Two functionally distinguishable cell types were employed: the SNR_1 and the SNR_2 cells. Both have broad receptive fields, and stop firing for targets with a motor error near an optimal value.

SNR_1 cells

Some SNR neurons are known to decrease their discharge before and during saccades (Hikosaka and Wurtz, 1983a,b). These cells are classified as SNR_1 neurons. Their activity is a mirror image in qualitative terms of the discharge pattern that is exhibited by the

TLLBs, although there is not a tight temporal relation between them. Because these cells are known to project to the SC (Hikosaka and Wurtz, 1983c), it is reasonable to assume that they gate the presaccadic activity of this structure, and more specifically the activity of the TLLB cells which are believed to form the main output of the SC (see 0, 0).

SNR_2 cells

The discharge of about 15% of SNR cells decreases soon after the presentation of a visual target and does not increase until a saccade to it has been executed (Hikosaka and Wurtz, 1983b). In other words, they stop firing soon after a target that was presented inside their receptive field becomes behaviourally important, and resume their steady firing rate around the time that a saccade is going to be executed towards a target. These cells are classified as SNR_2 neurons. Because the target is extinguished long before the movement starts, it is a remembrance of its location that continues to influence the rate of discharge of such cells, which are for this reason said to display "sustained memory contingent saccade responses". These cells have a firing pattern that is a mirror image of the firing pattern of the QV cells of the SC. In our model, we used them as a gating mechanism for the layer of QVs.

RTLLBs

Additionally, the SC is known to receive presaccadic input from a class of reticular long lead burst neurons (RTLLBs). RTLLBs have been recovered in a region of the mesencephalic reticular formation that is known to receive TLLB input, and their axons deploy terminal fields within the deeper layers of both the ipsilateral and the contralateral SC (Moschovakis, 1988b).

Electrical stimulation experiments of the SC

The electrical stimulation of neural structures is done with trains of spikes. These trains are defined mainly with two parameters, the frequency of the impulses and their intensity. These trains of pulses are thought to excite local neurons. It is not easy to model the consequences of electrical excitation. In gross terms, the higher the intensity of the current increases the wider area that is excited around the elecrode, whereas the higher the frequency of the pulses the stronger the excitation of the neurons. In our model, increase of current intensity were assumed to increase the number of units that we were activated during the simulation (due to wider current spread) (Fig 13).

Electrical stimulation at a single SC site

Effect of frequency and intensity of stimulation

The amplitude of the evoked saccade is only slightly influenced by the frequency and the intensity of the stimulation. The amplitude of the movement may slightly increase together with the intensity of stimulation (van Opstal et al., 1990), a fact that could be explained with the more extensive spread of current around the electrode.

Although the frequency and intensity of electrical stimulation do not influence much the size of the ensuing saccade, they influence the delay intervening from the onset of stimulation till the beginning of the saccade, as well as the peak velocity of the movement. The bigger the frequency or the intensity of electrical stimulation, the shorter

this delay becomes (Grantyn et al., 1996; Schiller and Stryker, 1972), whereas the peak velocity increases (Straschill and Rieger, 1973; Grantyn et al., 1996).

Staircase of saccades with continuous stimulation

Continuous stimulation results in a "staircase" of saccades, which is a sequence of saccades separated by an intersaccadic interval (Grantyn et al., 1996; Robinson, 1972). The amplitude of the saccades in the cat gradually decreases, due to the position sensitivity; this result is not obvious in monkey.

Simultaneous electrical stimulation of two SC sites

The electrical stimulation of the SC with two electrodes results in a saccade, whose vector is the average of the vectors of the saccades that would be elicited, if we stimulated each area separately (Robinson, 1972).

Figure 4 depicts this result. If the separate electrical stimulation of areas A and B gives saccades with vectors V_A and V_B respectively, then the simultaneous stimulation of areas A and B gives a saccade with vector V, which is the mean average of vectors V_A and V_B. Bold letters represent vectors.

$$V = (V_A + V_B) / 2$$

Generally, if areas A and B are stimulated electrically with currents of different frequencies F_A and F_B respectively and $F_A > F_B$, then the vector of the resulting saccade V_1 is:

$V_1 = (F_A V_A + F_B V_B) / (Fa + Fb)$, where V_1 lies closer to A than to B.

If $F_A < F_B$, then the result is a saccade with vector V_2, where V_2 lies closer to B than to A.

Thus, by manipulating the ratio of the frequencies at the two electrodes, it is possible to elicit any saccade intermediate between those that result when each area is stimulated in isolation. In other words, the endpoint of the vector V is at the line segment that connects the endpoints of V_A and V_B. This result is called "weighted average".

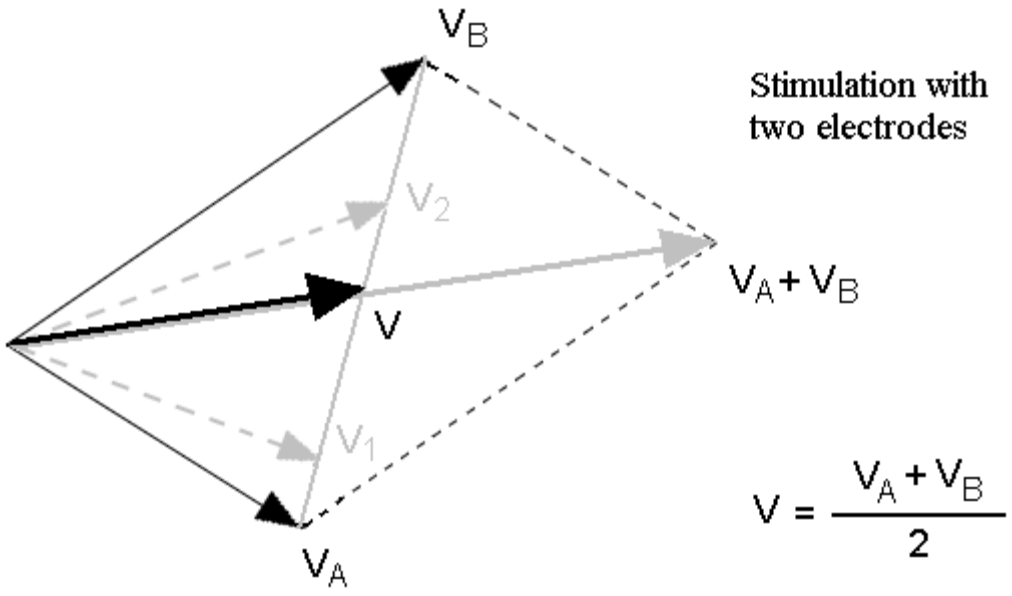

Fig. 4. Stimulation with two electrodes. Two sites A and B of the SC when electrically stimulated yield saccades with vectors V_A and V_B respectively. When both sites are simultaneously stimulated with currents F_A and F_B, they yield a saccade V (big arrow), which is the average of V_A and V_B weighted by F_A and F_B. When both sites are simultaneously stimulated with currents with equal frequencies $F_A = F_B$, they yield a saccade V which is the mean average of V_A and V_B. Stimulation with $F_A > F_B$ resulted saccade V_1, whereas stimulation with $F_B > F_A$ resulted saccade V_2.

If we suppose that the electrical stimulations somehow mimic the natural stimulation of the SC input after the presentation of visual stimuli, then the results of simultaneous stimulation resemble the "global effect"(see 0). It is sufficient to replace V_A and V_B, with the vectors of distance of visual stimuli from the fovea, and Fa and Fb with the luminance of the two targets.

We notice here a non-linearity at the SC output layer, as the sum of two inputs does not give as an output the sum of the two separate outputs. Getting the mean average result at the output of the SC is a well-defined property, which our model must be able to reproduce.

Lesion and transient inactivation experiments

Inactivations of SC regions produce a counterintuitive phenomenon. If the inactivated area corresponds to a region that gives saccades of bigger amplitude at the same direction, then the result will be a hypometric saccade, i.e. a saccade smaller than that physiologically expected. But if the inactivated area corresponds to a region that gives saccades of smaller amplitude at the same direction, then the result will be a hypermetric saccade, i.e. a saccade bigger than that physiologically expected (Lee, Rohrer and Sparks 1988)! This last result is quite unexpected, because we destroy or inactivate a motor structure and yet we get a stronger than normal response to a stimulus. This result is another quite challenging one for models of the SC.

Neural network models

Methods of rate neural networks.

Rate neural network models

A neural network (n.n.) is a dynamical system consisting of units and connections. Each unit i receives input from units connected to it, and gives output to other units.

Mathematical description of a rate n. n. model with border activations

A rate neural network model is a neural network in which each one of N units represents a cell or a group of cells. Every unit sends signals to other units via connections. Every connection is characterised by a unique number, called weight W, which corresponds to the strength of the synaptic connection between the cells.

States of the network

The state of this neural network evolves in time. At every instant, the state of every unit i of this network is described by a unique number $A_i(t)$, called activation .The state of the whole network, at every given instant, is described by the activations of all N units that constitute it. The activation of every element, at a given instant, corresponds to (or is supposed to model) the instantaneous firing rate of a group of cells, i.e. the number of action potentials that these cells give per unit of time.

Boundary restriction of the activation values

The activation of every element at any given instant cannot exceed A_{max}, which equals the maximum firing frequency that a particular cell can reach and which depends on its membrane properties. It also cannot become less than zero, as negative frequencies in nature do not exist.

If we call $A_i(t)$ the activation of unit i at time t, we have

$$A_{max} \geq A_i(t) \geq 0 \qquad \text{for i=1 to N at every t}$$

A_{max} and zero are the border activations of the unit.

A neural cell is a rather complicated device. It usually gets input from 1000 cells at its numerous dendrites, and gives output to 1000 other cells with its axon. The way the input to this cell is manipulated in order to give an output may be very complicated. There exist mathematical models of neural cells that use detailed information about cell geometry, ionic channels and cell membrane (compartmental models). In compartmental models, with the use of the linear cable theory, we assume that we can divide the cell into a number of compartments with simple geometry (spheres, cylinders or cones), and every compartment has uniform voltage at all its extent. The linear cable theory is a strong tool for understanding of single neuron function, although even in this case it may lead to very complicated models with many free variables, as it demands a lot of biological data for its application. When we deal with big populations of neurons, however, we may assume that each neuron may be modelled as one compartment with first order dynamics. The activations of all N units of the network are functions of time. These activations are the unknown functions of time of a system of N first order linear differential equations with constant coefficients. The values of these coefficients are the weights of the network.

Geometric representation of a partial solution of the rate model

The state of the whole network is represented, at every instant, by a fictitious point in the N-dimensional configuration space. Given the system of N first order linear differential equations with constant coefficients and a point in the configuration space (which corresponds to the initial conditions of the network), a unique solution is determined. This solution is a one-dimensional trajectory in the N-dimensional configuration space. The movement of a fictitious point on this trajectory represents the evolution of the network in time. Because of the additional boundary restriction of the activation values, this trajectory lies inside a hypercubic surface of N-1 dimensions. The 2N sides of this cube are all the N-1 dimensional surfaces in the N-dimensional configuration space, which are given by the 2N equations:

$A_i = 0, \qquad A_i = A_{max} \qquad$ for i=1 to N

When a trajectory reaches the edge of the hypercube, one unit of the network gets activation equal to Amax or to 0. As long as this unit remains with value Amax or 0, the trajectory moves in a space with one less dimension. The trajectory is continuous but, because of the boundary restriction of activation values, it is not differentiable at the isolated points where the trajectory meets or leaves the edge of the hypercube.

Figure 5 depicts the configuration space of a very simple rate neural network with only three units with activations A_1, A_2 and A_3. In this case, the N-dimensional hypercube is reduced to an ordinary three-dimensional cube of the three-dimensional configuration space, which has edge equal to A_{max}. The one-dimensional trajectory is depicted in red, and lies always inside the cube. In this figure, the network starts at the initial state that is represented by point p, and ends at point w. The six equations $A_i=0$, $A_i=A_{max}$ for i=1 to 3 give the six sides of the cube. These six sides represent states of the network where one of the units has activation Amax or 0. The twelve edges represent states of the network where two units have activation Amax or 0, and the eight corners are the states where all units have activation Amax or 0.

Analytical solution of a rate neural network model

Although the trajectory is not differentiable, we can still solve the system of the N first order linear differential equations analytically. To do this, we notice that every unit can be at 3 different states according to its activation, which can equal zero, A_{max} or a value in between zero and A_{max}. These three cases for every unit give 3^N possible cases for the whole network. The set of all states, which belong to every such case, form a subset of the N-dimensional configuration space. Every such subset has a dimension, which is from 0 to N. For example, the case where all units have activations, which lie between zero and A_{max}, is the N-dimensional interior of the hypercube. The case where one and only one unit has a border-activation (either zero or A_{max}) forms a N-1-dimensional side of the hypercube. If in our state two and only two units have border activations, then this state forms a N-2-dimensional edge of the hypercube. Zero dimensional cases are those where all units of the network have border activations. Every instant, the trajectory will lie inside one of these 3^N subspaces of the N-dimensional space.

We can now solve analytically the 3^N systems that correspond to the 3^N possible cases. Some of them may be trivial. To find a partial solution, we start to form the trajectory with the solution of the state that corresponds to the initial conditions of the network. When we reach the border of the subset of the N-dimensional space that corresponds to this case, we enter a second subset of the N-dimensional space, which corresponds to another case. We get the second part of the trajectory, which is the solution of the system in this case, starting with the point of entrance to the new subset

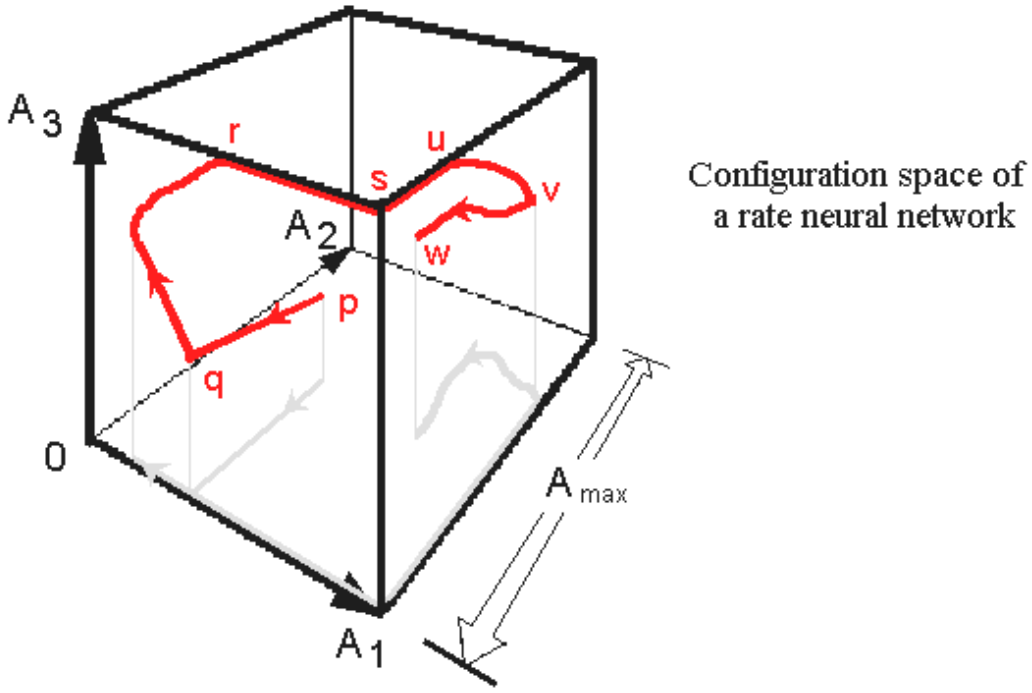

Fig. 5. The configuration space of a rate neural network with three units with activations A_1, A_2 and A_3. The three axes denote these activations. The trajectory is denoted with red and its projection on the A_1 and A_2 plane with gray. The arrows in the trajectory show the direction of the movement of the fictitious point that represents the state of the network. The trajectory in sections pq and vw lies inside the three-dimensional space, in sections qr and uv in a two-dimensional space, and in section ru in a one- dimensional space.

of the N-dimensional space as an initial condition, and ending again at the border of this second subset and a third subset. We can thus construct the whole trajectory of a partial solution in a piecewise manner.

Limitations of analytical approaches to a rate model

The number (3^N) of systems that should be solved is too big, and most of the systems are not interesting. At every instant there is a unit in the network with zero activation and certainly, at some point in time, maximum activation will be achieved by some units. We

can say that the model of the superior colliculus presented here works all the time at the edge of this hypercube in the configuration space. We are thus interested only in a few partial solutions, each derived with a well-defined initial condition. Only a few of the 3^N subsets of the N-dimensional configuration space will be entered by these partial solutions, and we need to solve only the systems corresponding to these subsets. It would be a waste of effort to solve all systems.

However, even with the above simplification, we still need to solve too many systems, and the solutions we get are lengthy and give no clear intuition about the networks' function. We thus preferred the numerical method to extract the particular partial solutions we are interested in, and which will be presented in the following paragraph.

Numerical solution and Euler's integration method

Instead of searching for an analytical solution, the simplest method for numerical integration was used, namely the Euler method. In this method we evaluate the trajectory in the configuration space at discrete points in time which are all integer multiples of a time interval Δt. We then evaluate the activation of every unit at any time with linear interpolation of the activation at the two nearest evaluated discrete points. The time interval Δt was chosen to be equal to 2ms, in order to be roughly equal to the synaptic delay for a signal transmitted from one cell to another. The activation ($n\Delta t$) of the unit j at time $n\Delta t$ equals the sum of the activations A_i of all units i at time $(n-1)\Delta t$, multiplied by the weight W_{ji}, plus A_i $((n-1)\Delta t)$ multiplied by a constant k. The weight W_{ji} is a constant real number which is proportional to the strength of the connection from unit i to unit j. The constant k is a number, which depends on the time constant of the unit.

$$A_j(n\Delta t) = \sum A_i((n-1)\Delta t)\, W_{ji} + K\, A_j\,((n-1)\Delta t)$$

Or, using matrix formulation,

$A(n\Delta t) = W\ A((n-1)\Delta t) + K\ A((n-1)\Delta t)$, where W is the matrix of the weights W_{ji}, and A is the vector of the activations A_i, and i, j are natural numbers from 1 to N. The constant K is related to the time constant τ with the following formula:

$$K = e^{-\Delta t/\tau}, \text{ or } \tau = -\Delta t/\ln(K)$$

The simple proof for the derivation of K will be explained in the following paragraph.

When the calculation of a unit's activation $A_j(n\Delta t)$ leads to a value greater than A_{max} or less than zero, then it is set equal to A_{max} or zero respectively, and the next step of the numerical integration takes place. This is equivalent to stating that the numerical integration is interrupted whenever it gets out of the hypercube, and is started again with new initial conditions, with the activation(s) that were found out of accepted borders set to the nearest border, which is either A_{max} or zero, and all other activations left as they were. In case that one and only one unit i has activation A_i equal to A_{max} or zero, the trajectory in the configuration space reaches the N-1 dimensional side of the hypercube. If a second unit reaches the N-1 dimensional side of the hypercube, then the trajectory enters inside the N-2 dimensional edge of the hypercube, which is defined as the

intersection of two N-1 dimensional sides. If m units at an instant t have activations equal to either E_{max} or zero, then the trajectory lies inside a N-m dimensional hypersurface.

Suppose the unit i obtains an out of border activation value, above A_{max} for example, and all other units have activations between zero and A_{max}. Then we can say that we start again with new initial conditions as described before for all units other than i, and construct a system with the N-1 equations of all units other than i, where the activation A_i is set to A_{max}. This system describes how the network behaves as long as $A_i > A_{max}$. Every time another unit exceeds a border-activation, we may reduce by one the equations of the system, and have an additional inequality requirement for the duration of this new system. The opposite of course happens when the inequality requirements no longer hold.

Evaluation of K as a function of τ.

Suppose that we have a first order unit, like those used in the present model, with activation function A(t). The activation A(t) is given by the differential equation

$$A' + A + C = 0,$$

Where A´ is the time derivative of the activation A

When this unit starts with an initial activation A_0, and receives no other input, then its activation function A(t) follows a decaying exponential law

$$A(t) = A_0 e^{-t/\tau}$$

When we evaluate A(t) using discrete time $t = n\Delta t$, the activation of the unit is

$$A(t) = A_0 K^n$$

Where K is the recurrent weight, which is used to model the time constant of the unit. Equating the above to relations for time $t = n\Delta t$, we have

$$A_0 e^{-n\Delta t/\tau} = A_0 K^n \Rightarrow$$

$$K = e^{-\Delta t/\tau} \text{ or } \tau = -\Delta t/\ln(K)$$

Model Presentation

Expectations from a superior colliculus model

In principle, it should be possible to incorporate the wealth of information described in paragraphs 0, 0 and 0, into models of the SC that can account for the properties of saccades that are due to its activation. More generally, models of the saccadic system should rely on units, which display realistic activation functions and are connected in a realistic manner. Further, model output should respect known psychophysics. Additionally, the properties of evoked saccades should be consistent with what is known from the electrical stimulation of the brain. Finally, lesions of model elements should replicate the symptoms of known neurological disease. A model of the burst generator, which satisfies these stringent verisimilitude tests, has been proposed (Moschovakis, 1994). The present report describes its extension to encompass the SC and the predictions that it leads to.

Model description

Our model of the SC consists of two models connected in series, one model for the input of the SC and one for the output. The model for the input encompasses units simulating the function of the L and Pv cells. The model for the output encompasses units simulating the function of the TLLBs and the QVs, where QVs receive input from the PVs of the input layer. The output layer of the TLLBs drives the MSH model of the burst generator in order to get saccades. RTLLBs receive also input from the TLLB layer, and feed it back to the PV layer in order to remap the location of targets in the input layers.

Computer simulation of the model

Model simulations were run with time steps of 0.1 - 1 ms on a Macintosh Quadra using commercially available software. The input-output characteristic of all model units consisted of a linear region (for inputs greater than zero), a threshold equal to zero and a saturating nonlinearity beyond 1000 Hz. As described in methods section, the saturating nonlinearity of 1000 Hz is due to the maximum firing frequency a neural cell can exhibit, whereas the threshold (zero) is the minimum frequency that it can display.

Transfer functions of the burst generator elements were similar to those of the leaky version of the MSH model (which employed non-integrating LLBs connected to RIN units with a time constant of 40 ms).

I will start the model description from the output machinery, where much more is known in terms of the anatomy and physiology.

The output of SC (motor part)

The upper part of Figure 6 is a diagrammatic illustration of layers close to the output of the simulated SC model; it includes a TLLB layer and a QV layer. The input to the model is information about target location (eye position error signal topographically coded), which comes from the PV layer.

The QV layer

The eye position error is fed to the layer of the quasivisual (Qv) units of the deeper tectal layers. In addition, Qv cell activity is gated by inhibitory input from cells of the substantia nigra pars reticulata, which display "sustained memory contingent saccade responses" (SNR_2; Hikosaka and Wurtz, 1983b) (see 0). Because the discharge of SNR_2 cells mirrors that of Qv cells, it is reasonable to assume that the former inhibit the latter and that the sustained pauses of SNR_2 cells would release Qv cells from tonic inhibition.

Every Qv_i receives excitatory input from the Pv_i, with a weight equal to 1. In addition, every Qv_i receives a self-excitatory connection equal to 1. This self-excitation works as a memory: once a QV is activated, it will not seize firing till a saccade near its optimal vector is over and the SNR_2 gets activated. The PV layer, which will be described in 0, keeps a record of all the presented visual stimuli in spatial code, and remaps them after every movement of the eye relative to the surrounding environment. Every time a visual stimulus becomes behaviourally important, as for example in experimental conditions when the thirsty animal expects a liquid reward, the SNR_2 cells of the substantia nigra stop firing, and QVs receive the input from PV units. QV cells, as described before, display long stretches of low frequency discharge that commences soon after the presentation of visual targets and ends soon after the end of a saccade to it (Mays and Sparks, 1980). Depending on the distance between their location and that of the eyes (i.e., the eye position error signal) different targets will activate different Qv cells. These are indexed by their location in an array of Qv cells. For our simulations, 40 indexed units were employed for one SC, so that small and large index numbers correspond to small and large eye position errors, respectively. The contralateral SC was not represented at the level of the Qv layer.

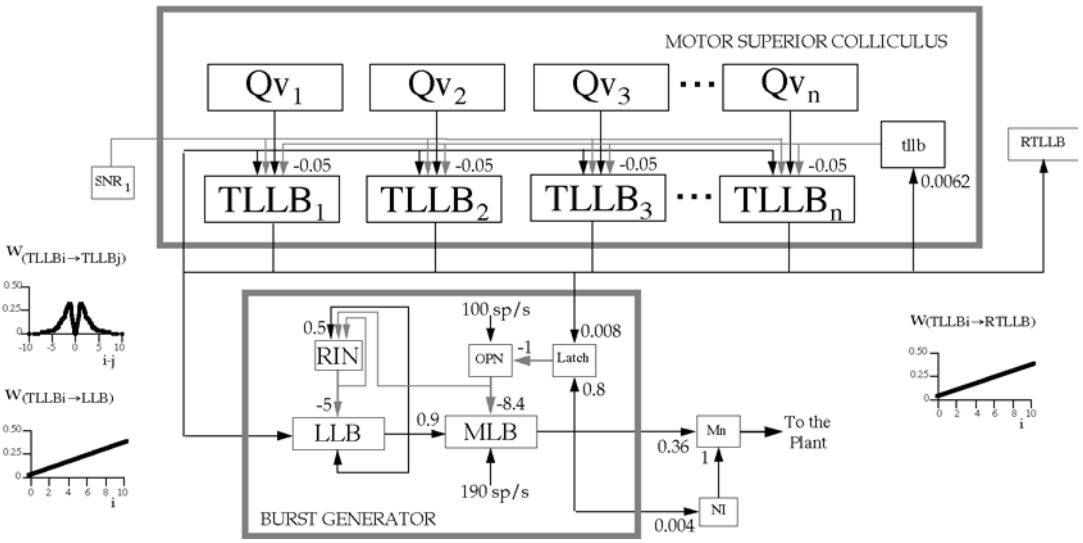

Fig. 6. Model of distributed population coding of saccade metrics in the motor layers of the SC. Solid lines indicate excitatory connections. All other connections are inhibitory. Numbers indicate connection strengths. Insets indicate spatially varying connection strengths (w), plotted as a function of the location of source (i), or the target (j) neurons within their respective arrays, or in terms of the distance between them (i-j). Abbreviations: LLB, long-lead burst neuron; MLB, medium-lead burst neuron; Mn, motoneuron; NI, neural integrator; OPN, omnipause neuron, RIN, resettable integrator neuron; RTLLB, reticulotectal long-lead burst neuron; SNR_1, neuron of the substantia nigra pars reticulata that pauses for saccades; Qv, quasivisual neuron; TLLB, tllb, excitatory and inhibitory tectal long-lead burst neurons.

Spatiotemporal transformation and connection to burst generator

Qv units in turn activate neighbouring (and thus similarly indexed) tectal long lead burst units (TLLBs; Moschovakis, 1988b). Each $TLLB_i$ unit receives input from Qv_i, with a weight equal to 0.01. Consistent with known anatomy and physiology, TLLBs carry the output of the SC to the burst generators. Accordingly, to evaluate the performance of the proposed SC model, we connected TLLBs to a leaky version of Moschovakis' (Moschovakis, 1994) MSH model of the burst generator (the bottom box of Fig. 15). Consistent with known anatomy (Scudder et al., 1996a,b), the TLLB signal has been routed to the long lead burst element (LLB) and the "latch" element of the burst generator. The strength of the TLLB→LLB connection ($w_{TLLB→LLB}$) is assumed to depend on the index (i) of TLLBs, so that cells preferring small saccades (small i) project less heavily to the burst generators than cells, which prefer bigger saccades (bigger i). A plot of $wTLLB_i→LLB$ as a function of the index number of TLLBs is plotted next to the pathway it concerns in Fig. 6. The weight of the connection from $TLLB_i$ to the LLB is a linear function of the index i, and was given by the following formula:

$$wTLLB_i→LLB = 0.003125\ i$$

This simple device is called "spatiotemporal" transformer because it connects a part of the brain that uses a "place" code to specify movement parameters (the SC) to a part of the brain (the burst generator) that uses a "time" code to specify the same movement parameters (cf. Moschovakis et al., 1996). As previously mentioned in TLLB physiology, there is experimental evidence for the spatiotemporal transformer, which is commonly used in models of the SC output (Moschovakis et al. 1998b). Its existence is of particular importance as it allows a motor circuit (the motor SC) to use a code (the "place" code) generally preferred by sensory systems. This provides an opportunity for the motor map to be brought in register with the sensory map of visual space in the manner to be described shortly. The spatiotemporal transformer of the present model is consistent with known anatomy in that SC regions encoding saccades with a large horizontal and a small vertical component project strongly upon the horizontal burst generator and weakly upon the vertical burst generator and *vice versa* for regions that encode saccades with a small horizontal and a large vertical component (Grantyn et al., 1997). In our model, which is one-dimensional, we used a graded projection from the SC to the burst generator, and areas of the SC coding for larger saccades project stronger to the burst generator than areas coding for smaller saccades.

TLLB dynamics

An important question that must be addressed by all models of the SC is the mechanism responsible for the generation of TLLB bursts. TLLBs were assumed to receive input from two sources. One is the aforementioned excitatory one from Qv cells. The second is inhibitory and originates from cells of the substantia nigra pars reticulata (SNR). Some of them are known to discharge tonically and to pause for saccades (SNR_1; Hikosaka and Wurtz 1983a,c). Because the discharge of SNR_1 cells mirrors that of TLLBs, it is reasonable to assume that the former inhibit the latter. This assumption is further supported by the fact that TLLBs belong to a class of tectal efferent neurons (T) all members of which display monosynaptic IPSPs in response to the electrical

stimulation of the SNR (Karabelas and Moschovakis, 1985; Moschovakis et al., 1988a,b). Neither excitation originating from Qv cells nor inhibition originating from SNR cells can fully explain the high frequency bursts of TLLBs. To account for such bursts, the present model relies on lateral excitatory connections between TLLBs. This is consistent with the fact that TLLBs emit recurrent collaterals, which invest tectal areas housing other TLLBs (Moschovakis et al., 1988a, b). Further, it is justified by the fact that the main axon of TLLBs joins the predorsal bundle and the fact that predorsal bundle efferents are glutamatergic (Mooney et al., 1990; Büttner-Ennever and Horn, 1994). To account for the eventual end of their burst, we assumed that TLLBs are reciprocally connected to local circuit inhibitory neurons, which display a discharge pattern similar to that of TLLBs and are for this reason called tllbs. This pattern of connections endows the SC with a biological oscillator.

Spatial constraints of intracollicular TLLB connections

Because of the important role they play in our model, we sought spatial constraints of the strength of connections between TLLBs. This and other spatially constrained connection strengths are shown in Fig. 7 as plots of $W_{(I_i \rightarrow A_j)}$ versus i-j (where i and j indicate the spatial location of units within the arrays I and A, respectively) next to the connections they concern. To obtain the spatial distribution of the boutons deployed by TLLBs inside the SC, we analysed quantitatively the recurrent terminal field of one such cell that was intraaxonally injected with HRP following its functional identification in an alert behaving squirrel monkey (Fig. 8). Methods used to functionally identify and study morphologically saccade related neurons have been described elsewhere (Moschovakis et al., 1988b; Moschovakis, 1991a,b; Scudder et al., 1996a,b). For the purposes of this report we plotted terminal fields with the help of a Zeiss microscope (Axioskope) equipped with a 2.5x and an x40 objective (x25 and x400 final magnification) and connected to a Compaq 486 microcomputer running the Neurolucida piece of software (MicroBrightField Inc., Colchester, Vermont). To obtain accurate spatial alignment of terminal fields distributed over several sections in widely separated regions of the SC (the SC of the squirrel monkey spreads over about 55 sections measuring 80 μm in thickness), we stored the outlines of the midline, the aqueduct and the dorsal surface of the SC, as well as the three dimensional coordinates of synaptic *boutons* belonging to the neurons studied. We aligned all the sections and performed a projection onto the horizontal plane of all boutons contained within the SC (with the exception of boutons contained within the stratum griseum superficiale). This way, we constructed horizontal composite plots. The resulting information was then exported to a Power Macintosh computer for re-sampling. To this end, we counted the total number of boutons contained within a voxel measuring 80 μm in width and length and comprising the total thickness of the deeper SC layers, with the help of the Transform piece of software (Fortner Research Inc., Sterling, Virginia). Figure 16 illustrates the spatial distribution of the recurrent terminal field of the TLLB we analysed. Consistent with this data, the present model assumes that TLLB recurrent projections (plotted in the inset of $w_{(TLLBi \rightarrow TLLBj)}$ versus i-j; Fig. 6) cover a considerable proportion of the ipsilateral SC and are spatially distributed in a bi-lobe fashion centered on the cell body they originate from. These connections spread also to the contralateral SC, through commisural fibers. We modelled the contralateral SC with an exactly symmetrical array of 40 TLLB units, where the areas corresponding to small movements of both colliculi were placed adjacent to each other, and the weights between

them were evaluated as if they formed a continuum. This way, both modelled colliculi form a functional continuum. The symmetric weights connecting $TLLB_i$ to $TLLB_j$, was a function of the absolute difference $|i-j|$. Weights are presented explicitly in the following table:

Distance $\|i-j\|$	Weight from $TLLB_i$ to $TLLB_j$
0	0
1	0.27
2	0.2122
3	0.1207
4	0.05303
5	0.02828
6	0.01768
7	0.0106
>8	0

Global inhibition in TLLB layer

All TLLB units give an excitatory connection to the lumped inhibitory unit tllb, which is equal to 0.03, and all TLLB units receive an inhibitory input from the tllb unit, which equals –0.2. Of course, only the product of these two weights is important for the function of the model. The tllb unit represents a lumped TLLB population of inhibitory cells, and it has not an upper bound for its activation.

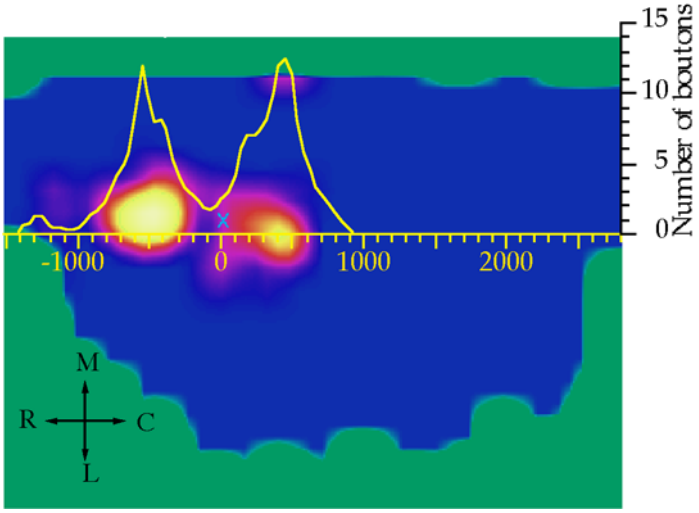

Fig. 7. Horizontal spatial distribution of terminals deployed in the deeper layers of the SC by a single functionally identified TLLB that was intraaxonally injected with HRP. Colors range from dark to light in proportion to the small or large number of boutons deployed in the corresponding point of the horizontal map of the SC. The yellow line is a plot of the number of boutons (ordinate) within 80 mm of a plane through the soma and normal to the SC surface as a function of the rostrocaudal distance from the soma (abscissa). Abbreviations: C, caudal; L, lateral; M, medial; R, rostral.

The input of SC (visual part)

The model of Fig. 6 fails to address the issue of how visual information can reach Qv cells. For this reason it was supplied with the additional machinery illustrated in Fig. 9

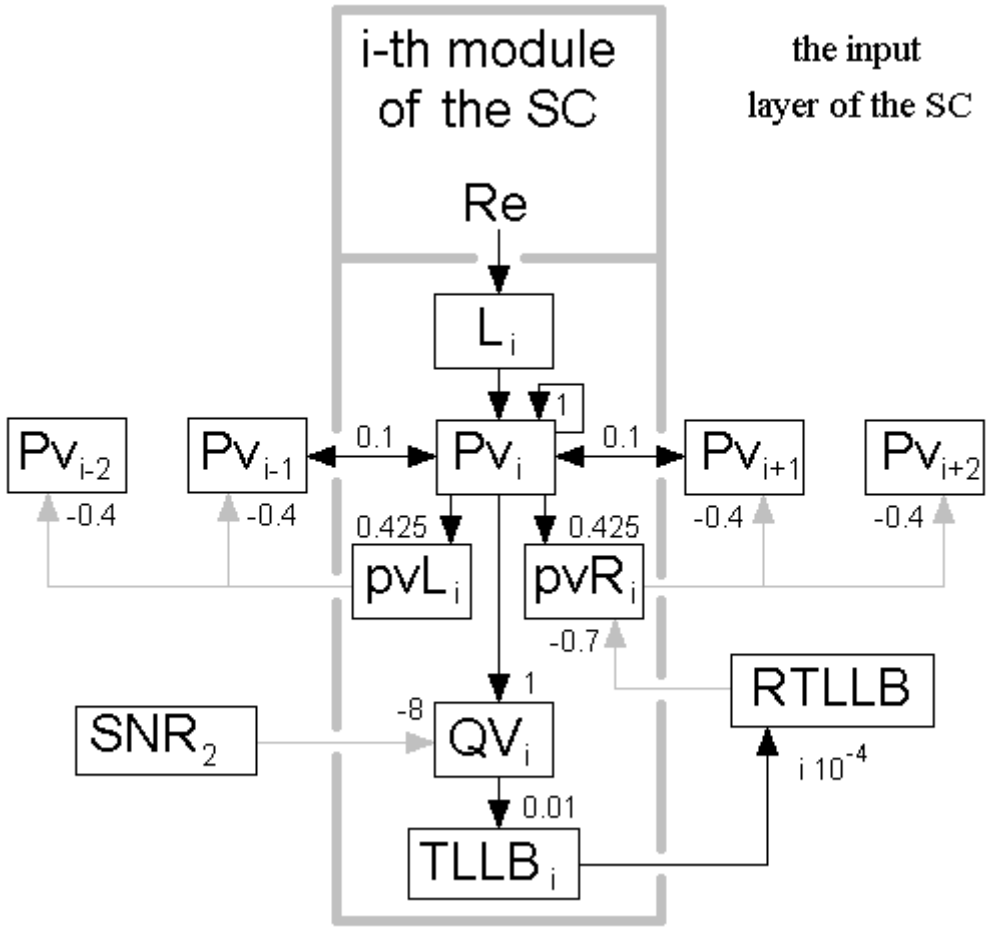

Fig. 8. The input layer of the SC. The *i*th module is inside the gray orthogonal. The neighbouring PVs and the connections from the *i*th module towards them as well as the connections from the neighbouring Pvs are depicted. Black and gray arrows indicate excitatory and inhibitory connections respectively. Pvs are excitatory predictive visual cells, whereas pvL and pvR are inhibitory predictive visual cells. SNR2 is a neuron of the substantia nigra pars reticulata with memory contingent responses. L is visual neuron of the superficial tectal layers.

L layer

The input stage of this additional circuit consists of a layer of units (L layer) simulating the visually responsive cells of the superficial tectal L-neurons, which receive input from the retina. L units code the retinal error signal, i.e. the distance of the visual target from the retina. L units were indexed in the same manner as the Qv and the TLLB

units, which they drive. Thus, L_i cells with small or large index number i are differentially activated by targets whose retinal images are close to or far from the fovea, respectively. Consistent with known anatomy (Moschovakis, 1988a), L neurons were assumed to project to cells of the deeper tectal layers, and in particular PVs.

PV layer

As was previously described (see 0, 0), the discharge pattern of PVs is very similar with that of Qv cells (Walker et al., 1995), with one additional constraint: The QV will not fire, unless a saccade pointed at its movement field is going to be executed in the future. Its firing pattern can thus be extracted by a one to one excitatory input from the QV layer, plus an inhibitory gate, which will allow only "interesting" visual stimuli of the PV layer to be transformed into coded decisions for action in the QV layer. The role of the inhibitory gate suits with the firing pattern of mirror cells of Substantia Nigra (SNR2 cells), which was used as mentioned above for the model of the output of the SC. Pv units were thus assumed to convey visual information to Qv units, and every Qv_i receives an input equal to 1 from every Pv_i. All Pvs (similarly with Qvs, as mentioned above) have autoconnections equal to one, i.e. every Qv_i and Pv_i sends to itself a connection with weight equal to 1. These autoconnections were used in order to model the memory properties of these cells, and they are equivalent with an infinite time constant.

Vector subtraction hypothesis

However, it is doubtful that this simple feed-forward scheme can always supply the deeper tectal layers with the requisite visual information. This is shown by the fact that monkeys and human subjects can execute a series of correct saccades to two targets both of which are extinguished before the onset of the saccade to the first target (Hallett and Lightstone, 1976; Schlag et al., 1990). In such double-step stimulation experiments, the desired displacement vector of the second saccade does not match the Re vector of the second target and thus cannot be computed from it if no other information is available. Instead it may be computed from the difference between the Re vector of the second target and the displacement vector of the first saccade (Moschovakis, 1988b), a hypothesis called "vector subtraction". In other words, according to vector subtraction hypothesis, every time a saccade with vector V is performed, and n other extinct visual targets with vectors V_1, V_2, … V_n are in memory, the vector -V is added to all V_1, V_2, … V_n, in order to continue to code the extinct visual targets in retinotopic coordinates. In the discussion, we will see the advantages of the vector subtraction hypothesis, in comparison with older hypotheses based on head centered coordinates. Of the several known classes of SC neurons, it is the Qv cells that are more likely to receive the signal that results from this "vector subtraction" process (the "eye position error" signal). The reason is that Qv cells respond not only when a target is present in a cell's receptive field, but also when a saccade moves the eyes in such a way, that the extinct target comes to lie within the cell's field (Mays and Sparks, 1980). In cases such as this, the superficial visual tectal cells activated are not in register with the Qv cells activated. In terms of our model, the index numbers of the L and Qv units which respond to the same target would differ by as much as corresponds to the size of the intervening saccade.

pvR and pvL layers; feedback from RTLLBs

Conceivably, cortical projections could bypass the superficial SC to engage the proper Qv cells (Sparks and Mays, 1982) and thus account for their discharge in instances such as this. In fact, the forebrain contains a multitude of cell classes, which display Qv like responses and could supply Qv cells with the requisite information (reviewed in Moschovakis et al., 1996). There is considerable evidence to suggest that the SC contains much of the machinery needed to compute the eye position error from the Re of targets and the efference copy of intervening movements (Moschovakis, 1987, 1996a,b; Moschovakis et al., 1988a,b). Accordingly, we felt that it would be worthwhile to explore the possibility that a circuit composed of known SC related neurons could carry out this process. Crucial in this regard are the reticulo-tectal long-lead burst neurons (RTLLBs) and their projections to the SC (Moschovakis et al., 1988b). In the model of Fig. 17, they have been assumed to contact inhibitory predictive visual (pv) units with asymmetric projections (pvR and pvL neurons) in the right and the left SC, respectively. For this scheme to be correct, RTLLBs of one side should contact tectal cells in both sides of the brain. In the model, the RTLLBs of the left side contact pvL cells of both superior colliculi, whereas RTLLBs of the left side contact pvR cells of both superior colliculi. This is consistent with the anatomical projections of single functionally and morphologically identified RTLLBs (Moschovakis et al., 1988b). In the model, there exist three layers of units, the PV layer, the pvR layer and the pvL layer, all indexed as all other layers and with the same number of modules. The three layers of Pv, pvR and pvL units in our model correspond to the Pv neurons, as they have been described. Every PV_i cell contacts the pvR_i and pvL_i units with the same index number. The pvL_i cell in turn contacts the two excitatory units $Pv_{(i+1)}$ and $Pv_{(i+2)}$, which lie right to pvL_i. The pvR_i cell, symmetrically, contacts the two excitatory units $Pv_{(i-1)}$ and $Pv_{(i-2)}$, which lie left to it. In summary, pvL cells receive input from the RTLLBs of the left side, and inhibit PV cells at their right. Tectal interneurons with asymmetric terminations, such as those of the pvR and the pvL layer, have been found in the snake (Dacey and Ulinski, 1986). Finally, consistent with known anatomy, RTLLBs have been assumed to receive input from TLLBs (Moschovakis et al., 1988b) in the weighted manner that was used in the connection between TLLBs and LLBs. This is important for our vector subtraction hypothesis, because RTLLBs have the information for the amplitude of the saccade that is being performed, and thus the vector that should be subtracted from all visual targets having vectors V_1, V_2, … V_n.

Since the circuit of Fig. 3 uses a place code, connection strengths were spatially constrained. Most of these projections are simple feed-forward point ones towards the immediately next element in a module's cascade. In particular, for every i between 1 and N, L_i unit connects to Pv_i unit, which in turn connects to pvR_i, pvL_i and QV_i units. The only exceptions were the asymmetric projections from pvL and pvR layers to the PV layer, and the extensive projection from the unilateral RTLLB population back to the TLLB layers of both superior colliculi, which were described above. Although this assumption can be relaxed without affecting the conclusions of our report, it accords quite well with the little relevant anatomical evidence that is presently available. This concerns the L cells which have been shown to be roughly coextensive with the spread of

the dendritic tree of the neuron they originate from (Moschovakis et al., 1988a). However, this pattern does not apply to one of the most important projections of our model (the SC projections of RTLLBs). To obtain information about the spatial distribution of the relevant boutons, we analysed quantitatively the axonal system of one RTLLB that was intraaxonally injected with HRP following its functional identification in an alert behaving squirrel monkey, in the manner described for TLLBs above. Figure 9 provides examples of the saccade related discharge of the analysed RTLLB (A), and illustrates its movement field (B) and the spatial distribution of the terminal field it deployed in the ipsilateral SC (C). As shown here, RTLLB projections are distributed throughout the ipsilateral SC and are roughly the same everywhere. Such a uniform distribution of RTLLB terminations in the ipsilateral SC, as well as the non-illustrated contralateral SC, was employed in the present model. The uniform distribution of RTLLB terminations is mirrored with a fixed weight (equal to –0.7) in Fig. 17. TLLBs send to RTLLBs a weighted input, which was

$$wTLLB_i \rightarrow RTLLB = i\ 10^{-4}$$

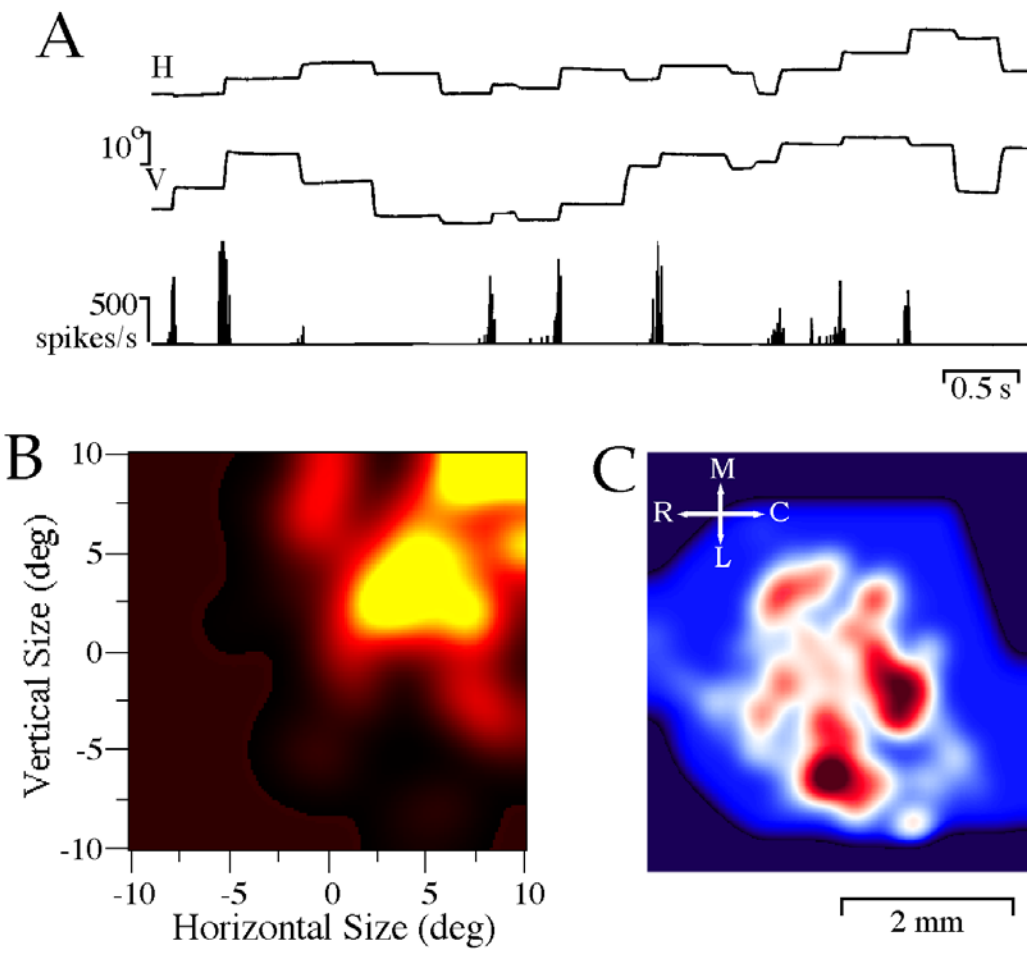

Fig. 9. A Saccade related discharge pattern of a functionally identified RTLLB that was intraaxonally injected with HRP. The top two traces indicate the instantaneous horizontal (H) and vertical (V) position of the eyes. **B** Color-coded plot of the movement field of the same RTLLB. Colours range from dark to light in proportion to the small or large number of spikes that the neuron emitted in its bursts for saccades of the corresponding horizontal (abscissa) and vertical (ordinate) size. **C** Horizontal spatial distribution of RTLLB terminals in the ipsilateral SC. Colours range from blue to dark red in proportion to the small or large number of boutons deployed in the corresponding point of the horizontal SC map. Abbreviations as in Fig. 7.

Choosing appropriate weights

In the absence of direct quantitative information, values of connection strengths (indicated by numbers next to the arrows in Fig. 6) are free model variables. Connections inherent to the MSH model were constrained in the manner described before (Moschovakis, 1994). Additionally, weights specific to the SC model were constrained in the following manner. Firstly, the strength of the connections between TLLBs and the reciprocal connections between tllbs and TLLBs determine the time course of their activation functions. Accordingly, they were adjusted so that the duration of the activation functions of model TLLBs roughly fit the experimentally determined duration of discharge of single TLLBs. In addition, the strength of the feedback and feedforward connections between predictive visual cells and the strength of the RTLLB feedback to the SC determine the dynamics of the vector subtraction process. Accordingly, the strength of these connections was adjusted so as to make its duration roughly equal to that of LLBs (Moschovakis, 1996b) and the possibly related time course of the illusory localization of visual stimuli flashed in the dark (Schlag and Schlag-Rey, 1995). Finally, anatomical evidence was used to spatially constrain connection strengths of the TLLB and RTLLB projections in the manner described above.

Model results

Psychophysics and activation functions

Main sequence

The present model produced realistic saccades ranging from less than 1 deg to about 30 deg, in response to stimulation of Qv cells with increasing index numbers. These simulated saccades are shown in Fig. 10. This is analogous to the activation of SC regions by targets located further and further away from the point of fixation and is largely due to the spatiotemporal transformer used to connect the TLLBs to LLBs of the present model. Activation of neighbouring Qv cells led to the generation of saccades that differed by about 1.2 deg. The inset of Fig. 10 illustrates the relationship between the size (ΔE) and the duration (S_d) of simulated saccades. The two variables are related through the expression, $S_d = A \cdot \Delta E^k$ where A and k obtain values equal to 17.7 and 0.26, respectively, showing a perfect fit with the known psychophysics of the main sequence (see 0).

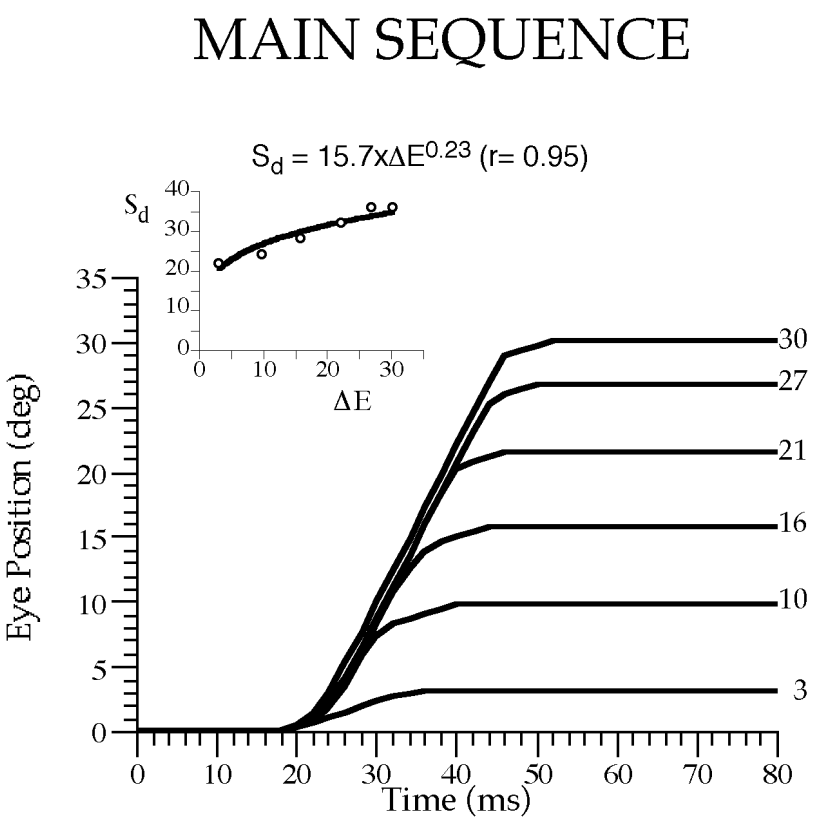

Fig. 10. Examples of saccades generated in response to the activation of Qv cells with different index numbers (indicated next to each saccade). The inset is a plot of the duration (S_d) against the amplitude (□E) of these saccades (open circles). The solid line is a power function fit to the data and obeys the expression $S_d = 17.7 \cdot \Delta E^{0.26}$ (r = 0.996).

TLLB dynamics

Figure 11 illustrates the activation functions of several units of the proposed SC model for a 12^{o} saccade. Inspection of the illustrated waveforms demonstrates their similarity to published curves describing the instantaneous frequency of discharge of saccade related units encountered in the SC and the SNR of primates (Moschovakis, 1996b). Of particular interest is the spatiotemporal profile of the activation functions of TLLB units. Figure 20B is a grey scale contour plot of the intensity of discharge of all TLLB units in the model as a function of time (ordinate) and unit index number (abscissa). To emphasize small differences between weakly activated units, activation functions were plotted on a Logarithmic scale instead of a linear one. Initially, activated cells include TLLBs located at a considerable distance from the Qv cells stimulated. Following their release from inhibition (originating in SNR_1 cells), and due to the recurrent plexus that connects them to one another, TLLBs start discharging more and more intensely. The profile of TLLB discharge progressively evolves so that the most intensely activated TLLBs are the ones that are fairly close to the stimulated Qv cells (the light region of the hill of activity depicted in Fig. 20B). Further into the saccade, TLLB activation progressively dies out around these units and it is around them that activity perseveres the longest.

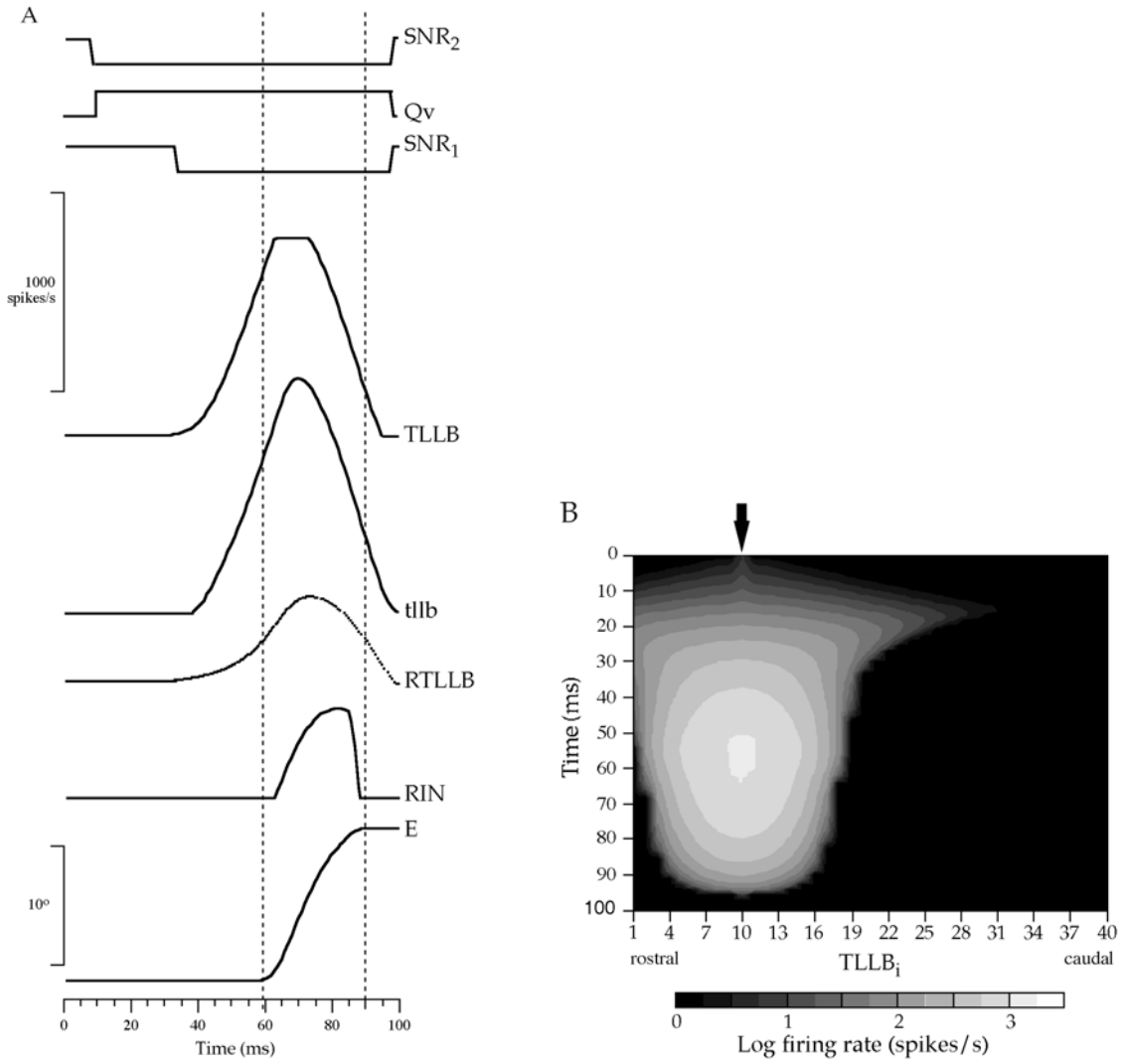

Fig. 11. A Waveforms of the instantaneous firing rate of model units for a 12^{o} saccade as a function of time (abscissa). Calibration bar of 1000 sp/s applies to all units. Abbreviations: E, instantaneous eye position. Other abbreviations as in Figs. 6 and 8. **B** Contour plot of the spatio-temporal profile of the discharge of all TLLB units employed in the model as a function of their index (abscissa) and time (ordinate). Small index numbers correspond to rostral SC sites and big index numbers correspond to caudal SC sites. The gray scale is proportional to the Logarithm of the activation function of depicted TLLBs. The arrowhead points to the spatial location of the Qv cell activated.

Double step stimulation

Figure 21 provides an example of the performance of our model in the somewhat more complex situation of a double step stimulation experiment. To see how it works, let us assume that two targets are presented simultaneously 6 and 18 deg away from primary position (Fig. 12A, open circles) and are extinguished after activating the two L units which correspond to retinal error vectors of 6 and 18 deg, respectively (L_5 and L_{15}). In turn, these activate units Pv_5 and Pv_{15}. Further assume that some time later the SNR gate is lifted permitting TLLB activation and the execution of a 6 deg saccade to the first target (Fig. 12C). The conceptual problems inherent in double step stimulation experiments are evident when the metrics of the saccade to the second target are considered. Clearly, the second retinal error vector encoded in both the L and the Pv unit array does not fit the desired displacement vector that must be executed if the eyes are to reach the second target (Fig. 12A, arrows). If the representation of the second target in the Pv array is not somehow compensated for the execution of the first saccade, the second saccade will be inaccurate (Fig. 12C, stippled line). It is here that the importance of the RTLLB activation manifests itself as it pushes the representation of the second target in the Pv array by 6 deg, from position Pv_{15} to position Pv_{10} (Fig. 12B). Because it is unit Pv_{10} that drives it, the saccade towards the second target is accurate (Fig. 12C, solid line). The second target is thus remapped on the Pv layer to a new position, which still codes correctly the extinct visual target in retinotopic coordinates.

How remapping works

It is important to give an intuitive feeling about how the Pv, pvR and pvL layers manage to do this remapping. First, all units of the Pv layer have integrating, self excitatory connections with weight 1, thus integrate every input they receive until they reach their maximum firing frequency of 1000 spikes/sec. Each unit of Pv layer, as we described it, gives direct excitatory input to its immediate neighbours, but also a stronger indirect inhibition through pvR and pvL layers. This stronger inhibition stops the excitation of one isolated Pv_i from spreading to the whole Pv layer. It also does not permit neighbouring Pv units to be activated simultaneously, because the described connections construct an architecture with local "winner take all" properties. Every Pv_i unit inhibits its immediate neighbours. Every Pv_i unit also excites itself with an autoconnection. On the other hand the simultaneous excitation of Pv units with a distance of 2 or 3 units is possible because they do not interfere with each other, as the weights are short range. This latest fact permits the simultaneous loading of multiple flashed targets V_1, V_2, … V_n on the Pv layer, which will remain in memory due to the self excitatory connections with weight 1, i.e. the infinite time constant of these units.

When a saccadic movement takes place, however, this balance is temporally perturbed. During a saccade to the right, RTLLB unit of the right side receive input from the left SC, which is proportional (due to the spatiotemporal transformation) to the amplitude of the movement. The RTLLB unit of the right side inhibits the pvR population of both colliculi. Each pvR_i unit, no longer exerts enough inhibition to the Pv_i-

$_1$ and Pv_{i-2} units, in comparison with the excitation the Pv_{i-1} unit receives from the Pv_i unit, which has a visual target memorised. The excitation thus spreads from the Pv_i unit, to the Pv_{i-1} unit. But, as the Pv_{i-1} unit integrates the signal of the Pv_i unit, it soon starts to fire maximally, and it transmits this firing to the pvL_{i-1} unit, which was not inhibited by the RTLLB unit of the right side. Now the "winner take all" architecture favours Pv_{i-1} unit against Pv_i unit. This happens because the Pv_{i-1} unit inhibits strongly Pv_i through the unaffected pvL_{i-1} unit, whereas the Pv_i exerts, as we saw, a net excitation to the Pv_{i-1} unit, through the algebraic sum of strong direct excitation and weak indirect inhibition through the pvR_i unit. The memorised target switches its position in the map, we could say that it moves to the left, erasing at the same time the trace behind it. As a result, as long as the RTLLB unit of the right side inhibits the pvR population, every memorised target will move to its left in the map, to a region which codes for smaller rightward saccades. The velocity of this movement, and thus the total distance, which the memorised target will travel, is directly proportional to the net excitation, which it receives from the unit right to it. This net excitation is proportional to the feedback that is received from the RTLLB unit of the right side, which in turn is proportional (again, due to the spatiotemporal transformation) to the amplitude of the movement. The total distance, which will travel the memorised target on the Pv layer, will be proportional to the amplitude of the movement. The distance which any memorised target in the Pv layer will travel, moves it from a region corresponding to a saccade with vector $V_{initial}$, to a region corresponding to a saccade with vector V_{final}. The difference $V_{initial} - V_{final}$ is the same for every memorised target V_1, V_2, … V_n, since the representation of movement fields of QV cells is an almost linear function of their index number in the layer. The small nonlinearity, which emerges at the region of small movements, is due to the non-linear performance of the MSH model at this region. This nonlinearity can be bypassed by an increase of the RTLLB weight at the region of pvR units corresponding to small movements, but we will ignore it here. By adjusting the weight from RTLLB unit of the right side to the pvR population, we can thus establish that $V_{initial} - V_{final}$ equals the vector of the saccade V that has been performed.

$$V_{initial} - V_{final} = V \rightarrow V_{final} = V_{initial} - V$$

The last relation shows, that the vector subtraction hypothesis is substantiated with success by our model.

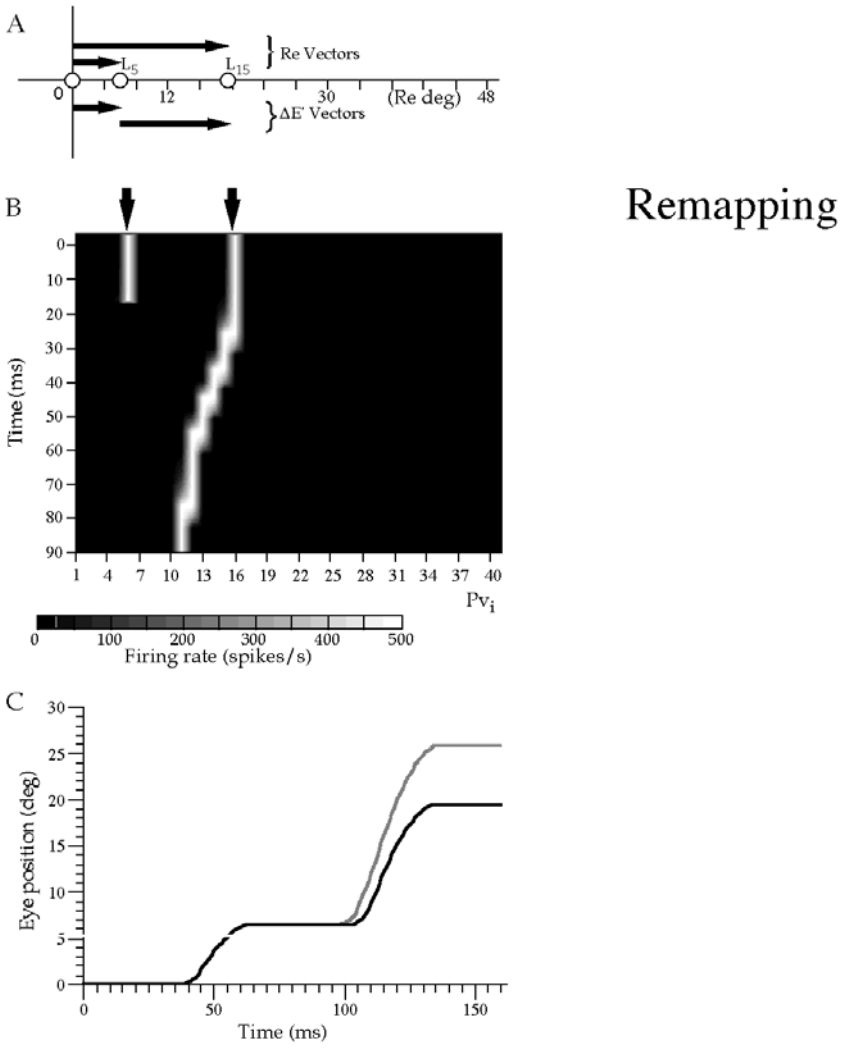

Fig. 12 A-C. Illustration of model performance in double step stimulation experiments. **A** Location of two L units (L_5 and L_{15}; open circles) activated in response to two targets that are extinguished before the saccade to the first one, as a function of the retinal error of the targets (abscissa). Arrows indicate the difference between the retinal error and the desired displacement vectors (above and below the abscissa, respectively). **B** Contour plot of the spatio-temporal profile of the activation function of all Pv units employed in the model as a function of their index (abscissa) and time (ordinate). The gray scale is proportional to the activation function of depicted Pv units. Arrowheads point to the spatial location of the L units activated. The horizontal white lines indicate the onset and offset of RTLLB bursts. **C** Saccades executed by the model (solid line) differ from those that would have been executed on the basis of Re alone (stippled line) if the representation of the second target by the Pv array had not been compensated for the execution of the first saccade.

Electrical stimulation experiments

Stimulation with varying current intensity at a single site

We also examined the performance of our model in situations resembling the electrical stimulation of the SC. To simulate this, the activation of Qv units was set to a constant value (200 Hz) for the duration of the stimulation. To study the effect of the strength of the stimulation, we assumed that the current spreads to Qv units further and further away from the stimulation site so that the number of activated units increases linearly with current intensity. Figure 13, illustrates examples of simulated saccades that were evoked in this manner and are arranged in order of the intensity of stimulation used to evoke them (in multiples of threshold, T). At the low end of the spectrum (1xT), the current was assumed to be just enough to activate a single Qv unit. At the other end of the spectrum (7xT), 7 neighbouring Qv cells were simultaneously activated (about 20% of the total number of Qv units of the present model). Despite the differences in the number of Qv units that were engaged, ensuing saccades were of roughly constant amplitude. If anything, the size of evoked saccades dropped slightly as the intensity of stimulation increased. This is due to the weak input from the QV layer to the TLLB layer, in comparison with the high values of connection strengths that were chosen for the TLLB layer. Decreasing the internal connection strengths of the TLLB layer leads to saccades, which increase slightly with increasing stimulus intensity. Figure 13 also demonstrates that the latency of simulated saccades decreases as the current intensity increases.

Simultaneous stimulation of two collicular sites

The effect of the simultaneous stimulation of two widely separated regions of the model's SC was explored next. Figure 14A illustrates the saccades that are evoked in response to activation of two widely separated Qv units (their index numbers were equal to 4 and 20 respectively). It also demonstrates that the size of the saccades evoked in response to the simultaneous stimulation of the same two Qv units (4&20) is roughly equal to the average of the size of the saccades that are evoked when the two Qv units are independently activated (stippled line). To capture the spatiotemporal profile of the TLLB activation functions that accompany these average saccades, we plotted the intensity of discharge of all TLLB units in the model (again in the form of a grey scale contour plot) as a function of time (ordinate) and unit index number (abscissa). As shown in Fig. 14B, TLLB activity initially builds up at two widely separated locations that correspond to the sites that are electrically stimulated (arrowheads). However, again due to the recurrent plexus that connects TLLBs to one another, the profile of TLLB discharge progressively evolves so that the most intensely activated TLLBs (the light region of the hill of Fig. 14B) are those located at a position intermediate between the two stimulated sites. Beyond this point, the spatiotemporal profile of the activation functions of TLLB units resembled that of the single point stimulation described above.

Long lasting electrical stimulation and staircases of saccades

Electrical stimulation of the SC has been known to produce a sequence of saccades in close succession (staircase of saccades) whose amplitude and direction depends on the location of the stimulating electrode. Figure 15 illustrates results obtained in the proposed model, after clamping the Qv unit responsible for a 9^{o} saccade to its peak value of 200

sp/s. As shown here, this results in a staircase of 9^{o} saccades, which lasts for as long as the colliculus is stimulated (about 250 ms). In addition, our model predicts that TLLBs (as well as burst generator units such as RINs) will emit one burst of discharge for each one of the saccades of the staircase (Fig. 15). The length of the interval between bursts depends on the synaptic weights, conduction delays and time constants associated with the TLLB and tllb units, which collectively comprise the biological oscillator of the SC.

Electrical stimulation of the SC soon after a natural saccade is known to evoke saccades whose amplitude (ΔE) depends on the size of the time interval (Δt) that separates them from the natural saccade (Nichols and Sparks, 1995). The relationship between the two variables (ΔE and Δt) decays exponentially to a site specific value with a time constant equal to about 45 ms. Figure 16A illustrates a simulation of the experimental situation in question. The second simulated saccade of this graph was evoked in response to activation of the Qv unit responsible for 15 deg saccades after a variable delay following a previous saccade of similar size. The size of such saccades (ΔE) has been plotted as a function of the time that elapses from the previous saccade (ΔT) in Fig. 16B. The two variables were related through the expression $\Delta E = 7.4 - 3.6 \cdot e^{-\Delta T/39.5}$, where 39.5 ms is the time constant of the phenomenon, 7.4 deg is the site specific value that it decays to, and 3.6 deg is the smallest size of saccades that can be evoked in this manner (when no time intervenes between the two saccades). For this result to obtain, the RIN unit of the present model's burst generator must not be reset at the end of the natural saccade. Because the resetting mechanism of the MSH burst generator that we used is due to connections between OPNs and RINs, the onset of the electrical stimulation of the SC must precede the resumption of OPN discharge at the end of saccades and somehow lead to strong OPN inhibition.

Lesions and saccade metrics

Although it was not tuned to replicate this, we examined the performance of our model in situations that resemble focal SC lesions. To this end, we disabled single TLLB units and examined the size of simulated saccades that were due to the activation of different Qv elements of the model. Figure 17A provides examples of two such saccades. As shown here, these can be either hypometric (left) or hypermetric (right) by comparison to simulated saccades produced after activation of exactly the same Qv elements prior to the "lesion". The direction of the change (hypo- or hyper-) and the magnitude of the effect depends on the distance between the Qv element activated and the TLLB element disabled. As shown in Fig. 17B, activation of Qv units with index numbers smaller than those of the disabled TLLBs leads to hypometric saccades. In contrast, stimulation of Qv units with index numbers larger than those of the disabled TLLBs leads to hypermetric saccades. To examine how such "lesions" affect the evolution of the spatiotemporal profile of TLLB activation functions, we again plotted the intensity of discharge of all TLLB units of our model as a function of time (ordinate) and unit index number (abscissa) in Fig. 18. As shown in Fig. 18A, B, TLLB activity is pushed to the left (more rostrally) when the site of stimulation (arrowhead) is rostral to the site of the lesion (x). Conversely, the contour plots of TLLB population activity illustrated in Fig. 18C, D, demonstrate that the hill of TLLB activity is pushed to the right

(more caudally) when the site of stimulation (arrowhead) is caudal to the site of the lesion (x).

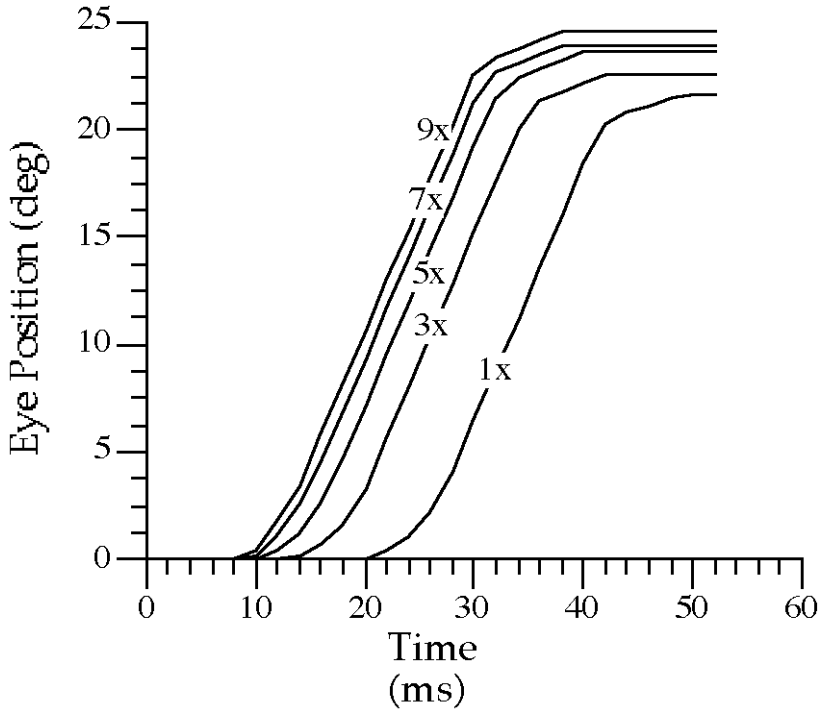

Fig. 13. Time course of saccades evoked in response to simulated electrical stimulation of the SC. Current strength is indicated in multiples of threshold.

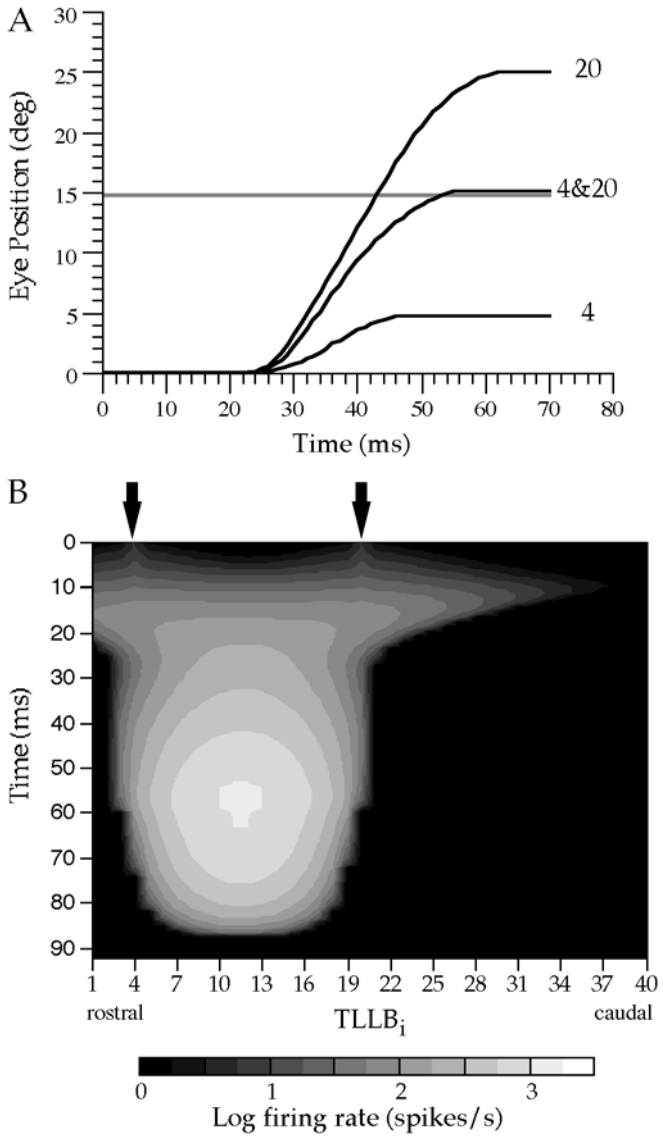

Fig. 14. A Comparison between simulated saccades evoked in response to the simultaneous stimulation of two widely separated Qv units (4&20) and those evoked when the same Qv units were stimulated in isolation (indicated by the index numbers, 4 and 20, respectively, of the two Qv units). Note that the size of the former (15 deg) is quite similar to the mean (stippled line) of the two latter (5 deg and 25 deg). **B** Gray scale contour plot of the spatio-temporal profile of the Logarithm of the activation function of all TLLB units employed in the model as a function of their index (abscissa) and time (ordinate). Arrowheads point to the spatial location of the two simultaneously activated Qv cells.

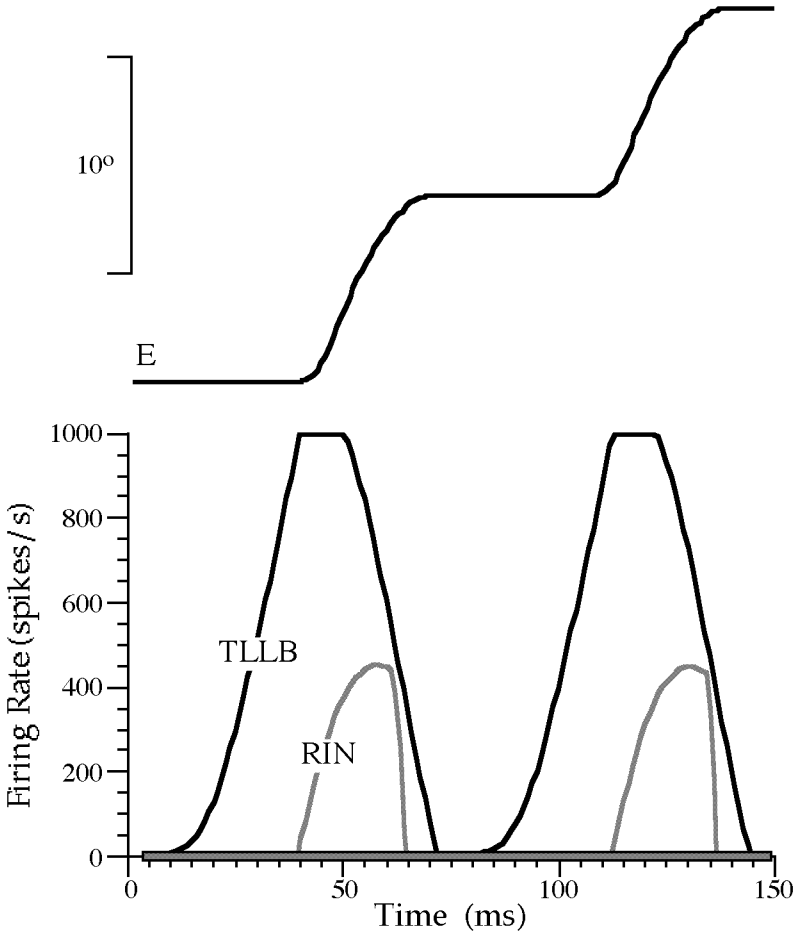

Fig. 15. Simulation of an experiment where the Qv unit responsible for 8 deg saccades was stimulated for a period of about 150 ms, to demonstrate network generation of saccadic staircase. Abbreviations as in Fig. 6.

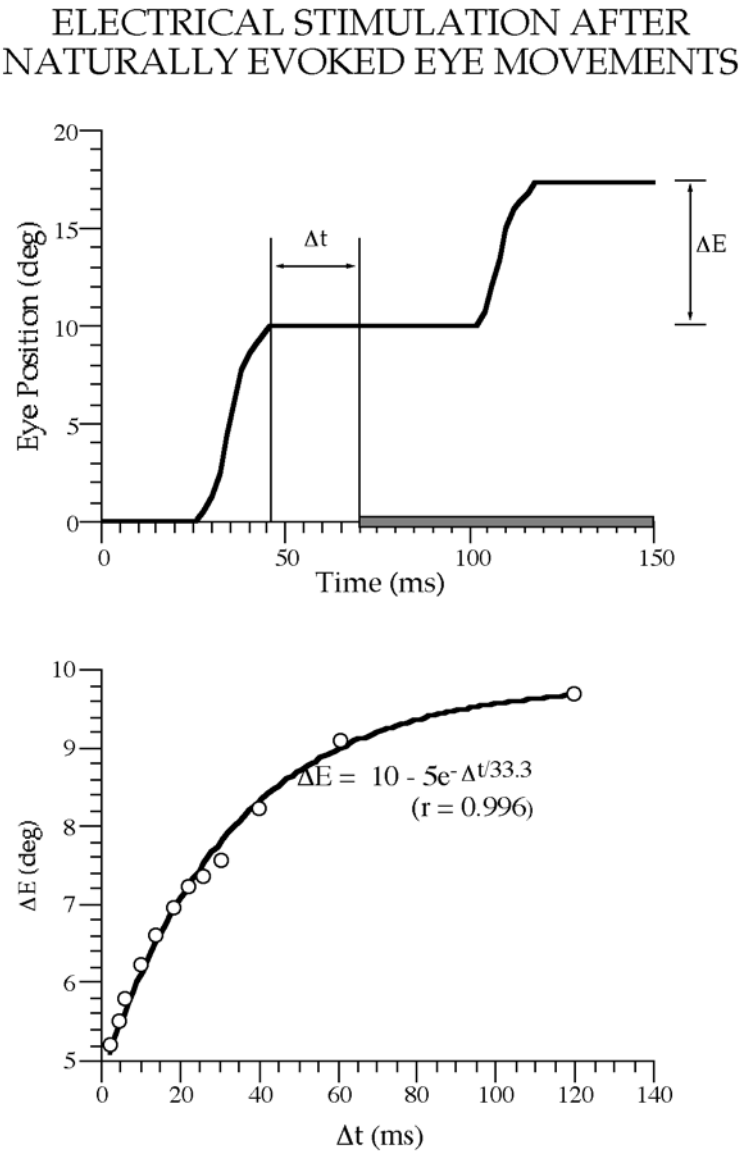

Fig. 16. A Simulation of an experiment in which the Qv unit responsible for a 10 deg saccade was electrically activated soon after the execution of another saccade. The bar covering the time scale indicates the time course of the electrical stimulation. **B** The size of the second saccade (ΔE) depends on the time that elapses from the first saccade (Δt). The solid line is the curve fit to the data (open circles) and obeys the expression $\Delta E = 7.4 - 3.6 \cdot e^{-\Delta t/39.5}$ ($r = 1$).

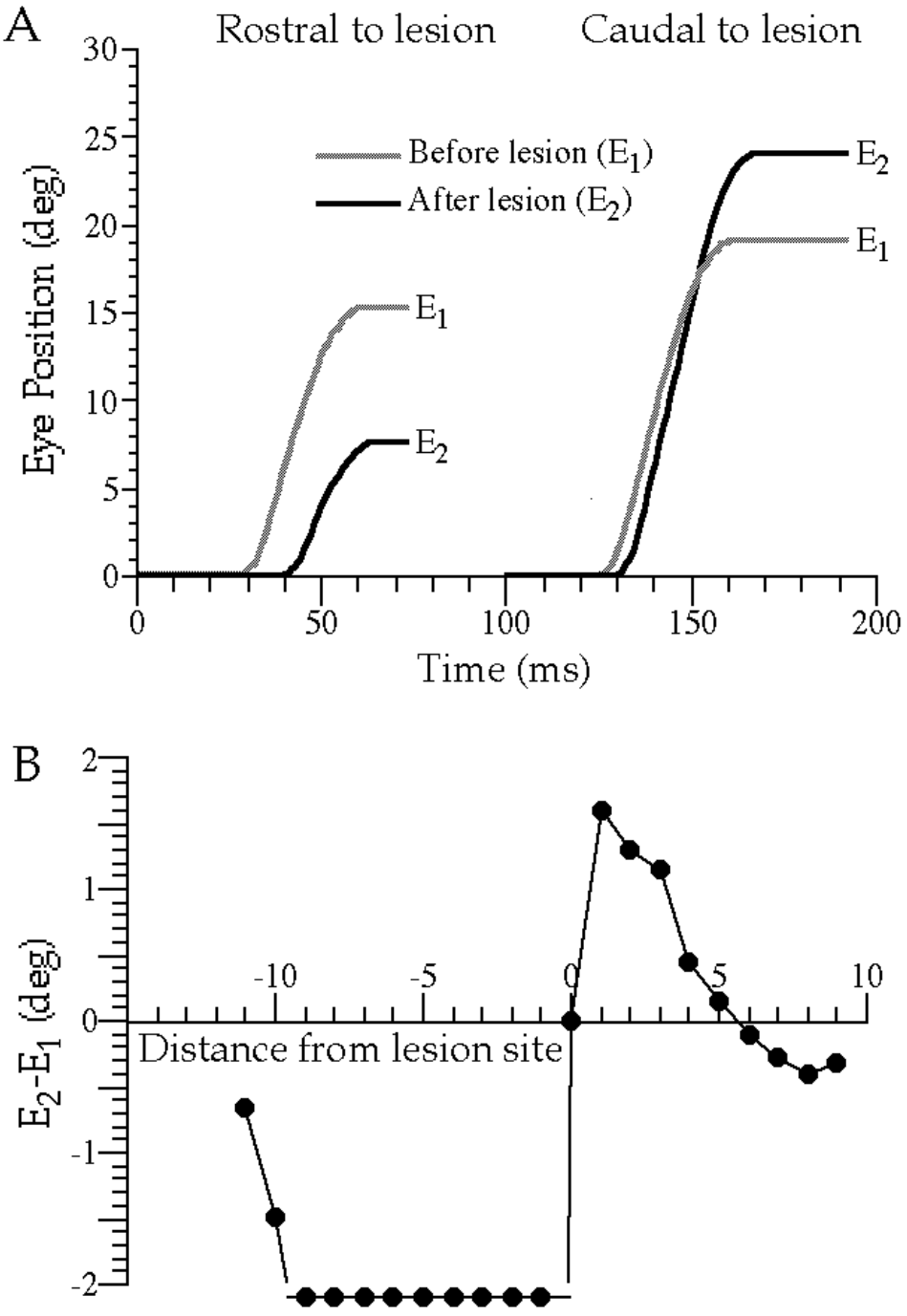

Fig. 17A, B. Simulation of focal SC "lesion" experiments. **A** Two examples of saccades produced before (stippled) and after (solid) TLLB lesions in response to activation of the same Qv unit. **B** Difference between the pre- and post-lesional size of saccades as a function of the distance between the activated Qv and the lesioned TLLB unit. Negative size indicates hypometric post-lesional saccades while negative distance indicates that the Qv unit is rostral to (has a smaller index number than) the TLLB unit.

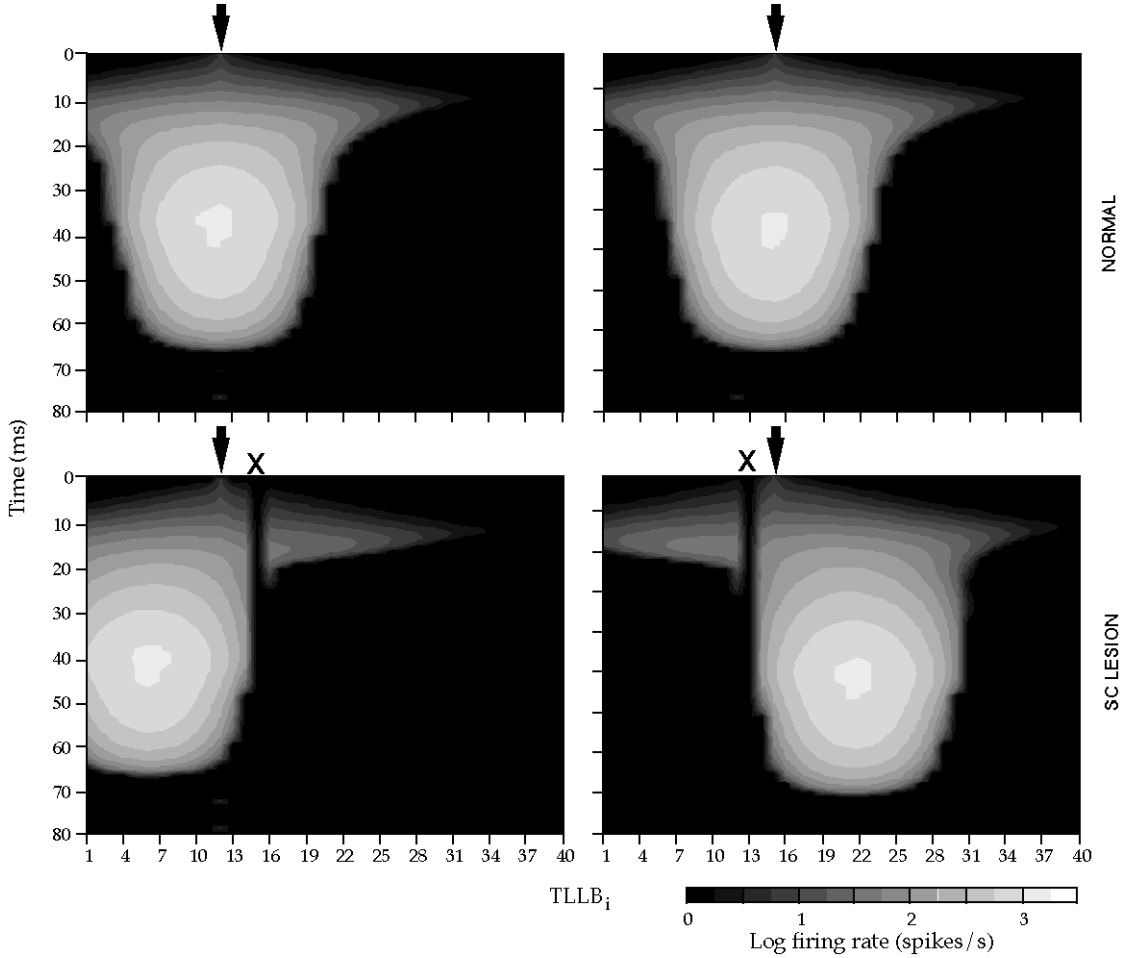

Fig. 18A-D. Contour plots of the spatio-temporal profiles of the discharge of all TLLB model units for saccades evoked from a normal (**A** and **C**) or a "focally lesioned" (**B** and **D**) SC. In **A** and **B**, the stimulation point (arrowheads) is rostral to the lesion (x), while in **C** and **D**, the stimulation point is caudal to the lesion. Conventions and abbreviations as in Fig. 14.

Discussion

The present report evaluates the performance of a one-dimensional, one-directional model of the superior colliculus which consists of an array of interconnected modules each one of which is composed of several vertically arranged processing steps and drives a model of the burst generator of the saccadic system. It demonstrates that it is possible to construct a model of the SC which is consistent with the known anatomy, physiology and psychophysics of the saccadic system and can account for phenomena observed when the SC is electrically stimulated or lesioned.

Experimental evaluation of assumptions and results

Anatomy and neurophysiology

Although complex, the herein proposed model is the simplest that can account for the facts known of the primate SC. Of particular importance are the recurrent collaterals that TLLBs are known to deploy (Moschovakis et al., 1988b); it is their presence which explains the intense bursts of TLLBs. The use of a spatially accurate plexus of recurrent excitatory connections between TLLBs (Fig 7) endows the TLLB array with attractor dynamics such as to account for known properties of saccades evoked in response to stimulation or following lesions of the SC. Also of particular importance is the saccade related efference copy, that the RTLLBs are known to send to the SC (Moschovakis et al., 1988b); their projections allowed us to construct a circuit that is largely confined to the SC and can implement the "vector subtraction hypothesis" in such a way as to account for the psychophysics of double step stimulation experiments and the attending discharge of Pv and Qv cells. Furthermore, of considerable importance are the point to point connections between the superficial and the deeper tectal layers subserved by the well known axonal collaterals of L neurons (Moschovakis et al., 1988a) as well as the several gating mechanisms subserved by the massive nigrotectal pathway (Hikosaka and Wurtz, 1983c; Karabelas and Moschovakis, 1985). The substantial anatomical and physiological evidence to support the existence of the units we employed in the present SC model and the connections between them was outlined in page 17. Much of the remainder of this section is devoted to functional classes of SC cells and their input/output connections that are known or suspected to exist but have not been employed and those that are not known to exist but have been employed.

Elements not included in the present model

Commisural projection to the contralateral SC

The herein proposed model employs the well-known commissural path that originates from TLLBs (Moschovakis et al., 1988b), only at the rostral pole of the superior colliculus. These projections are continuous with the ones that are targeted towards TLLBs of the ipsilateral superior colliculus. Our model does not include the projections between the caudal regions of the two superior colliculi. This projection should be also included in bi-directional extensions of our model to account for the fact that tectal presaccadic cells, which burst before saccades in one direction, are inhibited during saccades in the opposite direction (Infante and Leiva, 1986, Peck, 1990).

Projection from the zona incerta to the SC

The herein proposed model does not employ a well-known projection to the SC that originates in the zona incerta. This nucleus is known to send an inhibitory (Araki, 1984; Ficalora and Mize, 1989; Appell and Behan, 1990) projection to the intermediate and

deeper layers of the superior colliculus (Ricardo, 1981; Ma et al., 1991) and to contain cells which resemble SNR_1 cells in that they pause for saccades. Unlike SNR_1 cells, which pause for saccades to visual or remembered targets, the neurons of the zona incerta also pause for spontaneous saccades (Hikosaka and Wurtz, 1983c). Because we focused on visually elicited saccades, we did not include this projection. It would be important to include it in extensions of our model that concern spontaneous saccades.

Position sensitivity

The electrical stimulation of the SC is known to produce saccades, with amplitude and direction depending on the site of the electrode inside the SC, and linearly on the initial position of the eyes in the orbit. The amplitude of the movement ΔH which is elicited when we stimulate at a specific SC site, is

$$\Delta H = \beta_H + \alpha_H H_1 ,$$

Where the constant β_H gives the amplitude of the horizontal component of the elicited saccade when the eye starts from the primary position, H_1 is the initial horizontal distance of the eye from the primary position when we give the stimulation and α_H is the position sensitivity constant (Grantyn et al., 1996). The fact that the amplitude of the electrically elicited saccade depends on initial position is called position sensitivity. A similar relation holds also for the vertical dimension. The position sensitivity is different among different species, bigger in cats than in monkeys for example.

The existence of position sensitivity seems also to contradict, at first sight, with the recordings from the motor layer of the SC, where the TLLBs exhibit the same burst of activity for a fixed vector size, regardless of initial position (Hepp et al., 1993).

Position sensitivity seems to be a potential problem of our model. Our model produces stereotypical bursts at the output layer of the SC, and gives saccades with vectors independent of initial position of the eyes. In fact, as our model does not use anywhere eye position information, is in principle unable to explain position sensitivity alone.

Position sensitivity can be explained, however, with the electrical excitation of a pathway parallel to that of TLLBs. Apart from saccades, the electrical stimulation of the feline and also the monkey SC has been shown to produce slow eye movements. These slow movements have position sensitivity constant similar with the position sensitivity constant of the saccades. Fibers passing near the electrode could form the slow eye movement pathway that bypasses the TLLBs. When the electrode electrically excites both pathways, the result will be a composite movement consisting of a fixed vector saccade plus a slow eye movement that is position sensitive; the composite movement will be position sensitive. This explanation is in agreement with the common position sensitivity constant for both saccades and slow eye movements elicited at the same site (Moschovakis et al., 1998). As far as modelling the saccade producing circuits of the SC is concerned, we can thus ignore the position sensitivity, and explain it as an artefact of the electrical stimulation experiment that is due to bypassing fibers that are not part of our model.

Build-up neurons

Our model does not include the build-up neurons (in short BUNs) that have been found in the deeper layers of the SC (Sparks et al., 1976). In contrast to TLLBs, which emit discrete bursts for saccades within their movement fields, the discharge of BUNs

increases about 80 - 100 ms before the onset of the saccade, reaches a peak value that precedes saccade onset by 10 - 20 ms, and then decreases. The dynamics of the discharge of the TLLB elements of our model is determined by the strength and spatial distribution of connections established by excitatory TLLBs and their inhibitory counterparts. It is possible to change these to replicate the slow ascent and descent of the discharge pattern of BUNs. The inclusion of presaccadic cells with both fast (TLLBs) and slow (BUNs) dynamics would not affect the dynamics of saccades, which is determined by the burst generator. The inclusion of both fast TLLBs and slow BUNs could account for the large variability of intersaccadic intervals observed in the saccadic staircases evoked in response to the electrical stimulation of the SC (Grantyn et al., 1996).

Moving mountains of activity

The herein proposed model does not include mountains of activity that move over the topographic map of the SC during saccades (Fig 19). Such mountains have been thought to start from a location, which defines the desired displacement of the eyes, and to end at the rostral pole of the SC (a region which corresponds to 0^{o} saccades) (see 0, page 63). Their existence would provide the rationale for certain models of the feline gaze control system (Lefèvre and Galiana, 1992) and of the primate saccadic system (Optican, 1995). Evidence to support their existence was initially obtained from SC cells encoding gaze displacement (i.e., the sum of eye and head displacements) in alert, head free cats (Munoz et al., 1991a,b) and more recently from primate BUNs (Munoz and Wurtz, 1995).

On the other hand, there is considerable evidence to indicate that moving hills do not concern the cells that carry the output of the SC to the burst generators (the TLLBs), thus obscuring the causal relevance of such mountains of activity for saccades. Firstly, contrary to the predictions of moving mountain models, monkey presaccadic neurons remain silent during the execution of saccades that exceed their movement field (Sparks et al., 1976). More to the point, this is true of functionally and morphologically identified TLLBs (Moschovakis et al., 1988b; Anderson et al., 1998). Additionally, recording from BUNs during saccadic eye movements in monkeys revealed that the timing of their bursts as a function of their "optimal" motor error contradicts the moving hill hypothesis (Soetedjo et al., 2002).

Furthermore, the presence of moving mountains of activity in the SC has been directly disproved with the help of electrical stimulation of the OPN region (Keller and Edelman, 1994) and air puffed to the eye lid (Goosens and Van Opstal, 2000b). The procedure of OPN stimulation is known to interrupt saccades in midflight; after the end of the stimulation, saccades resume their course and acquire the target with a second saccade. This second saccade is called "resumed saccade". OPN stimulation also interrupts the discharge of tectal presaccadic cells, which emit a second burst during the residual saccades, which follow the end of the OPN stimulation (Keller and Edelman, 1994). Contrary to predictions of moving mountain models, presaccadic cells preferring small saccades are not the ones activated following the end of OPN stimulation even though the movement is well within the cells' field. Instead, it is presaccadic cells preferring large saccades that resume their spiking activity for the small second saccade despite the fact that this movement is shorter than the inner boundary of the cells' field (Keller and Edelman, 1994). The same cells resume firing after interruption of a saccade with an air puff (Goosens and Van Opstal, 2000b).

Studies in monkey with the use of the quantitative [^{14}C]-deoxyglucose functional imaging method (Moschovakis et al., 2001) give further proof for the stable hill hypothesis. The animal during the experiment executes repeatedly visually guided saccades of the same amplitude and direction. The radioactive [^{14}C]-deoxyglucose accumulates at the region with increased metabolic activity. This appears to be a well-defined circumscribed area at the two-dimensional reconstructed map of the SC contralateral to the movement. The precise rostrocaudal and mediolateral location of this area depends solely on saccade metrics. If a moving hill were the case, then the rostral pole of the superior colliculus would also be activated, and the activated area would be a strip connecting the region corresponding to saccade metrics, with the rostral pole of the superior colliculus.

All the above experiments provide unequivocal evidence, that there is no mountain of activity moving through the TLLB population during saccades. The present model does not imply any such moving mountain of activity.

Fixation cells

Our model does not include the "fixation cells" (FNs) or “Tectal pause neurons” (TPNs) (Munoz and Wurtz, 1993) of the rostral “fixation zone” of the SC, which are used by some other models of the SC (see 0, page 66).

During active fixation, when the eyes are immobile, FNs discharge tonically. Before and during the saccade, they seize firing, and they resume firing after the end of the saccade. Because these cells are known to pause for saccades, both ipsiversive and contraversive, they are also known as tectal pause neurons (TPNs; Moschovakis et al., 1996). They are called “Fixation cells” because some researchers believe that their firing during fixation keeps the eyes still by activating the OPNs (Munoz et al., 1996).

Fixation cells are located at the rostral pole of the SC, at the deep and intermediate collicular layers. They were originally described in the superior colliculus of the cat (Straschill and Hoffmann, 1970; Straschill and Schick, 1977; Harris, 1980), and later found in the monkey (Munoz and Wurtz, 1993).

TPNs are thought to be inhibitory cells and to establish connections with presaccadic neurons of the SC. Their targets in the SC are thought to be suppressed for as long as TPNs are active (i.e., in between saccades) and to be released from inhibition when TPNs become silent (i.e., during saccades). This gating mechanism has been thought to explain why electrical stimulation of the rostral pole of the SC inhibits the discharge of TLLBs and interrupts saccades in midflight (Munoz et al., 1996). Additionally, TPNs may also project to the OPN region with excitatory connections to give to OPNs their tonic discharge during fixation. These two connections inhibit the initiation of saccades, and can also stop them in midflight. In order for a saccade to be elicited, fixation cells should be inhibited. Recently, it was concluded that these cells encode the difference between desired and actual gaze position, i.e. that they participate in quite a different job than the one expected of “fixation” neurons (Bergeron and Guitton, 2000). Some models of the SC include fixation neurons as an essential part of their machinery (see 0 page 66) as the model of Lefèvre and Galiana (page 76), the model of Massone and Khoshaba (page 82) and the model of Quaia et al. (page 87).

It is doubtful that FNs gate the activity of the caudal 9/10 of the SC. Because TPNs are located in the anterolateral pole of the intermediate and deeper tectal layers (Munoz and Wurtz, 1993) and are presumed to project to the intermediate layers of the remaining

SC, biocytin injected anywhere in the SC should backlabel neurons in the rostral SC. Several hundreds of biocytin containing neurons have been recovered in the SC following tracer injections in the intermediate layers of the structure (Grantyn et al., 1997). None were recovered in the rostral SC. This casts doubt on the functional role that has been proposed for the "fixation zone" and the TPNs. All in all, there is ample evidence to suggest that gating mechanisms in the SC are better entrusted to the massive nigrotectal pathway (Hikosaka and Wurtz, 1983c; Karabelas and Moschovakis, 1985), which was incorporated in our model. In our model, the global inhibition by the element tllb is adequate to give an end to the fixed burst of activity, and the inhibition by substantia nigra, which is not temporally locked to the end of the saccade, comes after a variable time to stabilize by inhibition the TLLB layer. In this framework, the existence of FNs is not functionally or conceptually needed.

Other modalities and multi-modality neurons

Our SC model does not include neurons that respond to modalities other than the visual. Several examples of such additional cell classes can be found in the elegant studies of Stein and his colleagues (e.g., Meredith and Stein, 1985; Meredith et al., 1987; Wallace and Stein, 1994). Their inclusion would allow stimuli with the appropriate features to overpower the gating mechanisms of our model. Similarly, our model does not include cells that respond to auditory stimuli in the manner that Qv cells respond to visual ones (Jay and Sparks, 1987). Their inclusion would allow auditory cells to be connected to TLLBs, through a previously proposed neural network that remaps the head centered auditory receptive fields into retinotopic ones (Groh and Sparks, 1992). Neither does our model include machinery that would allow the SC to participate in the control of effectors other than the eyes. The SC is known to contain cells that discharge for complex orienting behaviour (Grantyn and Berthoz, 1985; Munoz et al., 1991a,b; Grantyn et al., 1993). This is particularly true of the caudal SC, which has been implicated in the control of head movements (Roucoux et al., 1980; Cowie and Robinson, 1994). The development of this part of the model will have to wait the collection of additional information about the neural elements that comprise the immediate premotoneuronal controllers of these other effectors. Finally, our model makes several assumptions about connections between tectal interneurons and their targets inside the SC. The fact that virtually nothing is known of such connections is a major problem for all models of the SC and should attract experimental attention.

Use of other burst generator models apart from MSH

To generate saccades, our model was connected to Moschovakis' MSH model of the burst generator. Interested readers are encouraged to consult the original literature for an account of the considerable evidence that supports this model (Moschovakis, 1994). Suffice it to say that this is the only model of the burst generator that places MLBs outside its feedback loop thus accounting for the fact that saccades are no longer normometric when the excitability of MLBs is affected (Scudder, 1997). Nevertheless, it would be of value to examine whether our collicular model can drive other well-accepted models of the burst generator such as Scudder's (Scudder, 1988).

Cerebellum

Needless to say, structures other than the SC are also indispensable if the burst generator is to function properly. A good case in point is the fastigial nucleus of the cerebellum, lesions of which are known to cause severe saccadic dysmetria (Robinson et

al., 1993). A model of the fastigial nucleus that accounts for such symptoms and is consistent with its physiology and projections to the burst generator has been presented (Dean, 1995). The model of Quaia, Lefèvre and Optican (see 0, page 87) also uses the fastigial nucleus, although the moving mountain it incorporates inside the fastigial nucleus has not received experimental support. It would certainly be of value to examine the performance of a burst generator simultaneously controlled by a collicular model such as ours and a model of cerebellar output such as Dean's (Dean, 1995).

Residual SC activity after saccade interruption and feedback to SC

When a saccade is interrupted by OPN stimulation or an air puff, a second saccade takes place after the perturbation is over, which drives the eyes to the point it would end, if the first saccade was not interrupted. The region, which starts to fire maximally after the perturbation is over, is the same that started to fire for the whole saccade, and not the region that corresponds to the amplitude of the residual saccade (Keller and Edelman, 1994; Goosens and Van Opstal, 2000b). This is strong evidence against the moving mountain hypothesis, as already mentioned. Additionally, the total spike count that TLLBs give during the interrupted and the residual saccade, equals the spike count that gives the whole uninterrupted saccade (Keller and Edelman, 1994; Goosens and Van Opstal, 2000b). This shows that the TLLB layer is inside a feedback (see 0, page 62); the control variable of this feedback loop could be the total spike count. Our model does not account for the residual activity, which emerges in the TLLB layer of the SC, just before the residual movement is performed. In our model, the mechanism generating the residual saccade was placed downstream of the SC, at the burst generator; as a result, the residual activity inside the SC equals the activity during the uninterrupted saccade. The residual activity of the RIN element, which decays exponentially in time, is subtracted by the LLB activity, and is responsible for the smaller metrics of the residual saccade, compared to the uninterrupted saccade. This mechanism, although it gives saccades with correct metrics, cannot explain the intracollicular residual activity after the end of the OPN stimulation or the air puff.

Because of the absence of specific biological information for a connection from the burst generator back to the SC, it was not attempted to implement this feedback here. However, a future extension of this model should also contain such a feedback to the SC. It is an interesting question, if this future model will manage to avoid the incorporation of artificial elements.

Simulated psychophysics

Main sequence

In agreement with the well-known map of the SC, activation of different Qv elements of the proposed model produces saccades of different size. Evoked saccades demonstrate a non-linear relation between the duration (S_d) and amplitude (ΔE) of the movement. Similar power functions have been observed in feline (Evinger and Fuchs, 1978), primate (van Gisbergen et al., 1981; Henn and Cohen, 1973), and human (Yarbus, 1967) saccades ranging from 0.5^o to 20^o (see 0). For example, the relationship found in primates ($S_d = 17.7 \cdot \Delta E^{0.25}$; van Gisbergen et al., 1981) is almost identical to the one that applies to the simulated saccades of Fig. 10B.

Double step saccade paradigm

The herein proposed model can account for the accuracy of saccades in double step stimulation experiments, despite the fact that it retains the vertical retinotopic organization of the SC assumed in the first and probably the best known SC model, namely the "foveation hypothesis" (Hess et al., 1946; Schiller and Koerner, 1971) (see 0, page 73). A model that retained the idea that saccades are programmed in a strictly retinotopic regime, made no use of eye position information, and was consistent with the accuracy of saccades in double step stimulation experiments was proposed in the form of the "vector subtraction hypothesis" for the SC (Moschovakis et al., 1988b; Moschovakis, 1996a,b) and the primate frontal eye fields (Goldberg and Bruce, 1990). However, the "vector subtraction hypothesis" assumes that to compute the vector of desired eye displacement (ΔE'), a neural replica of ΔE' is fed back to the SC where it is subtracted from the Re vector. To implement this process, the present model uses a biologically plausible RTLLB eye displacement feedback to push the representation of a visual target in the Pv array so as to compensate for saccades that intervene between target presentation and the execution of a saccade to it. A previous implementation of the "vector subtraction hypothesis" relied on a feedback signal proportional to the velocity of the actual eye movements (Droulez and Berthoz, 1991) (see 0, page 90). In contrast, the time course of the vector subtraction process we simulated reflects the time course of the RTLLB discharge and not that of the intervening saccades. This is consistent with the fact that the discharge of Pv cells can precede saccades by 50 ms or more (Walker et al., 1995). All in all, the present model demonstrates that it is possible to implement the "vector subtraction hypothesis" in a realistic model of the SC and that there is no need to use signals such as eye velocity or eye position to do so.

Lesion or stimulation of model elements

Single electrode stimulation

The herein described model accounts for a multitude of phenomena observed after electrical stimulation or lesion of the SC. Firstly, the present model accounts for the fact that the size of evoked saccades depends on the site stimulated and remains roughly constant despite increases of stimulation intensity and current spread further and further from the stimulating electrode. A previous model could also account for this phenomenon after assuming the existence of inhibitory connections between output neurons of the SC (van Opstal and van Gisbergen, 1989) (see 0, page 76). No justification for this assumption has been offered. In contrast, the herein proposed model relies on known properties of morphologically and functionally identified TLLBs. More specifically, it relies on the well-known existence of TLLB recurrent collaterals (Moschovakis et al., 1988b). It also relies on the excitatory influence that the latter are likely to exert on their targets as surmised from the fact that PDB axons (such as those arising from TLLBs) are known to employ glutamate as a neurotransmitter (Mooney et al., 1990; Büttner-Ennever and Horn, 1994). Finally, it relies on the herein demonstrated spatial extent of the terminal fields they distribute in the neighbourhood of the cell body they originate from (Fig 7). Consistent with previous observations (McIlwain, 1982, 1991) even low intensity stimuli engage a considerable proportion of the model's output units. Also consistent with previous observations in the cat and the monkey (e.g., Robinson, 1972; Grantyn et

al., 1996), the present model predicts that the latency of evoked saccades decreases with stimulus intensity.

Double stimulation and vector average

As shown here, the present model accounts for the fact that the size of saccades produced in response to the simultaneous electrical stimulation of two SC sites is the vector average of saccades evoked from the same sites when stimulated in isolation (Robinson, 1972). In the possibly related but less artificial phenomenon of "global effect" (see 0 page 13), the eyes of human subjects are attracted to the center of gravity of the visual stimuli they are presented with (Coren and Hoenig, 1972; Findlay, 1982). In principle, saccade vector averaging could be due to either extra-collicular or intra-collicular processes (see 0 page 68). In the extra-collicular scenario, two hills of activity build up when two SC sites are simultaneously stimulated, and flatten independently (Massone and Khoshaba, 1995). Two distinct models have been proposed that would extract the average saccade metrics from the saccade vectors that correspond to the two hills. The SC of the first one (Tweed and Villis, 1985) drives two independent burst generators through a vectorial comparator (the LLB). However, vectorial comparator models have been shown not to accord well with reality (Nichols and Sparks, 1996). The second model relies on quaternion operators to accomplish this task (Tweed and Villis, 1990), but no neural implementation of these operators has ever been elaborated.

Two of the models that invoke intra-collicular mechanisms to account for the vector averaging of evoked saccades (Fujita, 1989; van Opstal and van Gisbergen, 1989) (page 75), also predicted the presence of two separate foci of activity in the SC (corresponding to the two sites being stimulated). In contrast, a third previously proposed intra-collicular mechanism predicted that the active SC site occupies a region intermediate between the two stimulated sites (Arai et al., 1994) (see 0, page 78), due in large part to the "winner take all" combination of lateral excitatory and inhibitory connections it employed. Unfortunately, this mechanism does not work when the distance between the two stimulation sites is large; it was limited to sites corresponding to saccades that differ by less than 6 deg in the examples illustrated by Arai et al. (1994). Yet, averaging is known to occur in the monkey even when the two SC sites stimulated correspond to saccades that differ by more than 30 deg (Robinson and Fuchs, 1969). Largely due to the fact that it relies on realistic lateral excitatory connections between TLLBs, our model can account for the vector averaging of saccades even when the stimulated sites are widely separated. Our model further predicts that vector averaging is accompanied by a shift of the active SC site to a region intermediate between the two stimulated sites. Although this prediction has not been tested directly, there is some evidence to suggest that it may be true. Saccades that are executed towards positions intermediate between two simultaneously presented visual stimuli are known to be coded in the motor SC as single movements to an intermediate location (Glimcher and Sparks, 1993).

Nichols and Sparks experiment

The amplitude and direction of saccades evoked after electrical stimulation of the SC is known to depend systematically on the time that elapses from a previous visually guided saccade. Furthermore, this effect is known to decay exponentially with a time constant of about 45 ms (Nichols and Sparks, 1995). As shown here, the present model can account for such observations, after assuming that electrical stimulation of the SC

prevents the normal postsaccadic reactivation of OPNs thus disabling the active resetting mechanism of the burst generator (Fig 16).

Staircases of saccades

Furthermore, prolonged electrical stimulation of the SC is known to produce staircases of saccades (Robinson, 1972; Schiller and Stryker, 1972). Moschovakis' MSH model was the first to account for the generation of staircases of saccades over a wide range of amplitudes (Moschovakis, 1994). This was due to the resetting mechanism of that model's RINs and the assumption that continuous SC stimulation generates continuous TLLB discharge. The herein proposed model also accounts for the generation of staircases of saccades over a similarly wide range of amplitudes. However, it predicts that each saccade of the staircase is accompanied by the bursting discharge of the relevant TLLBs. The demonstration that this is not the case would refute much of our model (at least its output stage illustrated in Fig. 15).

Lesions

Despite the fact that it was not tuned to accomplish this, the present model is to our knowledge the first to account for the effects of focal SC lesions. Consistent with previous observations in the monkey, the present model predicts that lesions of a small part of the SC will lead to the generation of hypometric saccades if the inactivated region corresponds to saccades bigger than the executed one and of hypermetric saccades if the inactivated region corresponds to saccades smaller than the executed one (Lee et al., 1988). Further, our model predicts that this is due to shifts of the focus of excitation within the TLLB array so that it is pushed more rostrally (caudally) when the site of stimulation is rostral (caudal) to the site of the lesion. Whether this is the case or not, and consequently whether our model reflects reality, remains to be tested experimentally.

Comparison with other models of the SC

Classification of models

Models of the superior colliculus can be divided into categories, according to the following main characteristics:

SC outside or inside the feedback loop

When perturbed with OPN stimulation (Keller and Edelman 1994) or an air puff to the eyes (Goosens and Van Opstal 2000a) saccades are known to stop in midflight and to resume their course after the end of the perturbation. The resumed saccade brings the eye to the same position that it would have been brought if the perturbation did not stop it in midflight. This shows that saccade amplitude is controlled by a closed feedback loop.

Models placing the SC inside the local feedback loop receive a dynamic feedback during the movement, which could be a velocity or displacement signal. Examples of models that place the SC inside the feedback loop are those by Waitzman (1991), Tweed and Villis (1985 and 1990) (page 73), Lefèvre and Galiana (1992) (page 76), Arai et al. (1994) (page 78) and Moschovakis (1994) (Moschovakis, 1994).

Models placing the SC outside the local feedback loop (or open loop models for the SC) give a fixed signal to the brainstem, and place this feedback loop downstream of the SC at the burst generator. These models of the SC need a closed loop burst generator in order to give accurate perturbed movements. Examples of such models are those of Fujita (1989) (page 75), Opstal and Hepp (1995) (page 80), Massone and Khoshaba (1995)

(page 82), Krommenhoek and Wiegerinck (1998) (page 85), Quaia and Lefèvre (1998-1999) (page 87) and our model (1998) (see 0, page 59).

One of the first models to place the SC inside the local feedback loop was proposed by Waitzman et al. They recorded during the saccade from the motor cells of the SC. They found that activation is proportional to the motor error, consistent with placement of the SC inside the feedback loop controlling saccade metrics (Waitzmann et al., 1991). Later, OPN stimulation (Keller and Edelman 1994) and blink perturbation of saccades with air puff (Goosens and Van Opstal, 2000a,b) were used in order to stop saccade execution in midflight. Despite the perturbation, the eye still manages to reach its initial goal after the perturbation is over, with a resumed saccade. It was shown that superior colliculus stops firing and starts again during resumed saccade with a residual activity emerging at the same site (Keller and Edelman 1994; Goosens and Van Opstal, 2000b). These results strongly support models that place the superior colliculus inside the feedback loop. However, not enough biological evidence is available about the nature of this feedback

Our model is as mentioned before open loop for the SC, and should be extended to a closed loop model when more data is available about the nature of the feedback that reaches the SC.

Moving hill or stable hill

"Stable hill models" retain the same region of maximum excitation during the saccade (Fig. 19). This region corresponds to the desired displacement. Other researchers use the term "jumping hill" for the stable hill models, because activity seems to jump in space from the region corresponding to desired gaze displacement during the saccade, to the rostral pole of the superior colliculus when the saccade is over. Examples of stable hill models are those by Tweed and Villis (1985 and 1990) (page 73), Fujita (1989) (page 75), Arai et al. (1994) (page 78), Opstal and Hepp (1995) (page 80), Krommenhoek and Wiegerinck (1998-1999) (page 85) and our model (see 0, page 56).

In "moving hill" or "wave" models, on the contrary, the region of maximum excitation moves continuously in time and space during the saccade from the region corresponding to desired displacement towards the rostral pole of the SC (Fig.19). In every moment, the region of the SC with maximum activation codes the dynamic motor error. The dynamic motor error is the difference between the desired displacement and the amplitude of movement that has already taken place. Examples of moving hill models are those by Quaia and Lefèvre (1998-1999) (page 87) and Grossberg et al. (1997) (page 83). The model by Massone and Khoshaba (1995) (page 82) is a jumping hill model. The model by Lefèvre and Galiana (1992) (page 76) is a moving hill model, which with some simple changes at its weights can also work as a stable hill model.

The existence of moving hills of activity is still a controversial issue (page 56). Some researchers claim to see them in the cat (Munoz et al. 1991a,b) and the monkey (Munoz and Wurtz 1995), and others not to see them. It is not certain that they concern the output of the superior colliculus. Studies in the monkey with the use of functional imaging (Moschovakis et al., 2001) and recording (Sparks et al., 1976; Soetedjo et al., 2002; Anderson, 1998) show that only one hill of activity emerges during saccades, and strongly support the stable hill models, at least in the primate. Interrupting saccades by OPN stimulation during recording (Keller and Edelman 1994), showed that after saccade interruption the SC is reactivated in order to give the residual saccade. According to

moving mountain models, the activated region should correspond to the new motor error of the resumed saccade). However, the SC region that is reactivated is the same that started to fire for the whole saccade. The same result holds with the use of air puff to the eyelid as a perturbation (Goosens and Van Opstal, 2000b). These results directly disprove the spatial coding of dynamic motor error at the motor layers of the SC, which is essential to all moving hill models. We thus believe that although the simplicity of moving mountain makes them conceptionally and functionally appealing, they do not exist inside the SC.

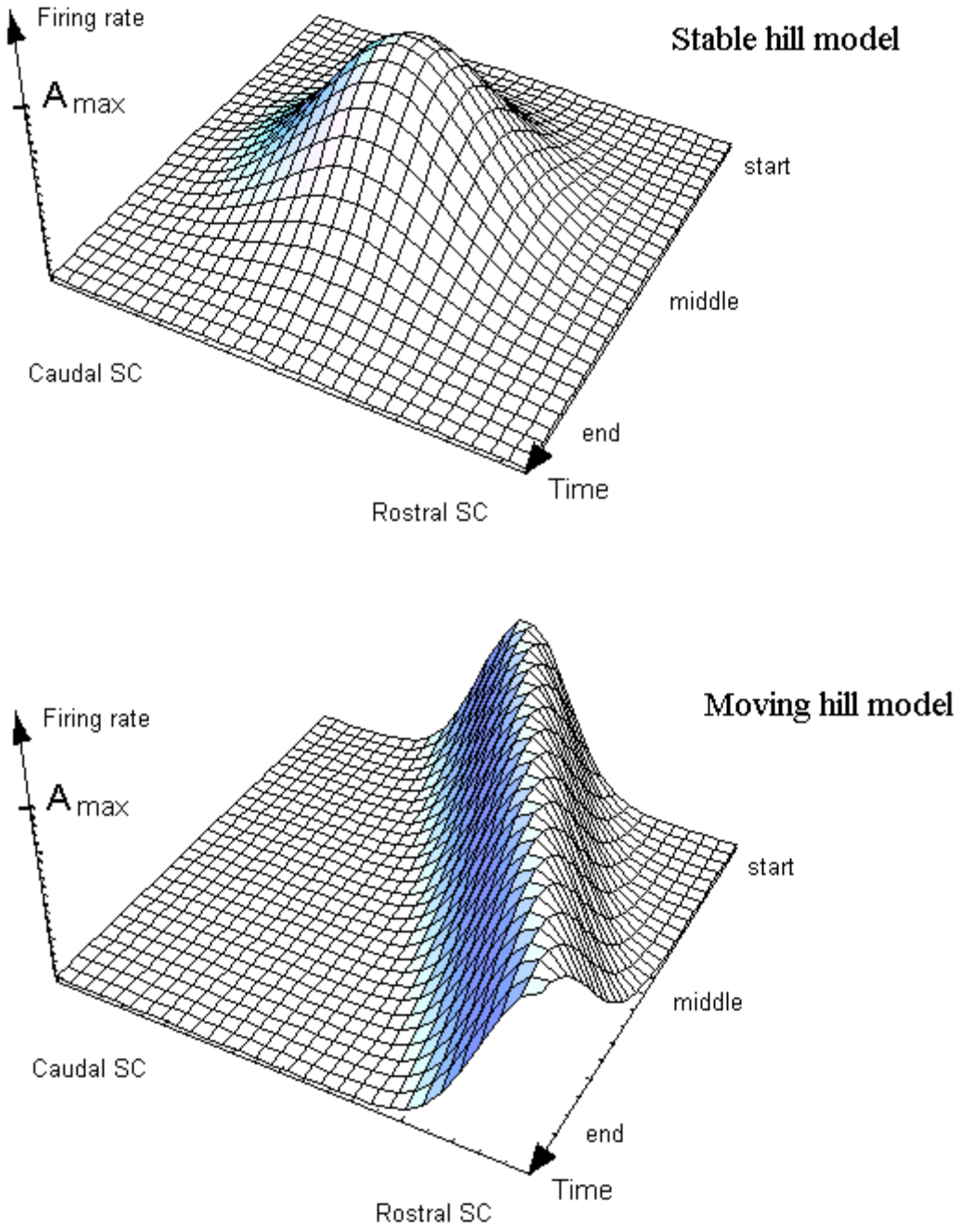

Fig. 19. Stable hill and moving hill models. In stable hill models the center of gravity of the excitation remains stable during the movement and corresponds to the metrics of the saccade. In moving hill models the excited region shifts during the movement towards the rostral pole of the SC.

Models with or without fixation cells

Moving hill models generally use fixation cells (page 57) in order to stop the saccade (Lefèvre and Galiana, 1992; Optican 1995). Stable hill models do not in general use fixation cells. An apparent exception is Lefèvre and Galiana model, which claims that it can also work as a jumping hill model and uses fixation cells, but in fact is a moving hill model. This distinction of models with or without fixation cells therefore coincides with the previous one in (B), between moving hill and stable hill models. However, in light of the new interpretation of their firing as coding the error between the desired and actual gaze positions (Bergeron and Guitton, 2000), models with a new functional role for them are expected to emerge.

Models which include fixation cells are those by Lefèvre and Galiana (1992) (page 76), Massone and Khoshaba (1995) (page 82) and Quaia et al. (1998-1999). (page 87) Models without fixation cells are those by Tweed and Villis (1985 and1990) (page 73), Arai et al. (1994) (page 78), Fujita (1989) (page 75), Van Opstal and Hepp (1995) (page 80), Groh (2001) (page 92) and Krommenhoek and Wiegerinck (1998) (page 85). Our model, as mentioned before, has no fixation cells (page 57).

One-hill or two-hill models

As was previously described, when two visual targets are simultaneously presented, then the oculomotor system responds with either a sequence of two saccades to the two targets, or with a saccade between the two targets (the weighted average response) (page 13); a similar result is obtained with the stimulation with two electrodes (page 22).

When the weighted average response takes place, two-hill models (Fig. 20) predict that two hills of activity will emerge, at the regions that would be activated when the two targets are presented separately.

Two-hill models can be further divided according to the height of their hills. The first category of two-hill models are those models, where each of the two hills of activity emerging after the presentation of two targets is identical with the single hill after presentation of one target. This kind of models assumes that the averaging takes place downstream of the SC (see 0 page 68). In the first category of models, the integral of activation over time and space when the model receives input consisting of two targets is twice the same integral when the model receives one target input. Two hill models of the first category are the models by Tweed and Villis (1985 and 1990) (page 73), Groh (2001) (page 92) and Massone and Khoshaba (1995) (page 82). The model by Tweed and Villis gives the weighted average result because the height of the mountain does not influence saccade metrics. The model by Groh (2001) gives the average result with a downstream of SC mechanism. The model by Massone and Khoshaba cannot give the weighted average result and places it outside the SC, in an undefined region.

The second category of two-hill models includes those models, where the two hills of activity have half the height of the single hill. In these models the averaging takes place inside the SC, but the activity inside the motor layer of the SC during a saccade depends also on target configuration, and not just saccade metrics. In the second category of two-hill models, the integral of activation over time and space when the model receives input consisting of two targets is the same with the integral when the model receives one target at its input. Two hill models of the second category are the Fujita m. (1989) (page 75),

the Van Opstal and Van Gisbergen m. (1989) (page 76) and the Lefèvre and Galiana m. (1992) (page 76). The Arai model (page 78) is also a two-hill model of the second category for distant targets, but for targets closely spaced is a one-hill model.

In 0 (page 68) we will discuss distinction between two-hill models in relation to the potential sites that could implement vector averaging. Figure 20 shows the different outputs that one-hill or two-hill models give when they are presented with one or two targets.

When the weighted average response takes place, one-hill models (Fig. 20) predict that the activity inside the output layer of the SC is identical to that when a one-target saccade of the same metrics is executed. In other words, the activity at the output layer is completely motor in its nature and depends solely on the metrics of the saccade that is going to be executed, and not on the context of the stimulus. The model by Krommenhoek and Wiegerinck (1998) (page 85) presents one hill of activity at the output layer when presented with two targets, but with twice the total activation that it presents with one target. The model by Arai et al (1994) (page 78) is a one-hill model when the two targets are close, and becomes two-hill for distant targets. Our model displays one hill of activity with fixed height and dynamics, even for distant targets (see Fig. 14).

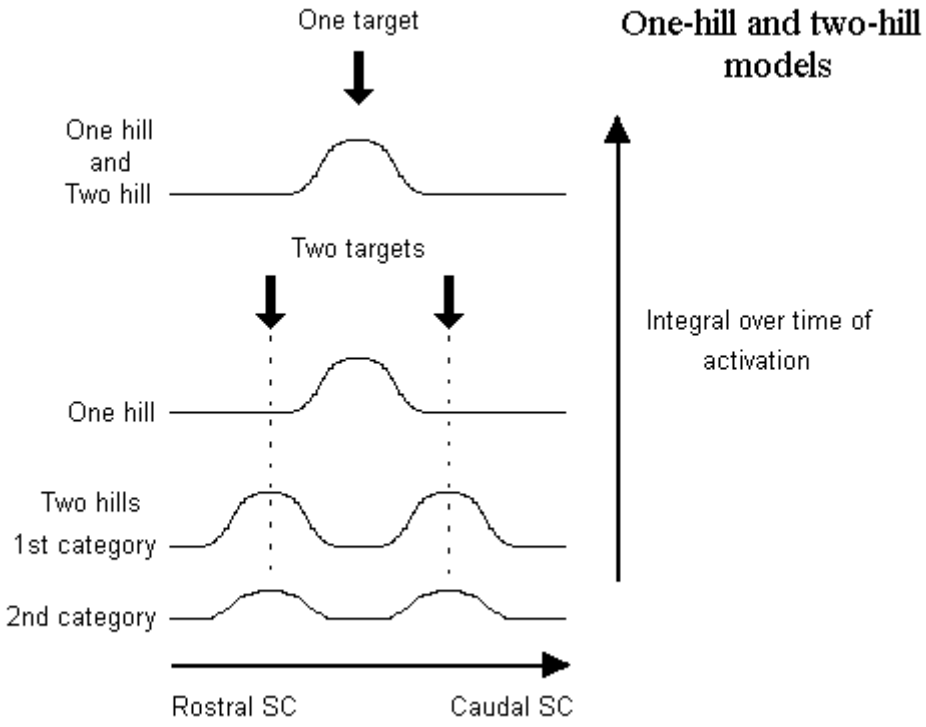

Fig. 20. Two-hill and one-hill models. All models give the same output when they execute a saccade to a single target (upper part of the figure), but give a different output (total spike count) when they are presented with two or more targets (lower part of the figure). The integral of activation is taken during the whole duration of the movement, and it corresponds to the total spike count of natural cells. Note that the area under the curve in first category, which corresponds to the integral of activation over both time and space, is double from the one target case, whereas in first category models is the same.

The empirical status of one hill and two hill models is still open. Most recordings (Glimcher and Sparks, 1993; Van Opstal et al., 1990) show one hill of activity during averaged responses. There are recordings, however, which favour the two-hill hypothesis, and more specifically the first category mentioned above (Edelman and Keller, 1998).

Intracollicular, upstream or downstream averaging

Averaging could take place inside the SC (intracollicular models), before the appropriate signal enters the SC (upstream models) and after the exit of the SC (downstream models).

In upstream models (Fig. 21), structures upstream of the SC (which could be the LIP or the FEF) make all the appropriate averaging calculations. When the animal makes an averaged response to two simultaneously presented visual stimuli, the SC receives an input identical with the one that it would receive for a target at the weighted average of the two stimuli. Inside the output layer of the SC, there is one hill of activity, which corresponds to the correct metrics of the averaged saccade. In other words, the SC activity is independent of target configuration, and depends only on saccade metrics. An upstream model is the one by Krommenhoek and Wiegerinck (1998) (page 85).

In downstream models (Fig. 21) the output of a two-hill SC model is passed through a mechanism that intervenes between the SC and the burst generator. This mechanism is termed here vector averager, and computes the vector average of the vectors that correspond to the two regions that have been activated. The models by Groh (2001) (page 92) and Tweed and Villis (1985-1990) (page 73) are downstream. In both these models the height of the mountain inside SC does not matter for saccade metrics.

In an intracollicular model (Fig. 21), two cases emerge. It may have one hill of activity, as with our model (see Fig 14), and the model by Arai et al. (1994) (page 78) when the two targets are close. Alternatively, it may display two hills of activity, scaled in such a way, that the sum of their activations equals that of one hill; this is the case for the model of Van Opstal and Van Gisbergen (1989) (page 76), Fujita (1989) (page 75). It is also the case for the model by Arai et al. (1994) (page 78) for distant targets. All these models belong to the second category of two-hill models, presented in 0 (page 66). This means that the integral over time and space of the SC activation during a single saccade (which corresponds to the total spike count of the SC output cells) remains constant, independently of the stimulus configuration (Fujita et al., 1989) (page 75), although the activity inside the SC motor layer is different in the one-target and the two-target case.

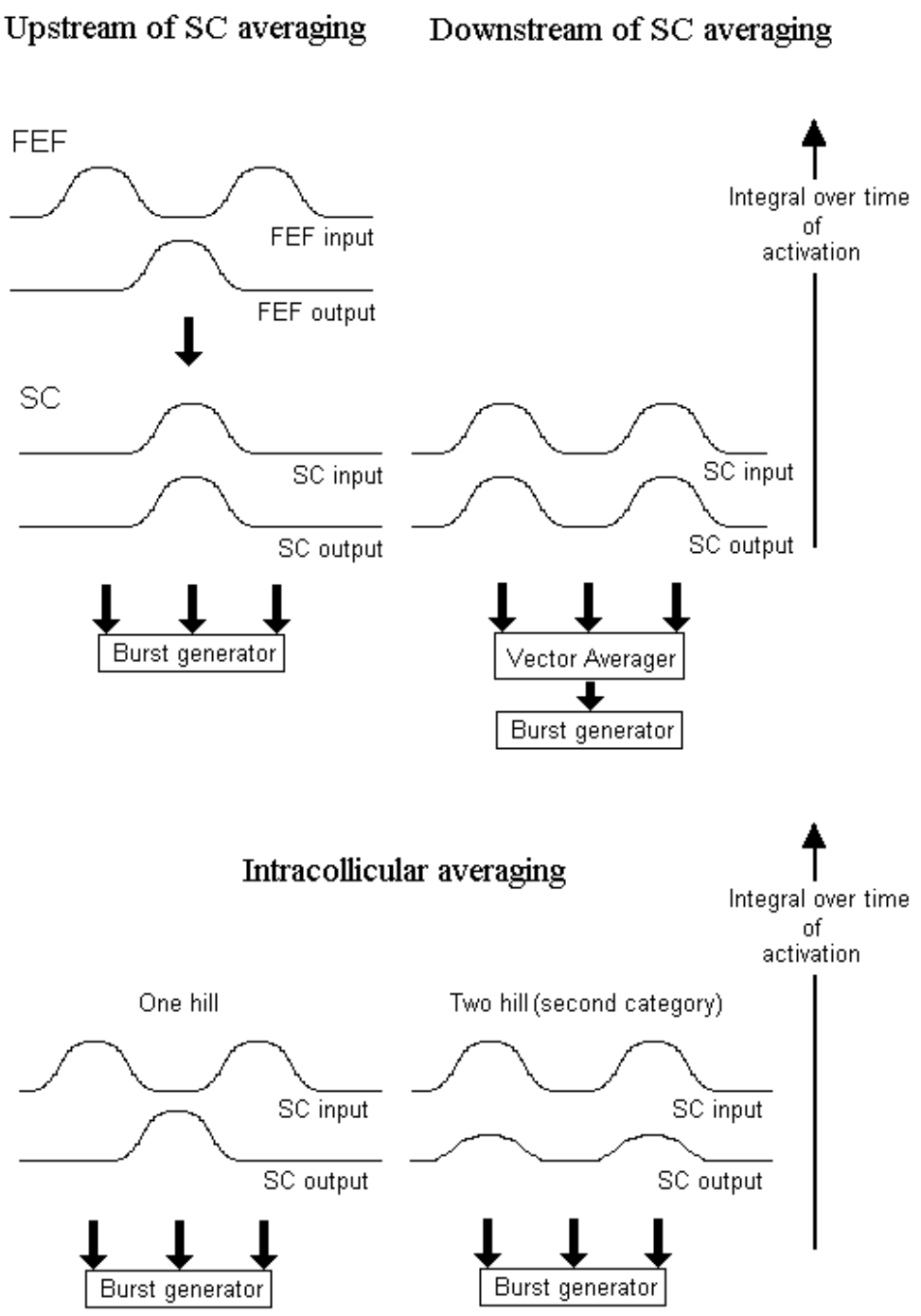

Fig. 21. Intracollicular, upstream or downstream of SC averaging. All three above models receive two simultaneous visual stimuli. The horizontal dimension at all above figures denotes the spatial extent of the SC, whereas the vertical dimension denotes the integral over time of the activation.

Upstream models cannot account for the result of simultaneous stimulation of the SC with two electrodes. Conceivably, this result could be due to involvement of the Frontal Eye Field (FEF) of the cortex, which is connected with the SC. When is stimulated with two electrodes, the signals could travel to the FEF where the mean average is calculated and coded in space code, and then sent to the burst generator. But most of FEF output passes through the SC whereas the direct projection from the FEF to the burst generator is weak, and the average that was calculated in the FEF would interfere with the two electrical signals inside the SC; this mechanism could not therefore account for normometric saccades.

On the other hand if averaging takes place downstream of the SC then, given the place coding of saccade metrics in the output layers of the SC, the amplitude of the ensuing saccade once activation emerges in the SC should be the vector average weighted by the activation in the whole output layer of the SC. This means that we should count the spike count of every TLLB cell, multiply this with its optimal vector, add for all TLLB cells and divide by the total spike count in order to get the vector average. In other words, at the level of the output layer of the SC the amplitude of the saccade is the vector average of the preferred directions of all TLLBs, weighted by their total spike counts and divided by the total spike count of the whole TLLB layer. On the other hand, in both upstream and downstream models, the vector sum of all preferred direction vectors of activated cells weighted by their spike counts gives the saccade amplitude. In this case, we do not need to divide the amplitude of the ensuing vector by the total spike count in order to get the saccade amplitude. This is called the ensemble coding for the output of the SC (Mc Ilwain 1976,1982; Sparks et al., 1976). Our model belongs to this later category.

The vector average coding hypothesis fails to explain the results of saccade perturbations. After OPN stimulation (Keller and Edelman 1994) and blink perturbation of saccades with air puff (Goosens and Van Opstal, 2000a,b), activation reappears at the same site that was originally activated, but the resumed saccade is smaller in amplitude than the whole unperturbed saccade, despite the fact that in both the unperturbed and the resumed saccade the vector average of the TLLB layer is the same. This dissociation between vector average of the TLLB layer and the metrics of the ensuing saccade is strong evidence against the vector average coding at the exit of the SC and in favour of the vector sum coding, and thus against the downstream averaging and in favour of the intracollicular and upstream averaging models. Taken together with the problems of upstream averaging exposed above, experimental data seem to favour intracollicular averaging.

Two-dimensional or three-dimensional SC output

Listing's Law has important implications for all models of eye movement control. In fact it states that a two dimensional motor command has all the necessary information to direct the eye to the appropriate target. But how is Listing's Law implemented in the oculomotor system? In other words, how does a torsion signal, appropriate for the horizontal and vertical position of the eye (Listing's Law) appear at the eye?

One hypothesis states that Listing's Law is due to the computation of the appropriate torsion by a mechanism called "Listing operator", which may use as an input the desired

horizontal and vertical eye position. The horizontal and vertical motor error is not an adequate signal for the Listing operator. This Listing operator could lie upstream, inside or downstream of the superior colliculus. In the first two cases, the exit of the superior colliculus would be a three-dimensional motor command. The most important model with a three-dimensional exit of the SC is the model by Tweed and Villis (1985 and 1990) (page 73). Another model presented below which is able to give a three-dimensional SC output is that by Opstal and Hepp (1995) (page 80). However, experimental evidence so far favours the hypothesis that the motor command, which exits the superior colliculus to enter the brainstem burst generator, is two-dimensional. This two-dimensional motor command specifies horizontal and vertical displacement alone, and not torsion. These facts argue against the quaternion model of the superior colliculus, where the exit of the SC specifies torsion, and all models with a three-dimensional output that it motivated.

Another hypothesis states that Listing's Law is a consequence of the mechanical properties of the eyes, and a Listing operator does not exist.

The question of whether and where a Listing operator exists still remains open. In our model we do not deal with the problem of torsion. We accept that the superior colliculus issues a two dimensional motor command, and torsion is specified somewhere downstream of the SC, possibly by a Listing's operator.

Examples of models

The models presented here are attempts to explain a large set of experimental results. As a consequence, it is hard to present them in brief, and even less judge them objectively. In order to make their presentation easier for the reader, some symbols have been changed and the structure of the models outside the SC simplified. The figures have been modified from the original presentations, in order to use unified symbolism. Black and gray arrows denote excitatory and inhibitory connections respectively. Rounded squares denote units that belong to a layer; orthogonals denote lumped elements or bigger structures. Circles denote summing junctions, which do not obligatorily exist as neural elements, but are included by the authors for a clearer presentation of the model's function.

The table of model classification in next page gives in summary the basic characteristics of the models that are presented below. The "X" denotes which are their characteristics. The symbol ± shows characteristics that are not clear or certain. Our model is placed for comparison at the last row.

	SC outside loop	SC inside loop	Moving hill	Stable hill	With fixation cells	No fixation cells	Two hill 1st category	Two hill 2nd category	One hill	No averaging	Upstream averaging	Downstream averaging	Intracollicular averaging	3D SC output	2D SC output
Foveation hypothesis (1946)	X			X		X	X			X					X
Tweed and Villis (1985, 1990)		X		X		X	X					X		X	
Fujita (1989)	X			X		X	X						X		X
Van Opstal and Van Gisbergen (1989)	X			X		X		X					X		X
Lefèvre and Galiana (1992)		X	X		X			X		X					X
Arai et al. (1994)		X		X		X		X	X				X		X
Van Opstal and Hepp (1995)	X			X		X	X			X				X	
Massone and Khoshaba (1995)	X		X				X			X					X
Grossberg et al. (1997)	X		X			X	±			X					X
Krommenhoek and Wiegerinck (1998)	X			X		X			±		±				X
Quaia et al. (1998, 1999)	X		X		X		X			X					X
Droulez and Berthoz (1991)										X					X
Groh (2001)	X			X			X					X			X
OUR MODEL	X			X		X			X				X		X

Foveation Hypothesis, 1946

Hess W.R., Burgi S. and Bucher V. proposed this model in 1946, in the article "Motorische Funktion des Tectal- und Tegmentalgebietes."

General features and description

The "foveation hypothesis" was based on the simple assumption that the superficial cells of the SC excite those presaccadic neurons that are located underneath them. The superficial layers of the SC receive their input from the retina. Because the motor map of the deeper tectal presaccadic cells is in register with the visual map of the superficial tectal layers, neurons with the appropriate movement fields will be activated so that the eye is accurately displaced.

Evaluation

The foveation hypothesis is simple, and furthermore it explains the correspondence of the visual fields of the superficial layers and motor fields of the deep collicular layers. The proximity and correspondence of sensory and motor structures in the SC is more evident than in any other place in the brain, and an effort to explain it is reasonable. The foveation hypothesis also accepts that the SC receives a retinal error input, and does not make use of more artificial signals at the input of the SC, as the position of the target in craniotopic coordinates used in the Krommenhoek and Wiegerinck model of the SC (page 85).

The major shortcoming of foveation hypothesis (discussed in Moschovakis et al., 1996) was the fact that foveating saccades cannot be accurate in double step stimulation experiments. If the only input received by the motor cells of the deep layers of the SC were visual, then the vector of the saccade to the second target would be equal to the retinal error at the moment of target presentation. The model by Droulez and Berthoz (page 90) and also our model for the input layers of the SC can complement the foveation hypothesis and give correct metrics for the second saccade. In our model, the additional mechanism (incorporating the predictive visual PV cells) intervenes between the visual cells V and the quasivisual cells, and corrects target representation after every eye movement, in order to keep all targets coded in retinotopic coordinates. The same is achieved by Droulez and Berthoz model, outside the SC.

Tweed and Villis, 1985, 1990

This model was presented in the article "The superior colliculus and spatiotemporal translation in the saccadic system" (Tweed D. and Villis T., 1990). An older article by the same authors with the title "A two-dimensional model for saccade generation" (Tweed D. and Villis T., 1985) presented a "vectorial" model, which evolved to the quaternion model in 1990.

General features

This model places the SC inside a feedback loop (page 62). It produces a spatially stable hill (page 63) of activity whose height increases together with the strength of the electrical stimulation. It is a downstream, two-hill model of the first category (page 66) and makes no use of fixation cells (page 66).

The most remarkable feature of this model is the three-dimensional output of the SC and the use of quaternion operators inside the SC. The exact manner that quaternions are encoded with the use of firing rates by natural neurons is not specified. Quaternions are mathematical entities invented by W.R. Hamilton in 1843 (For a concise description, see Birkhoff and McLane, 1962). Quaternions constitute a four-dimensional vector space over the field of real numbers, with a basis of four special vectors denoted by 1, i, j and k. A quaternion q is a vector, which can be written as

$$q = q_0 + q_1\, i + q_2\, j + q_3\, k,$$

Where q_0, q_1, q_2 and q_3 are real numbers. The set of quaternions is equipped with the usual operations of vector addition and scalar multiplication, plus the new operation of quaternion multiplication. The real parts are multiplied with the use of ordinary real number multiplication, and the vectors i, j and k are multiplied with the following rules:

$$i^2 = j^2 = k^2 = -1$$

$$ij = -ji = k, \quad jk = -kj = i, \quad ki = -ik = j$$

For every quaternion q, the vector of the quaternion q is defined as the quaternion if we set $q_0 = 0$. The norm, or magnitude of a quaternion |q|, is defined as

$$|q| = (q_0^2 + q_1^2 + q_2^2 + q_3^2)^{1/2}.$$

Every quaternion can be written in the form

$q = |q| (\cos\theta + n_1 i \sin\theta + n_2 j \sin\theta + n_3 k \sin\theta)$, where (n_1,n_2,n_3) is a unit vector and θ is the angle of the quaternion. It is proved that if r is the axis of the eye at a given time, then the operator $q ( ) q^{-1}$ applied to vector r gives the vector obtained by rotating r about an axis parallel with q, through twice the angle θ of q.

Every unit of the motor layer codes for a specific quaternion q, and when stimulated it produces a movement with amplitude 2 θ around the direction of q. The norm |q| of the quaternion q does not influence saccade metrics.

Description

Every region of the SC codes for a specific eye rotation, and in particular the unit quaternion r* representing that rotation. Each output unit, when activated, provides the brainstem oculomotor circuit a signal that is composed of the four real components r_0^*, r_1^*, r_2^* and r_3^* of a quaternion error signal E. The brainstem feeds back to the SC a quaternion signal r, the quaternion that corresponds to the displacement so far in the saccade. The quaternion r* is multiplied by r^{-1} in order to give the error signal E. The saccade stops when the error quaternion E equals 1, which is the quaternion representing no displacement The result is a movement which turns the axis of the eyes for an angle 2 θ around the direction of r*.

The quaternion model gives the result of constant size with stimulation with increasing intensities, and the weighted average result. The underlying reason for both of them is that all nonzero scalar multiples of a quaternion q represent the same rotation. When one stimulates with increasing frequencies f_1, f_2, f_3 where $f_1<f_2<f_3$, he still gets the same rotation that corresponds to the quaternion f_1 q, f_2 q or f_3 q. Whenever one stimulates with increasing intensity, he gets more units working, but the result is again the scalar multiplication of the quaternion q by the number of units, which leaves unchanged the rotation that the quaternion q codes.

The weighted average result is extracted as follows: When one stimulates simultaneously two sites coding for quaternions p and r with frequencies f and g respectively, he gets a summated input to the comparator that is equal to

$$f p^* + g r^*.$$

Since every scalar multiple of a quaternion represents the same rotation, the quaternions

$$f p^* + g r^*$$

and

$$(f p^* + g r^*)/(f+g)$$

code for the same rotation. The last quaternion is the weighted average of p* and r*.

Evaluation

The quaternion model has an advantage on the control of three-dimensional eye movements. Although eye movements are associative, they are not commutative. The order we perform eye movements determines the final position of the eye and its torsion. The quaternion model gives an accurate mathematical explanation for this phenomenon. It also gives the weighted average result and the constancy of size result in stimulation with increasing intensities.

However, neither the electrical stimulation data (Van Opstal et al., 1991) nor the recordings (Hepp et al., 1993) seem to support a 3-D output for the SC implementing the Quaternion model and favour more a 2-D output of the SC. The electrical stimulation of the SC elicited two-dimensional saccades with no torsional component, rather than three-dimensional saccades with variable torsional component as the quaternion model predicts. The quaternion model could be very useful for the neural integrator that keeps the eye fixed in position after saccades, but it seems that at the level of the SC the only information available is a two-dimensional representation of desired eye displacement.

In addition, no proof for the ability of biological neurons to perform quaternion operations has been found, neither signals in the SC that could be interpreted as the real components of quaternions. The complexity of this model makes hard the search for such signals. Our model can extract both the result of constant size with stimulation with increasing intensities, and the weighted average result with a simpler and more biologically motivated mechanism.

Finally, it has the problems of downstream models (see 0 page 68).

Fujita M., 1989

Fujita M. presented this model in 1989, included in the publication "Neural programming" (Fujita M., 1989).

General features and description

This is a stable hill (page 63) model that places the SC outside the feedback loop (page 62) and does not use fixation cells (page 66). It is also an intracollicular averaging model (page 68) and a two-hill model of the second category (page 66). It obtains the weighted average result with a simple mechanism that relies on lateral inhibitory interactions. The motor layer of the SC contains a two dimensional map of targets. Every motor unit inhibits through activation of inhibitory units all other motor units, with the same strength (weight). When the model is presented with two stimuli simultaneously, then the two areas that correspond to the retinal error of the two targets are simultaneously activated and appear as two competing hills of activity. Due to lateral inhibitory interactions, every hill of activity inhibits the other, and the result is that each hill has half the height that it would have had only one of the targets been present when we present to it one target. If three targets are present, each hill would have one third of the height that it would have if only one target were present; and so on with multiple targets. The total activity at the exit of the SC is the same in all cases, due to the lateral inhibitory interactions between SC subregions.

Evaluation

This model can give a weighted average result at the exit of the SC with a simple intracollicular mechanism. This exit is however static and not dynamic, as the model does not deal with dynamics. When the model is presented with two stimuli simultaneously, it gives two hills of activity, which have half of the height that a single hill of activity would have. This model belongs thus to the second category of two-hill models. However, evidence supporting the two-hill hypothesis is in favor of the first

category of one-hill models, i.e. the height of the hills is the same regardless of their number (Edelman and Keller, 1998).

Van Opstal A.J. and Van Gisbergen J.A.M., 1989

This model was presented by Van Opstal A.J. and Van Gisbergen J.A.M. (1989), in the article "A Non-linear model for Collicular spatial Interactions Underlying the Metrical Properties of Electrically Elicited Saccades", almost at the same time as that of Fujita (see 0).

General features and description

This model obtains the weighted average result in the same manner as that of Fujita model. It uses the same uniform inhibition from every motor unit to all others. In addition, it uses a more precise non-linear motor map of the SC.

Evaluation

All arguments concerning the model of Fujita apply here as well.

Lefèvre P. and Galiana H. L., 1992

This model was presented by Philippe Lefèvre and Henrietta L. Galiana (1992), in the article "Dynamic Feedback to the superior colliculus in a neural network model of the gaze control system."

General features

This is a two-hill model (page 66) of the output layer of the superior colliculus. It places the output layer of the superior colliculus inside a closed feedback loop (page 62), and the two-dimensional output signal of the SC specifies the vector of desired gaze displacement. It incorporates fixation cells at the rostral pole of the superior colliculus (page 66), in order to stop the saccade. Interestingly, it is able to give results simulating both the stable hill and the moving hill hypothesis, by manipulating its variables (page 63). Therefore, it attempts to show that there is in fact a continuum between these apparently contradictory modes of functioning.

Description

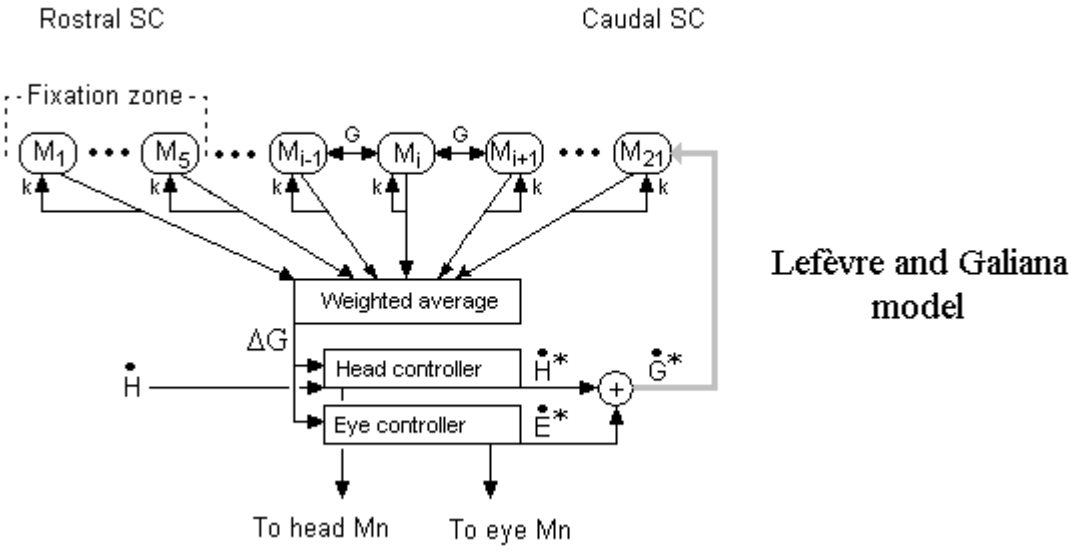

Fig. 22 Lefèvre and Galiana model.

The superior colliculus output units form a one-dimensional array of 21 M (motor) units (Fig. 22). The M units have a time constant equal to 3ms, like many biological

cells. Additionally, each unit receives an excitatory input G from its immediate neighbours. All this connectivity gives to the whole layer a time constant equal to 1 sec (short term memory). The superior colliculus output units project to downstream structures with a spatial gradient of weights. This is common to most superior colliculus models, in order to accomplish the spatiotemporal transformation, and easy to implement.

The variable, which is coded at the output layer of the superior colliculus, is the desired gaze displacement ΔG. A signal of dynamic motor error (or gaze error) E is fed from the output layer of the superior colliculus to an eye-head controller, which drives the eye and head motoneurons. The head controller receives also as an input the actual head velocity $\dot{H}$. The eye-head controller adds the separate signals of eye velocity $\dot{E}^*$ and head velocity $\dot{H}^*$ and feeds back to the output layer of the superior colliculus an efference copy of gaze velocity $\dot{G}^*$, which is integrated and subtracted from ΔG, in order to give the dynamic motor error E (Lefèvre et al., 1992, fig. 1C and fig. 2). The signal $\dot{G}^*$ is fed back with a negative weight to the 21st unit, which corresponds to the more caudal region of the superior colliculus. This gaze velocity signal $\dot{G}^*$ could originate from perihypoglossal nuclei, which carry a mixture of eye velocity, head velocity and eye position signals and project to the contralateral SC.

A switch is also included, which mimics the function of fixation cells. When the activity reaches the 5th unit, the activation of all units is set to zero. This switch-mechanism, in co-operation with the feedback to the 21st unit, put an end to the activity inside the layer.

The localised feedback of $\dot{G}^*$ to the caudal unit 21 and the internal dynamics of the interconnected output layer, causes the center of the active population to move toward the rostral pole of the SC during the saccade, giving a moving hill of excitation, despite the symmetrical connections inside the layer. This moving hill will stop the saccade, as soon as it reaches the rostral pole of the SC and excites the fixation units, which lie there.

Evaluation

One interesting feature of this model is the involvement of an inverse temporal-spatial transformation, which is required in order to translate the efference copy of gaze velocity $\dot{G}^*$, coded in the temporal domain, to a signal appropriate for the spatial coding of ΔG in the superior colliculus output layer. The model claims that it achieves this transformation by appropriately manipulating the feedback to the 21st unit. However, from the data presented, it seems more probable that the excitation of the 5th unit terminates the saccade and achieves fixation, rather than the feedback towards the 21st unit. Furthermore, as this feedback reaches only the caudal 21st unit, makes it a strong anatomical prediction (feedback fibers contacting selectively the caudal SC), which has not been confirmed.

Another interesting claim is that by increasing the strength of the connection between neighbouring units in the foveal region, i.e. between the units 4,5 and 6, this model can give a response that looks like a jumping hill. At the beginning of the saccade, a hill of activity emerges at the area corresponding to saccade metrics, and near its end activity gradually increases at the foveal region, and puts an end to the saccade. In fact, the only thing that changes at the transition from the moving hill to the jumping hill, is that the hill (which travels from the initially activated area towards the fixation units of the rostral pole) is lowered, whereas the final activation of the fixation units of the rostral pole, at the end of the saccade, is increased. Therefore, from a functional point of view, this is a moving hill model, which can simulate a jumping hill model.

When presented with two visual stimuli, the model does not give a weighted average result intracollicularly, although the center of gravity of the activation codes the residual motor error and can thus be the appropriate signal for a downstream of SC averaging mechanism. The sum of the collicular activity does not give the weighted average result, and a downstream averaging mechanism is still needed. The downstream model, however, has the problems, which were exposed at the general presentation of SC models.

Arai K., Keller E.L., Edelman J.A., 1994

This model was presented in the article "Two dimensional neural network model of the primate saccadic system" (Arai K, Keller EL, Edelman JA 1994).

General features

This intracollicular model (page 68) places the SC inside a feedback loop. It produces a stable hill (page 63) of activity and contains no fixation cells (page 66). It is a two-hill model of the second category (page 66), but when it gets as an input two targets close enough, it gives as an output one hill of activity.

The Arai et al. model uses an interconnected layer of motor units with both excitatory and inhibitory connections, and a visual layer, which gives input to the motor layer (Fig. 23). It also uses a burst generator in order to feed a first order model of the eye with the appropriate signals for accurate saccades. The weights of the connections inside the motor layer are controlled by local shunting inhibition from the substantia nigra. The SC is inside the dynamic local feedback loop. The eye position and eye velocity signals were shown to be effective candidates for this feedback.

Description

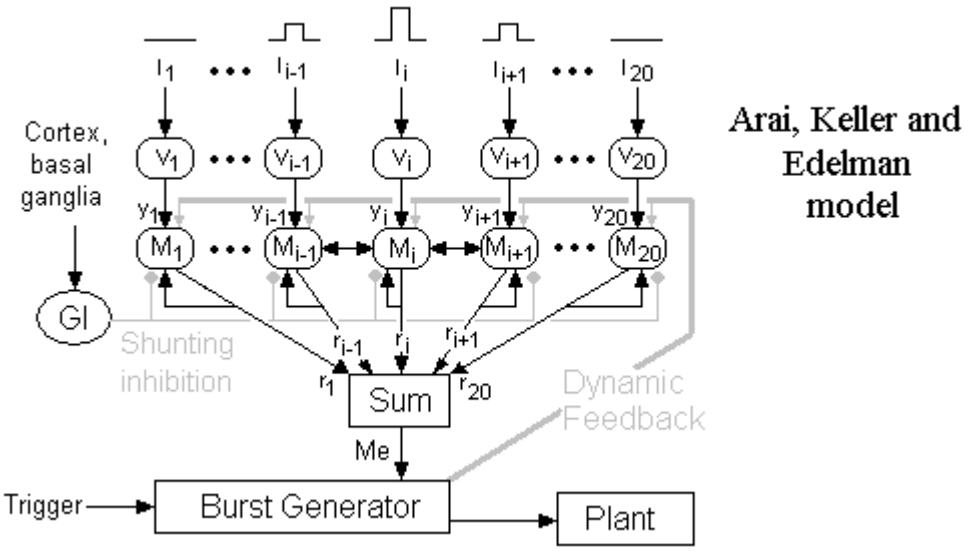

Fig. 23. Arai, Keller and Edelman model. Black and gray connections are excitatory and inhibitory respectively. The gray circular connections represent global inhibition. The visual input is represented by I_1-I_{20}. GI: global inhibition, Me: motor error. M: motor cells, V: visual cells, Sum: a summing junction.

The model has two layers of SC units, the visual and the motor layer (Arai et al., 1994, Fig 2). Each layer consists of 400 units, arranged in a two dimensional grid with an edge equal to 20 units. In the motor layer, one edge represents the amplitude and the other the direction of the saccade. The mapping is non-linear, based on the motor map constructed by Robinson with electrical stimulation (Robinson, 1972). Units in the visual layer (labelled V_i) connect in a one-to-one fashion with weights w_i to the units

M_i of the motor layer. The motor layer connects with weights r_i to the brainstem burst generator. Every visual unit V_i connects only to the motor unit exactly beneath it. Motor units M_i are interconnected by lateral connections w_{ij}, both excitatory and inhibitory. Higher brain centers including cortex and basal ganglia and in particular substantia nigra exert global shunting inhibition to the motor layer. This shunting inhibition controls the dynamics of the motor layer, and does not allow it to give movements to uninteresting stimuli, by controlling the strength of self-excitation weights w_{ii}. If GI(t) is this global inhibition as a function of time, then the strength of the self-excitatory weight w_{ii} is given by the formula:

$w_{ii} = w0_{ii} / [1 + GI(t)]$, where $w0_{ii}$ is the constant self-excitatory weight when the unit M_i is not inhibited by the substantia nigra.

The weights r_i to the brainstem burst generator and the interconnections between the units of the motor layer were found with a back propagation learning algorithm, in order to give saccade metrics corresponding to the position of the unit inside the map. In order to avoid border effects, only saccades small in amplitude were used for the back propagation. After learning, weights inside motor layer turned to be excitatory for units with distance 4 units or less, negative for units with distance ranging from 6 to 10 units, and zero for units with bigger distance.

The feedback signal comes from the burst generator and is directed towards the motor layer. The dynamic feedback signal could be either an efferent copy of eye position or eye velocity. The model could be trained to produce realistic discharge profiles for collicular motor layer and accurate saccades with either of these signals.

The activation functions of the motor layer are realistic. In particular, the short-term memory due to the shunting inhibition mimics effectively the initial visual response of the motor units. One small hill of activity emerges at one site of the SC after the presentation of the visual target, and decays with time. This is the initial visual response. Shunting inhibition also permits the motor layer to function as a short-term memory. When the substantia nigra, ordered by higher brain structures, decides to permit a saccade to take place, it releases the SC motor layer from shunting inhibition.

When the shunting inhibition is removed, the system acts as a modified winner-take-all network. The increase of local excitatory weights results in an active buildup of activation at the site were shunting inhibition was removed. This site is associated with a previously presented target. The output of the motor layer is fed to the burst generator, and moves the eyes. The inhibitory feedback signal from the burst generator finally drives the motor layer back to zero activation. The releases of the SC motor layer from shunting inhibition may happen after a variable time interval, because the initial visual response remains above zero for long. The model can thus perform accurate delayed saccades even after many hundreds of milliseconds after the visual stimulus is over. The presence at the motor layer of the visual response is interesting. This is because most cells of the SC have a mixed visual and motor response, forming a continuum from superficial layers (pure visual responses) to deeper layers (weaker visual and stronger motor response). This continuum was described in the paragraph about the responses of L-cells.

The model is also able to produce one hill of activity, when simultaneously presented with two closely spaced visual stimuli, and give an averaged saccade (Arai et al. 1994, Figure 11).

Evaluation

This model has many common features with our model. It relies on excitatory collaterals and to intracollicular inhibition to build up the burst of activity. A difference of this model with ours is that it places the SC inside the feedback loop; we believe this placing is in the right direction, and as was mentioned in discussion we should find a good way to modify our model similarly. Another good point of this model which could and possibly should be incorporated to future models of the TLLB layer is the global shunting inhibition from the substantia nigra, which gives a simple explanation for the presaccadic activity of TLLBs and the mixed visual and movement responses of collicular neurons.

The Arai et al. m. is not a clear one-hill model. When presented with two targets closely spaced, it gives one hill of activity; but when the two targets are at a bigger distance, then two hills of activity emerge with half the height of the single hill (second category of two hill models). However, the only experimental evidence in support of two hill models favours the first category of two hill models (Edelman and Keller, 1998). In comparison, our model manages to give one hill of activity even for widely separated targets. This is due to the global inhibition that we used, and the realistic bi-lobal excitatory connections inside the TLLB layer. In Arai model every output unit inhibits only units with distance from 6 to 10 units and excites units with distance 4 or less; therefore, when two targets are presented with big distance, they do not inhibit each other and two independent mountains of activity emerge.

Van Opstal A.J., Hepp K., 1995

This model was presented in the article “A novel interpretation for the collicular role in saccade generation” (Van Opstal A.J., Hepp K., 1995).

General features

The creators of this model are mostly interested in how the known output from the Superior Colliculus may be used downstream of the Superior Colliculus (page 68) to generate eye movement signals in either two or three dimensions (page 70). These signals could be the classical "eye position", the currently more acceptable "desired eye displacement" or the three-dimensional ocular rotation vector for saccades in Listing's plane. It is a stable hill model (page 63) that places the SC outside the feedback loop (page 62) and does not use fixation cells (page 66). The authors do not deal with averaging and two-point stimulation.

Description

According to data collected by these researchers (Van Opstal et al., 1995) there is eye position information at the output layer of the SC, in the form of "gain fields", similar to that encountered in Posterior Parietal Cortex (Andersen '85 Science 230) and area LIP (Andersen '90). These gain fields will modify the output of SC for a given fixed vector saccade, depending on the initial position of the eye in the orbit. The modification is seen at the mean firing rate of a specific neuron, which, for the same eye displacement, varies as a function of initial eye position. A good fit was given with the use of the following formula:

$$F(M, E_0) \sim [F_0 + e_0 \bullet E_0] \bullet G [(M-M_0), s_0],$$

All bold symbols in the above formula are vectors, and the dots represent the inner product between vectors. F is the mean firing rate of one cell during a saccade, which is expressed as a function of the displacement vector of this saccade M and the initial position of the eye E_0. M_0 is the optimal saccade size for this cell. F_0 is the peak-firing rate of the cell for optimal saccades. G is a two dimensional gaussian, centered at the optimal motor vector M_0 with width s_0. The eye position sensitivity (or modulation) vector e_0 has the direction where maximum increase of firing as a function of position

emerges, and its amplitude is proportional to this increase. The vectors e_0 were found to have a uniform distribution towards all directions, in all regions of the superior colliculus.

In order to give these gain fields at its output, the SC needs an eye position input. This input could originate from the contralateral nucleus prepositus hypoglossi (NPH) and from the medial portion of the vestibular nuclei, as retrograde studies indicate (Hartwich-Young et al 1990). Both of these nuclei are probably involved in the extraction of an eye position signal by the integration of eye velocity related inputs (Cannon and Robinson 1987, Cheron et all 1986).

The SC is represented by a two dimensional map. Each area in the map contains EM (EM =9 usually) units and corresponds to a fixed vector movement, i.e. its units fire mostly for a saccade of a fixed horizontal and vertical component. The eye position modulation vectors e_0 of the single units (Van Opstal and Hepp, 1995) are randomly varied within each area. The SC output thus contains enough information in principle to exert an eye position dependent influence on the Burst Generator circuitry of the Brainstem.

All units of the SC project linearly to six output units, representing the horizontal and vertical components of the three vectors M, E and H=M+E, where M is the motor displacement, E is the eye position and H is the desired eye position in head-centered coordinates. All units of the SC also project to three additional units corresponding to the torsional, horizontal and vertical coordinates of the 3D ocular rotation axis q=(qx, qy, qz). Except for these feedforward connections originating form the output layer of SC, there are no other connections in this model. The weights of these connections were initially set randomly. By the use of the Widrow-Hoff learning rule, the weights at the output of SC were modified to give successfully all the desired outputs. Learning was accomplished successfully with the addition of noise, and the model was also shown to operate successfully with only slight increase of mean error after lesions followed by additional learning epochs. The authors seem not to favour any single output signal, and furthermore they claim that an "Eye Position" and an "Eye Displacement" comparator could feed the Pulse Generator in parallel, if they are fed back with the appropriate "current eye position" and "current eye displacement" signals, respectively.

Evaluation

This model takes advantage of the diversity of responses encountered in output neurons of the SC, and shows that this diversity and the existence of gain fields makes a 3-D signal extractable. Neither the electrical stimulation data nor the recordings (Hepp et al., 1993) collected by the same researchers seem to support a 3-D output for the SC implementing the Quaternion model (Van Opstal et al., 1991) and favour more a 2-D output of the SC (see 0, page 70). The gain fields that the same authors claim to see are very weak: the differences in the peak firing rate are slightly visible only with initial eye position varying between the four visual quadrants, and the variability they observe obscures the result (Van Opstal and Hepp, 1995). The present model still makes an interesting theoretically point, namely that the appropriate signal for a neural implementation of Listing's Law could in principle be extracted from the output layer of SC, if we admit that they display eye position gain fields.

The notion of a 3-D SC could survive Van Opstal's electrical stimulation data by admitting that when we stimulate the SC, we stimulate simultaneously both the desired eye displacement input to the output layer, and at the same time the position input to the output layer. However, the recordings from single neurons in SC, which show them not to be influenced by initial eye rotation seems to be a serious obstacle for the quaternion model.

Massone L.L.E., Khoshaba T., 1995

This model appeared in an article by Massone L.L.E. and Khoshaba T. entitled "Local dynamic interactions in the collicular motor map: a neural network model", in 1995.

General Features

The motivation of this work was to explore if a model of the SC could be constructed, which places the SC outside the feedback loop (page 62) and incorporates fixation cells. This model of the SC displays a jumping hill (page 63) of activity during saccades, and two hills of activity when stimulated by two targets simultaneously (page 66). The learning algorithm of recurrent back propagation was used, and the network was trained in order to present an activity, which ends with the activation of the fixation zone. The authors do not deal with averaging, and even conclude on the basis of their results that this must take place outside the SC.

Description

The SC was represented as a two dimensional layer consisting of 25x25 units. This layer contains an area with 5x5 units, which is called fixation pool. This area represents the fixation zone at the rostral pole of the SC. The remaining units belong to the movement pool. Every unit connects to its neighbouring units with bidirectional connections and with a recurrent connection to itself. These weights are initially set to random values both positive and negative. The architecture described above forms a recurrent network, which can be trained to settle into specific stable-equilibrium points when it starts from a set of initial states. The initial states used were a hill of activation at randomly selected sites of the map. The only equilibrium configuration for this network was that in which all units of the fixation pool were active, and all units of the movement pool inactive. The cost function, which was used for the training of this network, was the distance of the network's state from this equilibrium configuration.

After the end of the training, the weights set to negative interconnections at the movement pool, and to positive interconnections at the fixation pool. The decline of the initial hill was too fast, lasting 20 steps. As the dynamics of the network where not taken into account at the formation of the cost function, this duration is not an adjustable variable. When the network was presented with two hills of activity at the movement pool, these hills declined independently with similar dynamics and ended up to zero with the activation of the fixation zone.

Evaluation

Based on their results, the authors claim that a recurrent network with a structure including lateral interconnections, cannot give one hill of activity inside the SC when the SC gives an averaged response. However, both Arai's and our model (Fig 14) can get this response with recurrent networks for the motor layer of the SC. This could be due, first of all, to the additional requirement for the existence of a fixation zone. Second, they did not train the network to get the one-hill response, and cannot claim that this is not possible. But even if they tried to train the network to give one hill of activity, it should be emphasized that the failure, with the use of a learning rule, to get a desired result from a neural network does not mean that this result is in principle unobtainable. It simply means that the random weights initialising the network were not appropriate for this result. The training of the network thus ended to a local minimum, different from the desired one. A network with so many units has a very big number of local minima, and in fact it would be a surprise if the initially randomly set weights were initially randomly set at the neighbourhood of this minimum. Learning rules should be used to get positive results about what the architecture of a neural network is able to do, but not negative results about what it cannot do.

Grossberg S., Roberts K., Aguilar M. and Bullock D. (1997)

This model was presented in an article by Grossberg S., Roberts K., Aguilar M. and Bullock D with the title "A neural model of multimodal adaptive saccadic eye movement control by superior colliculus".

General features.

This model places the SC outside the local loop of the saccadic system (page 62), and contains an adaptive mechanism for the transformation of target locations from a head centered to a retinotopic coordinate frame. It contains a burst cell layer with a stable hill of activity (peak decay layer) and a buildup cell layer with a moving hill activity (spreading wave layer) (page 63). It uses a representation of eye position relative to the head in order to explain the learning of saccades to auditory targets and planned saccades, and also to explain the double step saccade paradigm.

Description.

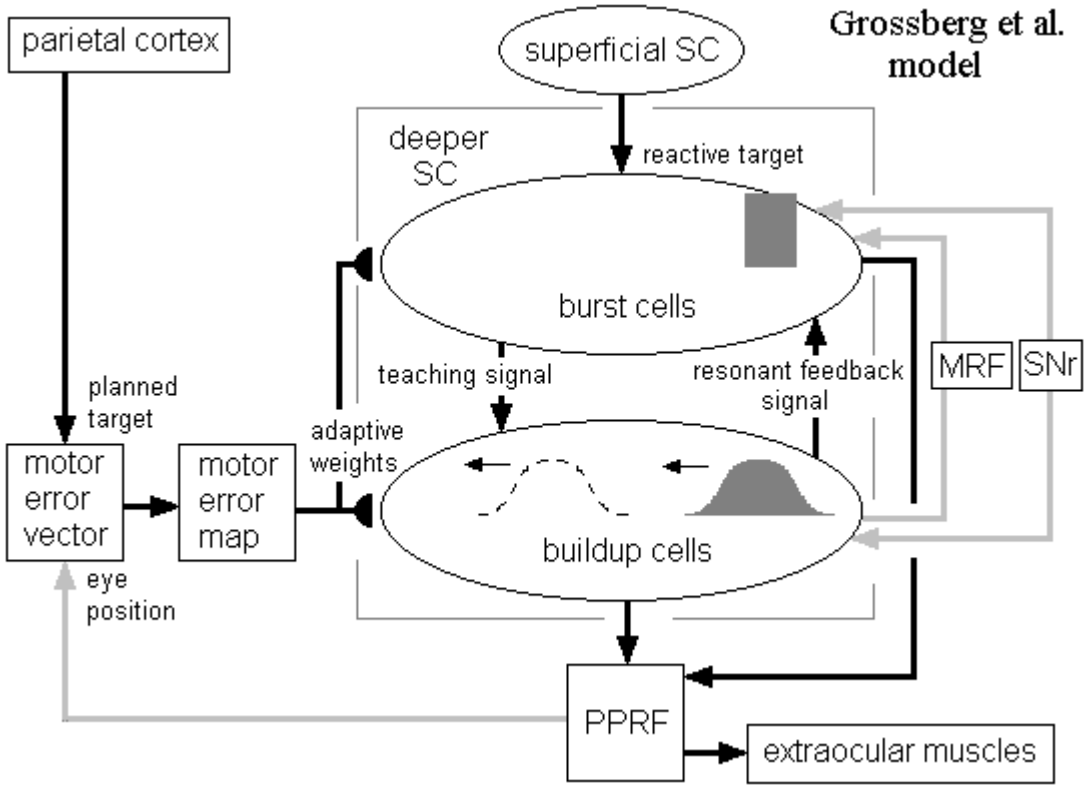

Fig. 24. The Grossberg et al. model. SNr: substantia nigra pars reticulata. MRF: mesencephalic reticular formation. PPRF: Paramedian pontine reticular formation. The black semicircular connection (◖) represents adaptive weights. The gray box encloses the cell groups that are located at the deeper layers of the SC. The output of the parietal cortex, the planned target, is the target of a conscious saccade coded in head centered coordinates. Any target coded in head centered coordinates, an auditory target for example, could serve as an input to the motor error vector box.

The model of Grossberg et al. contains a head centered representation of targets in the parietal cortex, which is used after a transformation to retinotopic coordinates in order to drive the retinotopic representation of gaze at the SC (Fig 24). This model attributes different functions to the burst and buildup cells of the SC. The burst cells receive direct visual input from currently present targets, and are therefore able to give "reactive saccades" to visual stimuli. The buildup cells receive input from stimuli of all

modalities, and are used in the learning procedure, which makes possible the alignment of the head centered map of the parietal cortex (or another unknown yet subcortical region) and the retinotopic map of the SC. The brainstem saccade generator (SG) circuit, which is located in the PPRF, gives an eye position feedback (the output of the neural integrator), which is compared with the planned target coded in head centered coordinates. Both eye position and planned target are in rate code. The result of the comparison is the motor error vector in rate code, which is translated to the motor error vector in space code at the motor error map. The motor error vector in space code drives the buildup and burst layers. The burst layer projects to the buildup layer with local connections, where the stronger connection is to the cell with the same index number, weaker connections target the neighbouring cells and no connections target distant cells; the graph of the weight from the burst layer to the buildup layer as a function of the difference between index numbers resembles a Gaussian. As the saccade progresses, the motor error decreases and this results a shift of the activity at the buildup cell layer from caudal regions that represent large motor errors, to the rostral regions that represent small motor errors. At the same time, the activity at the burst layer falls and becomes zero at the end of the saccade.

When a visual queue is present simultaneously with the planned target in head centered coordinates, it gives a stable hill input to the burst cell layer. This hill is used as a teaching signal for the adaptive weights of the figure 24. The result is that by using the target coding in spatial retinotopic coordinates from the burst layer, the model adapts the weights from the motor error map to the buildup and burst layers and can thus minimize the error between buildup cell starting point and the stable hill at the burst cell layer. The adaptive weight z_{ij} from the ith cell in the spatial error map to the jth cell in the burst layer grew if their activities were simultaneously large. After the learning epochs are over, the adapted weights from the motor error map to the deeper SC are maximum for units with the same index number, zero for distant index numbers (more than 3) and have intermediate values for index number difference less than or equal to 3. The learned weights provide an accurate mapping from the spatial error map to the buildup layer. The head centered command can thus accurately drive the retinotopic coding of gaze error in the SC, because the motor error map and the deeper SC layers are in register.

The buildup cells give a topographically arranged, excitatory resonant feedback to the burst cells, and a global inhibition signal, which is mediated through the mesencephalic reticular formation (MRF). This inhibition eliminates all irrelevant targets at the burst layer, and the resonant feedback excites the burst cells coding for the same motor error.

Evaluation

The model predicts that at infancy, when the connection between the retinotopic head centered maps has not yet been established, burst cells alone suffice to give visually reactive saccades. This model gives a distinct functional role to the buildup cells, and simulates their firing successfully.

However, a recent study (Anderson, Keller, Gandhi and Das 1998) shows a continuum between burst and buildup cell responses, and puts in question their distinction into separate groups. The model uses a moving hill only in the buildup layer, and a stable hill at the burst layer. As argued in 0 (page 56) and 0 (page 63) the use of a moving hill is a problem, although in real buildup cells the big lateral spread of excitation makes the distinction between moving hill and stable hill difficult. This model cannot account for the weighted average result.

It is also not true that a representation in head coordinates is needed in order to simulate the double step saccade paradigm. With the vector subtraction mechanism

that we used in our model, a head-centered representation of visual targets is not needed for the simulation of the double step saccade paradigm.

Krommenhoek K.P., Wiegerinck W.A.J.J. (1998)

This model was presented in an article by Krommenhoek K.P., Wiegerinck W.A.J.J. with the title "A neural network study of precollicular saccade averaging".

General features

This model places the SC outside the loop. It produces a stable hill of activity (page 63). It is a one-hill model but the height of the hill varies with current intensity as it does in the model by Tweed and Villis (page 73). It makes no use of fixation cells (page 57).

Although this model attributes the function of averaging to structures upstream of the SC and contains only the motor layer of the SC as an output non-functional layer, it is briefly described here as an example of an upstream model, and also as an effort to expand on Robinson's model. Robinson's model explains the double step saccade paradigm, which as mentioned above is the execution in sequence of two accurate saccades without visual feedback. In fact, this model is an effort to generalise the Robinson model for saccade generation. This generalization includes spatial coding of retinal error R; initial eye position measured at the moment of target selection E_T, instantaneous position of the eye E_A, and motor error M. All the two-dimensional vectors mentioned above are coded in frequency code in Robinson's model, by single lumped elements, which are transformed to layers of units in this model.

Description

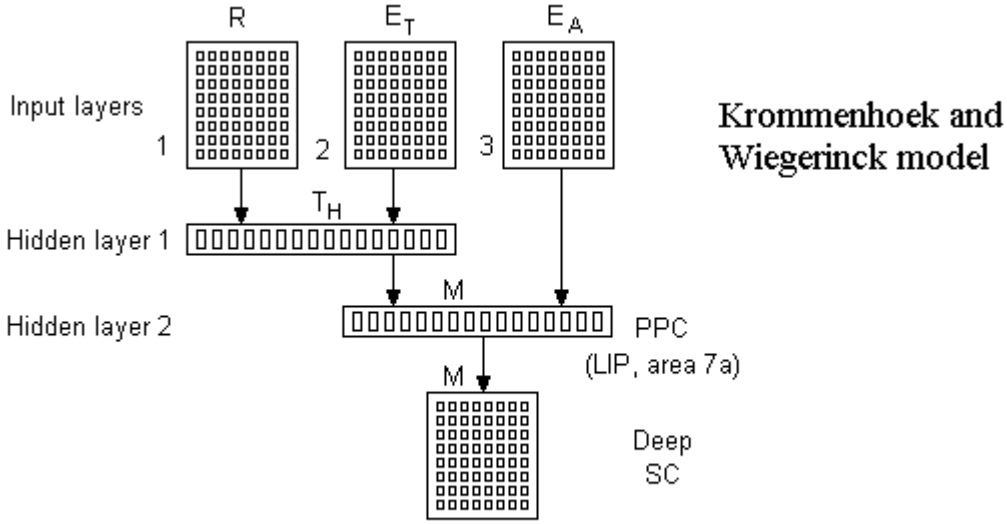

Fig. 25. Krommenhoek and Wiegerinck model. The big squares represent the input and output layers, and the orthogonals represent the hidden layers. The small orthogonals inside all layers are the model's units.

The architecture of the neural network includes three input layers, one output layer and two hidden layers. The first, second and third input layers code R, E_T and E_A respectively. The output layer codes M. Two hidden layers intervene between the input and the output layers. Hidden layer 1 gets input form the first and the second input layers and gives output to hidden layer 2. Hidden layer 2 gets input from the third

input layer and hidden layer 1, and gives output to the output layer. The input and the output layer are two-dimensional layers of units, and the position of every unit in this map corresponds to its preferred vector. The retinal error input map and the motor error output map are topographically coded by a single Gaussian mountain of activity. The centers of gravity of the mountains in these maps represent R and M for the input and output layers respectively. The first and second eye position input layers code E_T and E_A respectively in a recruitment/firing rate format in four directions. Each unit belongs to one of the four directions (up, down, left and right). If the eye position is above a recruitment threshold specific for this unit, then the unit will be active. Above that threshold, the activity of the unit increases linearly with a slope specific for this unit.

The output layer was trained to code $M = R + E_T - E_A$ using the back propagation learning rule (Rumelhart et al., 1986). After training, hidden layer 1 turns out to code the target position relative to the head T_H, where $T_H = R + E_T$, similarly to the first summing junction in Robinson's model. Hidden layer 2 turns out to code M (not in spatial coding), similarly with the second summing junction in Robinson's model.

The physiological interpretation of the various layers goes as follows. The output layer represents the motor cells of the deeper layers of the SC, i.e. the TLLBs. Hidden layer 2 may represent cells in area FEF, which project to the SC and code motor error. The units in the hidden layer 1 have gain-fields, and the gain of their visual response is modulated by eye position. Cells in area 7A in the PPC and cells in area V3a have gain fields, project to the LIP area and may code T_H. Hidden layer 1 could thus represent either of these two cell populations.

Evaluation

This is another model constructed with the use of learning algorithms, and the way it functions is not intuitively clear. Although it gets a weighted average result at the output layer of the SC, this result is influenced by both eye position at the moment of target selection E_T and by the total input drive, which both targets exert together at the input layer. The authors show that when the total excitatory drive to the input layer is less than 100% of the normally given, then the total excitatory drive to the input layer influences the total spike count at the output layer. This means that although the vector average remains correct, the vector sum output changes. But, as was shown in 0 that concerns where averaging takes place, we need to have a vector sum output coding saccade metrics at the output layer of the SC, in order to have intracollicular or upstream averaging. Thus, this model does not appear to achieve averaging.

The model does not reproduce the dynamics of natural cells, as the training procedure was only concerned with the coding of M at the output layer. The model output ends up with a steady mountain of activity some time after the presentation of the target, despite the fact that physiologically identified TLLBs show a burst of activity lasting for about 60 ms. These dynamics could be important for model evaluation, as the TLLBs have been repeatedly recorded from during eye movements.

Although the authors give physiological interpretation for the two hidden layers, the first input layer coding Re and the output layer, they avoid doing so for the other two input layers, which code for E_T and E_A. The explicit coding of E_T has not been located anywhere inside the brain, and this is a drawback inherited to this model by Robinson's model. The model by Droulez and Berthoz (page 90), manages to give a more realistic explanation of double step saccade paradigm.

Quaia C., Lefèvre P., Optican L.M., 1998-1999

This model, which places the cerebellum inside the feedback loop which controls saccade amplitude, was presented in the articles "Distributed model of control of saccades by superior colliculus and cerebellum" (Lefèvre P., Quaia C., Optican L.M., 1998) and "Model of the control of saccades by superior colliculus and cerebellum" (Quaia C., Lefèvre P., Optican L.M., 1999).

General features

This model places the SC outside the feedback loop (page 62). It is a moving hill model (page 63) that makes use of fixation cells (page 66). It is also a two-hill model of the first category (page 68). It does not deal with averaging and two-point stimulation.

In this model both the cerebellum and the superior colliculus work in parallel, in order to provide the drive for the generation of the saccade. The cerebellum receives feedback from the burst generator of the brain stem. It can thus keep track of the residual motor error, and end the movement when the target has been foveated. In other words, the cerebellum performs the function classically ascribed to the displacement integrator, which receives an efference copy of the MLB output (similar to the RIN element in the MSH model). The cerebellum codes this displacement in space and not in frequency code, as the classical displacement integrator. The model uses also burst, buildup and fixation neurons inside the SC.

The use by the cerebellum of on line information and its contribution to the metrics (amplitude) and heading (direction) of the saccade is in contrast with the role more often attributed to the cerebellum by other models (Dean et al. 1994; Grossberg and Kuperstein 1989; Optican 1986; Optican and Miles 1985). This traditional role is the long-term adaptation and control of saccade accuracy; the cerebellum compensates for alterations of the oculomotor plant due to age or injury and adjusts the saccadic command as a function of the orbital position, compensating this way for plant nonlinearities.

This paragraph presents Quaia et al. viewpoint. They emphasize that the cerebellum is not given the appropriate attention at models of the saccadic system, which include only the superior colliculus (colliculocentric) as the source of the motor command for the burst generator. This contradicts the more dramatic effects on saccades of cerebellar lesions, in comparison with the effects after collicular lesions. Lesions to the SC disrupt saccades only for a brief period (Schiller et al., 1980) and even at the acute phase the trajectory and speed of saccades may be affected without loss in accuracy (Quaia et al., 1998; Aizawa and Wurtz, 1998). Colliculocentric models do not explain why lesions of the SC do not result in large and permanent deficits. On the contrary, cerebellar lesions increase the variability of both amplitude and direction of saccades (Robinson et al., 1993; Robinson, 1995; Tagaki et al., 1998).

Description

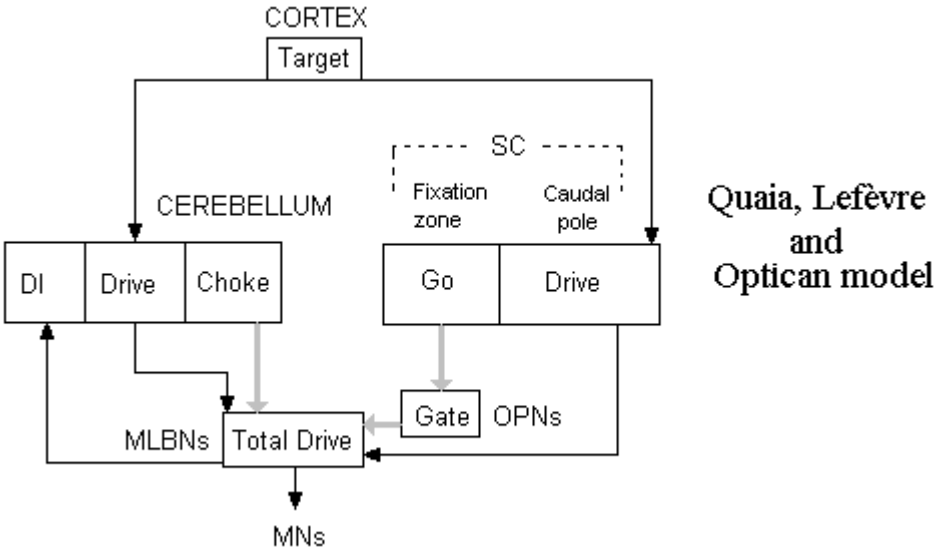

Fig. 26. Quaia, Lefèvre and Optican model

The general structure of the model is very similar to other models, which include a main pathway from the cortex to the motoneurons and a side pathway including the cerebellum (Albus, 1971; Grossberg and Kuperstein, 1989; Dean, 1995; Contreras-Vidal et al., 1997). In this model two pathways work in parallel, the collicular and the cerebellar. Both pathways activate the Medium Lead Burst Neurons (MLBs). The MLBs activate the extraocular motoneurons (MNs), which drive the eyes. The collicular pathway, which is the main pathway, originates in the motor cells of the Frontal Eye Fields (FEF), and the motor command drives the SC, which activates the MLBs. The cerebellar pathway originates from the SC and the FEF, which drive the Nucleus Reticularis Tegmenti Pontis (NRTP), which activates the cerebellum (CBLM) (lobuli VI and VII of the vermis and the caudal fastigial nuclei). The CBLM then drives the MLBs.

The SC, the FEF and the NRTP code the signal of desired displacement ΔE in spatial coordinates, as was described in the section concerning TLLBs. In this model, the authors propose that the CBLM also codes ΔE in spatial coordinates. Topographically organised projections from FEF to SC and NRTP and from NRTP to CBLM suffice to keep the spatial coding of the ΔE signal.

The FEF motor cells project to Buildup neurons (BUNs) and Burst Neurons (BNs) in the SC. BUNs receive another input from Lateral Intraparietal Area (LIP). In this model, the activation of LIP is neither necessary nor sufficient to produce a saccade and has a weaker influence on BUN activity, whereas the FEF activation is necessary. The spatial distribution of the LIP output changes during the saccade. The output of the LIP is taken to be a spreading activity, inducing a spread of activity from caudal BUNs toward rostral BUNs.

The model of the SC contains also fixation neurons (FNs), which gate the input from FEF to BUNs and BNs, and give the tonic excitation to the OPN neurons, which inhibit the MLBs. This way, the FNs gate the motor command in both the SC and the burst generator level. The FNs get a steady input FIX, which is the "fixation command". FNs receive inhibition from the BNs. When eyes fixate, FNs are tonically active and prevent the BNs from firing, but allow BUNs to fire in response to LIP activation.

When the FEF provides an ΔE command to the BNs, the BNs inhibit the FNs and stops their firing. The OPNs no longer receive input from the FNs and pause, allowing

the MLBNs to start firing and begin the saccade. The FNs thus give a "GO" signal to the burst generator. At the same time the CBLM gives an additional input, which contributes to the acceleration of the saccade. The efference copy of the signal that the MLBNs send to the MNs is fed back to the CBLM. The CBLM integrates this signal and keeps track of the residual motor error (coded in space code) since the beginning of the saccade. This residual motor error is coded as a spreading hill of activity in the CBLM. During saccades, the CBLM sends an inhibitory signal to the SC, making thus the burst of activity of BNs and BUNs decay as a function of residual motor error. When the eyes approach the target, the CBLM starts to drive the MLBNs and IBNs contralateral to the movement. The contralateral to the movement IBNs 'choke off' the drive provided by ipsilateral EBNs at the level of the MNs. When this choke is applied, the eyes stop although the excitatory drive from the MLBNs to the MNs is still active. This choke signal is only temporary, but the stability of fixation in mid-saccade time intervals is assured by the OPN reactivation.

Evaluation

One disadvantage of this model is that it makes a lot of controversial assumptions as the spatial coding of the ΔE in the fastigial nucleus, the connections from FNs which gate the input to BUNs and BNs from the FEF and the spread of activity in LIP, BUNs and the fastigial nucleus. Second, the model makes use of a moving hill of activity. As was mentioned in the section concerning the general features of SC models, experiments favour the stable hill hypothesis. In order to escape this apparent difficulty, this model transfers the mechanism for the moving hill from the SC to the cerebellum, a hypothesis, which seems to be ad hoc. Third, it provides no explanation for the global effect.

We disagree with the authors' criticism concerning "colliculocentric" models. First, the authors' claim that the spatial coding of residual motor error ΔE in the fastigial nucleus is essential for the accurate performance of curved oblique saccades is not correct. There is no need in principle of a heading feedback. Two independently working feedback loops for the horizontal and the vertical component of the saccade are equally capable of producing accurate saccades. In this last case, the curvature is produced by different durations of the horizontal and vertical components. Second, SC lesion may result only transient consequences on saccade metrics because the FEF takes over collicular function. Third, the slow dynamics of saccades with the preservation of accurate metrics after SC lesion (Schiller et al., 1980) is good evidence for putting the SC inside the local feedback loop, whereas in Quaia et al. model the cerebellum is inside the loop and drives the SC which is outside the loop.

Lesions to the SC disrupt saccades only for a brief period (Schiller et al., 1980) and even at the acute phase the trajectory and speed of saccades may be affected without loss in accuracy (Quaia et al., 1998; Aizawa and Wurtz, 1998). Colliculocentric models do not explain why lesions of the SC do not result in large and permanent deficits. On the contrary, cerebellar lesions increase the variability of both amplitude and direction of saccades (Robinson et al., 1993; Robinson, 1995; Tagaki et al., 1998).

Droulez J. and Berthoz A., 1991

This is a model of the retinotopic maps in general, and the way these maps could be updated during saccades or head movements, in order to maintain an accurate representation of interesting stimuli. It was presented in 1991 in the article "A neural network model of sensoritopic maps with predictive short-term memory properties".

General features

This model addresses the problem of double step saccades and of memorising visual targets and the execution of saccades towards them, although they are no longer visible. The authors do not place the proposed model necessarily inside the SC, so this is not a SC model, but a theoretical model that could be implemented inside the SC. The function of this model is equivalent with the vector subtraction that is achieved in our model at the input (visual) layers of the SC, and more specifically at the layer of PVs (Predictive Visual Cells). It is meaningful to present this model here, in order to compare it with our remapping mechanism of the PV (presented in model description section).

This model keeps all visual stimuli memorized in a two dimensional layer of units, which codes their location in a spatial, retinotopic frame of reference. Every unit in this layer codes for a specific preferred retinal error, and is activated whenever a stimulus, not necessarily a visible one currently, has the same retinal error. The retinal error of this target at the time of presentation plays no role in the activation of this layer. In other words, the layer of memorized stimuli keeps all presented stimuli as mountains of activity, whose position in the map code the retinal error Re. Every time a movement is performed, every mountain of activity shifts its location in the layer, and its new position after movement offset codes the new corrected Re of the target.

Description

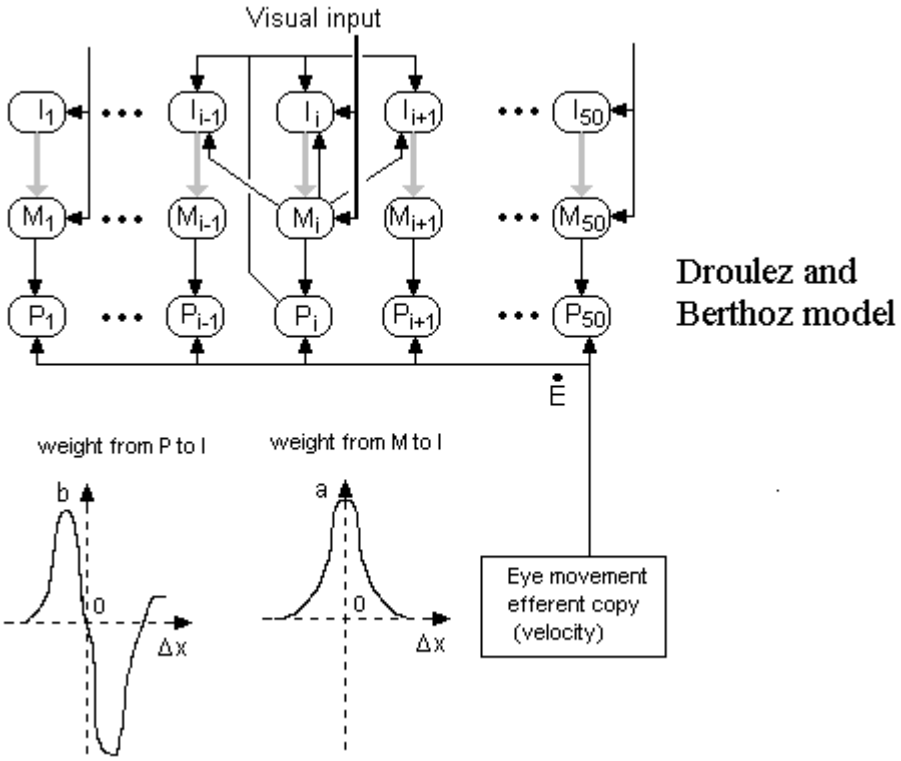

Fig. 27. Droulez and Berthoz model. The two graphs below depict qualitatively the strength of the weights from layer P to layer I and from layer M to layer I, as a function of the distance between the elements of the different layers.

Simulations were done with both one-dimensional and two-dimensional layers. The two-dimensional model includes: one input layer (I), one main layer (M) and at least two interneuron layers (P). Each interneuron layer P corresponds to movement in one of the four directions (up, down, left and right), so at least two are needed for the functioning of a two-dimensional SC map. The two dimensional map was formed by 31x31 modules of 4 units, which are 2 units for layer I and M and 2 more for two layers P. Visual input S enters layers I and M from the retina, in a one-to-one fashion. Each unit of layer I receives input from the units of layers M and P of the neighbouring modules. When visual information is available, the activity of input neurons reflects the error between the stored information and the stored visual map. This is in agreement with the transient visual responses of real visual neurons of the SC. When visual input is not available, the activity of the layer I is a mirror image of the predicted activity in the visual pathway, i.e. the activity that would be present if all interesting stimuli were still present. This means that the main output unit M receives, apart from the visual input S, an inhibitory connection from the I neuron of the same module. The unit M thus compares the external visual input S with the activity of the corresponding input neuron. The resulting activity of the M neuron is thus a non-linear sigmoid function f(x,y,t) of the result of this comparison. P units get two inputs: one from the M unit and an external input, which is proportional to an eye velocity signal. Each layer of P units receives a velocity signal that corresponds to one of the four directions (up, down, left and right). The output of the P units is the product of their inputs. This means that the transformation function of all P units is multiplicative and not additive, as for most models of simplified neurons.

The synaptic weights were set to zero, and a learning procedure was applied to a one-dimensional version of the above network. The learning concerned the connections from layers M and P to the layer I. The model was exposed to periods of fixation when velocity feedback to P neurons was zero and visual input constant, and to saccades when velocity feedback was present and the visual input was displaced accordingly. A modified Hebbian learning rule was applied to synaptic weights from M layer to I layer and from P layer to I layer. The cost function was minimised when the weighted sum of every mountain of activity predicted, as accurately as possible, the visual input to the next step. After learning, the synaptic weights from M layer to I layer as a function of their units' distance in the map, formed a single hill with its maximum at zero distance. The aforementioned weights were mostly excitatory, with a very small inhibition at the edge of the mountain, which could be ignored. The weights from P layer to I layer formed an antisymmetric function of the units' distance in the map, with positive weights towards the direction that the P layer pushes the mountains of activity in the I layer, and negative weights in the opposite direction.

After training, the input (I) and main (M) layers were able to keep in memory multiple targets, after the initial visual input was gone. When a saccade occurred, the velocity feedback to the P layer was fed to the layer I, and produced a continuous shift of the center of gravity of all mountains of activity. When the saccade was over, all mountains of activity were equally displaced in the map.

The activation pattern of units of layer M resembles that of QV cells and visual-motor cells in the deep layers of the SC. The activation pattern of P units is very similar to the pattern of activity described in the posterior parietal cortex (PPC) of monkeys (Andersen et al., 1985). It contains neurons with retinotopic receptive fields, whose firing is modulated by eye position. The prepositus hypoglossi nucleus and various cells in the brain stem show discharge profiles related to eye velocity, and could serve as a the source of the feedback signal to the P units.

Evaluation

This model has a major advantage in comparison with the Andersen model, and also the Krommenhoek and Wiegerinck model described before. It avoids the use of head-centered or inertial coordinate systems in order to explain the double step saccade paradigm. Instead, it uses only retinotopic spatial coding of targets, which has been seen in the QV and PV cells of the superior colliculus.

A difficulty for a biological implementation of this model is its complexity. First of all, as Dale's principle does not hold for P neurons (they give rise to both excitatory and inhibitory connections), each P layer should be duplicated in order to transform this theoretical network to a biologically plausible model. In a two dimensional layer, we need a mechanism able to shift the activity towards all four directions; this would give 8 layers of P units, and if we add the layers I and M we end up with a full model containing 10 distinct layers of units. It would be very hard to give experimental proof for such a diversity of layers. Another possible problem is the presence of the multiplicative neurons M. Multiplicative neurons have not been identified in structures possibly involved in remapping target location in retinotopic coordinates, as the Frontal Eye Fields (FEF) and the PV and QV layer of the SC. This of course does not exclude their discovery in the future, and the firing pattern of PPC neurons seems to multiply somehow place coded retinotopic targets with an eye position signal. If the PPC neurons are the M units in this model, then we still need an eye position signal to be multiplied; however, this would bring us back to the discovery of such an eye position signal, in order now to explain the firing pattern of the PPC. In our model, we managed to avoid the use of multiplicative units, and used only one additional layer for the movement to every direction and one layer for target memory, i.e. a total of five layers in sum (in comparison with ten in this model) which suffice for the shift of activity in the network (and the resulting remapping of targets) to all four directions.

Groh J., 2001

Two downstream models (page 68) were proposed in the article "Converting neural signals from place codes to rate codes" in 2001.

General features and description

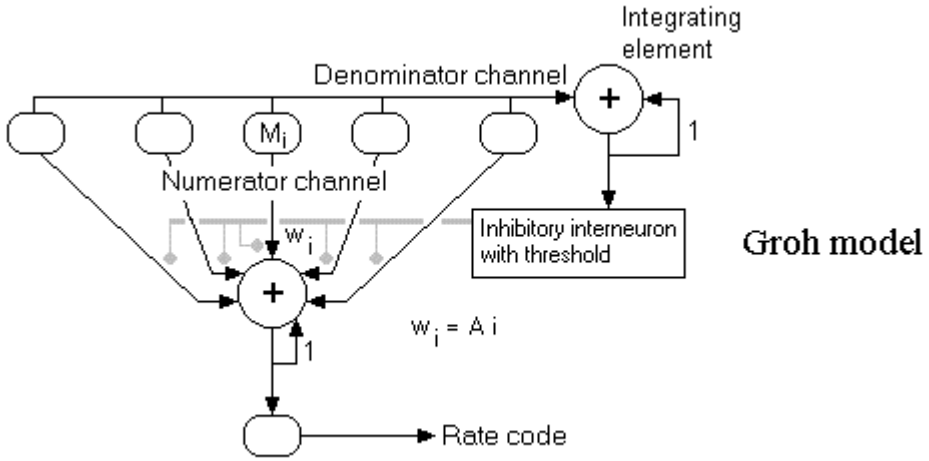

Fig. 28. The Groh model. Gray circular connections are inhibitory. The layer of M units is motor, and contains the information of saccade metrics in place code. The output of the model contains the same information in rate code.

Groh model is a two-hill model of the first category (page 66). It does not contain fixation cells (page 66) and does not deal with saccade dynamics. Both averaging

models in this article contain an array of motor units, which are the output layer of the SC and two channels, the numerator and the denominator channels. The numerator channel sums the output of the SC weighted by the index number of the motor unit, and this is denoted with the equation w_i= A i in the figure. The denominator channel sums all the activity of the SC and thus calculates the total activation.

We will summarize here "model 3" of the article, which is the one favored by the author. The model transforms a place code signal to a rate code signal, and evaluates the mean average of its input signal. The numerator and denominator signals are integrated in space and time, as shown in figure14 by two summing neurons. The denominator channel gives input to an inhibitory interneuron with threshold. As long as the total activation, i.e. the integral of all activation over time and space is below the threshold of this inhibitory interneuron, the activity of the integrator builds up. When the total activation reaches the threshold, the inhibitory interneuron starts to fire and inhibits totally the numerator channel. The inhibitory interneuron thus cuts off all additional excitation, when the correct amount of total activation is reached. When given to mountains of activity in its input that correspond to two targets, this model will give two identical mountains at the output of the SC (see Fig 8). The additional excitation will be clipped off and the ensuing saccade will correspond to the center of gravity of the two mountains.

Evaluation

The model has the disadvantages of all downstream models. In addition, it requires two summing elements and also an inhibitory interneuron with a threshold. The mechanism of this inhibitory interneuron is in fact a spike counter: it counts the number of spikes that the output motor layer of the SC has given in total, and does not permit the spike count to exceed a threshold. The total spike count at the motor layer of the SC seems to be the best preserved variable during perturbations of eye movement with OPN stimulation or air puff, as was mentioned in 0. A spike counter mechanism or a similar feedback device is expected to reflect the workings of the SC motor layer, and it is true that such a mechanism would also give the weighted average result. A spike counter could also in principle replicate the residual activity inside the SC after OPN stimulation or air puff. The spike counter presented by Groh is an all-or-nothing resetting mechanism and is not able to accomplish this. A future extension of our model would be expected to include a modified spike counter mechanism in order to replicate the residual activity result.

Abstract

Our goal was to construct a biologically motivated neural network model of the primate superior colliculus (SC). SC is a brainstem nucleus involved in the programming and execution of fast eye movements called saccades.

Assumptions

Our model is based on the following assumptions:

1) It is a neural network model, consisting of units (or elements) that represent groups of neurons, and their activation represent the firing rate of the groups of neurons.
2) It contains among its simulated collicular neurons the layers of motor (TLLBs), visual (Vs), quasivisual (QVs) and predictive visual (PVs) units.
3) It uses the "MSH" model of the brainstem oculomotor nuclei. This does not mean that it is not compatible with other models of the same structure (e.g. the model by Scudder).
4) All real collicular two-dimensional layers of cells are simulated with one-dimensional arrays of units. This is merely a simplification. The generalization to a two-dimensional model resembling the real SC poses no difficulties.
5) It contains excitatory connections between the output motor elements of the superior colliculus, whose strength varies realistically with the distance between the units of the motor layer.
6) It contains global inhibition at the motor (TLLB) layer.
7) It contains an intracollicular mechanism of local inhibition at the PV layer.
8) It contains a gating mechanism from the substantia nigra to keep the SC silent when the eyes fixate a target.
9) It does not use eye position or eye velocity information as an input to the SC. Instead, a realistic signal originating from the RTLLB neurons of the reticular formation is used as a feedback signal to the PV layer of the SC (and more specifically to inhibitory PVs). The time integral of this signal is directly proportional to the total eye displacement of the eye.
10) It makes no use of a head fixed frame of reference for visual targets either inside the SC or as an input to it. Instead, it uses only the experimentally well justified representations of retinal error and static motor error that are present inside the SC
11) It places the SC outside the feedback loop that is believed to control saccade metrics.
12) It assumes that the electrical stimulation of the deep collicular layers does not directly excite the output of the SC, but instead is stimulates the axons that give input to the motor (output) layer of the SC.
13) The position sensitivity (dependence of the size of an electrically elicited saccade on the initial position of the eye) is a result of the parallel excitation of axons that elicit slow eye movements. We do not deal with the position sensitivity because we assume that it is not related with the collicular mechanism that produces saccades.

Results

Our model produces the following results:

1) It can produce in cooperation with the MSH model of the burst generator eye movements in agreement with known psychophysics.

2) It produces movements towards the center of gravity of two or more targets (weighted average result). It is thus able to perform a nonlinear vectorial evaluation of its inputs.
3) It always gives one hill of activity at the motor output layer of the SC, with either visual or electrical stimulation. The anatomical position of this activity inside the superior colliculus depends only on movement metrics and not on the number of targets that evoked this movement. The development of this hill of activity is due to the lateral excitatory connections.
4) It contains a retinotopic map of visual targets in the PV and QV layer that is dynamically updated during eye movements (remapping of targets). It thus offers a model for the activation profiles of PVs and QVs.
5) It gives a sequence of two accurate visually guided eye movements (double step saccade paradigm) despite the fact that no visual information is available before the execution of the second saccade. It is shown that the realistic eye displacement signal of reticular origin to the PV layer of the SC is adequate to recalculate saccade metrics in retinotopic coordinates.
6) It gives roughly constant saccade metrics with electrical stimulation, irrespective of current frequency and intensity.
7) It gives a weighted average result when two SC sites are simultaneously electrically stimulated with two electrodes.
8) It gives a sequence of consecutive movements (staircase) with continuous electrical stimulation at a single site.
9) It generates a fixed burst of activity at the output layer of the SC with either a transient visual stimulus or a continuous electrical stimulation. This burst drives the aforementioned MSH model. At prolonged electrical stimulation, it gives a series of bursts at SC exit with latency between them, which give the aforementioned staircase of saccades.
10) It does not simulate the experiment of OPN electrical stimulation. During the residual saccade after release from OPN stimulation, it gives a residual collicular activity, which is the same fixed burst that is elicited for the whole saccade.
11) It reproduces the effects of SC lesions after partial inactivation of its units. It produces smaller than normal (hypometric) horizontal saccades when a region corresponding to bigger horizontal saccades is deactivated, and bigger than normal (hypermetric) horizontal saccades when a region corresponding to smaller horizontal saccades is deactivated.

Experimental evaluation of our model

All the above assumptions and results are amenable to experimental test. Some experiments have already been done, and are retrodictions for our model or possible falsification for it. Others have not been done yet or remain unresolved as a result of contradictory results from different researchers, and serve as predictions. The following table shows the extent to which our assumptions and results reflect empirical evidence.

Retrodictions	Predictions	Possible falsifications	
(5) Excitatory TLLB interconnections **(8)**SNR gating mechanism **(11)**Retinotopic coordinates inside SC	**(6)**Global inhibition at the TLLB layer **(7)**Local inhibition inside PV layer **(9)**RTLLBs connected to inhibitory PVs. **(12)**Simulation of deep SC electrical stimulation	**(11)**SC outside the feedback loop	**Assumptions**
(2) Weighted average **(4)**Remapping in PV and QV layers **(5)**Double step saccade paradigm **(6)**Roughly constant saccades with electrical stimulation with different intensity and frequency **(7)**Weighted average result when electrically stimulated at two regions **(8)**Staircase of saccades at prolonged electrical stimulation **(10)**Lesions	**(3)**One hill of activity with double stimulation **(9)**Fixed burst in motor output layer irrespective of stimulation parameters	**(9)**Fixed residual SC activity after OPN stimulation release	**Results**

ΠΕΡΙΛΗΨΗ

Σκοπός μας σε αυτήν την μελέτη ήταν να κατασκευάσουμε ένα νευρωνικό δίκτυο το οποίο θα χρησιμεύσει ως μοντέλο του άνω διδυμίου (Α.Δ.) των πρωτευόντων. Το Α.Δ. είναι ένας πυρήνας του στελέχους ο οποίος εμπλέκεται στον προγραμματισμό και στην εκτέλεση γρήγορων κινήσεων των ματιών οι οποίες ονομάζονται σακκαδικές.

Παραδοχές του μοντέλου

Το μοντέλο μας κάνει τις ακόλουθες βασικές παραδοχές, ή αλλιώς έχει τα ακόλουθα χαρακτηριστικά:

1) Είναι ένα νευρωνικό δίκτυο-μοντέλο, αποτελούμενο από μονάδες.(ή στοιχεία) τα οποία αντιπροσωπεύουν ομάδες νευρώνων, και των οποίων η δραστηριότητα αντιπροσωπεύει την δραστηριότητα των ομάδων των νευρώνων .
2) Εμπεριέχει μονάδες που εξομοιώνουν πολλά νευρικά κύτταρα του άνω διδυμίου, όπως τα κινητικά τα οποία ονομάζονται TLLB, καθώς και τα οπτικά κύτταρα V και τα κύτταρα QV και PV.
3) Χρησιμοποιεί το μοντέλο "MSH" των οφθαλμοκινητικών πυρήνων του εγκεφαλικού στελέχους. Αυτό δεν σημαίνει ότι δεν είναι συμβατό και με άλλα μοντέλα των πυρήνων του εγκεφαλικού στελέχους (π.χ. το μοντέλο του Scudder).
4) Για να απλοποιήσουμε την προσομοίωσή μας, χρησιμοποιήσαμε μονοδιάστατες στοιβάδες μονάδων για να εξομοιώσουμε τις δισδιάστατες στοιβάδες κυττάρων του πραγματικού άνω διδυμίου. Θεωρούμε ότι η γενίκευση σε ένα δισδιάστατο μοντέλο του άνω διδυμίου, το οποίο θα μοιάζει περισσότερο στο πραγματικό άνω διδύμιο, δεν παρουσιάζει δυσκολίες.
5) Τα κινητικά κύτταρα στην έξοδό του συνδέονται με διεγερτικές συνάψεις μεταξύ τους. Η ισχύς των συνάψεων αυτών μεταβάλλεται ρεαλιστικά ως συνάρτηση της απόστασης μεταξύ των συνδεόμενων μονάδων της κινητικής στοιβάδας.
6) Εμπεριέχει έναν μηχανισμό εκτεταμένης αναστολής μέσα στις κινητικές στοιβάδες του άνω διδυμίου.
7) Εμπεριέχει έναν μηχανισμό τοπικής αναστολής στην στοιβάδα PV.
8) Εμπεριέχει έναν μηχανισμό λογικής πύλης στον πυρήνα της μέλαινας ουσίας, οποίος κρατά το Α.Δ. σιωπηλό όταν τα μάτια είναι ακίνητα εστιάζοντας έναν στόχο.
9) Δεν χρησιμοποιεί πληροφορία σχετική με την θέση ή την ταχύτητα του ματιού ως είσοδο στο Α.Δ.. Αντί αυτής, χρησιμοποιείται ένα αληθοφανές σήμα, προερχόμενο από τους νευρώνες RTLLB του δικτυωτού σχηματισμού το οποίο επανατροφοδοτείται στην στοιβάδα PV του Α.Δ.. Το ολοκλήρωμα στον χρόνο αυτού του σήματος είναι ευθέως ανάλογο της συνολικής μετατόπισης του ματιού.
10) Δεν χρησιμοποιεί πουθενά μέσα στο Α.Δ. ή ως είσοδο σε αυτό το σήμα της θέσης των οπτικών στόχων σε σχέση με σύστημα συντεταγμένων προσκολλημένο στο κεφάλι. Αντί αυτού, χρησιμοποιεί μόνο τις αναπαραστάσεις του αμφιβληστροειδικού λάθους και του στατικού κινητικού λάθους, των οποίων η παρουσία στο Α.Δ. είναι πειραματικά τεκμηριωμένη.
11) Τοποθετεί το Α.Δ. έξω από τον βρόγχο ανάδρομης ρύθμισης, ο οποίος πιστεύεται ότι ελέγχει το μέγεθος των σακκαδικών κινήσεων.

12) Η ηλεκτρική διέγερση των εν τω βάθει στοιβάδων του Α.Δ. δεν διεγείρει απ' ευθείας την έξοδο του Α.Δ., αλλά διεγείρει τους άξονες οι οποίοι δίνουν είσοδο στην κινητική στοιβάδα εξόδου του Α.Δ..
13) Η ευαισθησία θέσης (εξάρτηση του μεγέθους της εκλυόμενης σακκαδικής κίνησης από την αρχική θέση του ματιού σε ηλεκτρική διέγερση των εν τω βάθει στοιβάδων του Α.Δ) οφείλεται στην παράλληλη διέγερση αξόνων οι οποίοι προκαλούν αργές κινήσεις των ματιών. Δεν ασχολούμαστε με την ερμηνεία της ευαισθησίας θέσης επειδή θεωρούμε ότι δεν σχετίζεται άμεσα με τον μηχανισμό του Α.Δ. που παράγει σακκαδικές κινήσεις.

Αποτελέσματα

Το μοντέλο μας δίνει τα ακόλουθα αποτελέσματα:

1) Σε συνεργασία με το μοντέλο MSH της γεννήτριας παλμών του εγκεφαλικού στελέχους, παράγει κινήσεις του ματιού συμβατές με ψυχοφυσικά δεδομένα.
2) Παράγει κινήσεις προς το κέντρο βάρους δύο ή περισσοτέρων στόχων (αποτέλεσμα του σταθμισμένου μέσου όρου). Είναι συνεπώς ικανό να κάνει μια μη γραμμική διανυσματική σύνθεση δύο διαφορετικών εισόδων.
3) Δίνει πάντα ένα βουνό δραστηριότητας μέσα στην κινητική στοιβάδα του Α.Δ.. Η ανατομική θέση αυτής της δραστηριότητας στο εσωτερικό του Α.Δ. εξαρτάται μόνο από το μέγεθος της κίνησης και όχι από τον αριθμό των στόχων οι οποίοι προκάλεσαν την κίνηση. Η ανάπτυξη αυτού του βουνού δραστηριότητας οφείλεται στις παράπλευρες διεγερτικές συνδέσεις.
4) Περιέχει έναν αμφιβληστροειδοκεντρικό χάρτη των οπτικών στόχων, ο οποίος ανανεώνεται δυναμικά κατά την διάρκεια των κινήσεων των ματιών (επαναχαρτογράφηση των στόχων). Προσφέρει έτσι ένα μοντέλο για τις δραστηριότητες των κυττάρων PV και QV.
5) Δίνει μια ακολουθία δύο ακριβών σακκαδικών κινήσεων προς οπτικούς στόχους (διαδοχικές σακκαδικές κινήσεις σε δύο στόχους), παρά το γεγονός ότι καμία οπτική πληροφορία δεν είναι διαθέσιμη πριν την εκτέλεση της δεύτερης κίνησης. Δείχνουμε ότι το αληθοφανές σήμα της μετατόπισης του ματιού που προέρχεται από τον δικτυωτό σχηματισμό επαρκεί για τον επαναϋπολογισμό του μεγέθους της κίνησης σε αμφιβληστροειδικές συντεταγμένες.
6) Δίνει σακκαδικές κινήσεις σχεδόν σταθερού μέτρου ανεξαρτήτως της έντασης και της συχνότητας του ρεύματος σε διέγερση με ένα ηλεκτρόδιο.
7) Δίνει το αποτέλεσμα του σταθμισμένου μέσου όρου όταν διεγείρουμε ηλεκτρικά ταυτόχρονα δύο περιοχές του Α.Δ.
8) Δίνει μια ακολουθία διαδοχικών σακκαδικών κινήσεων (σκάλα) με συνεχόμενη ηλεκτρική διέγερση σε μία περιοχή.
9) Δίνει έναν αμετάβλητο παλμό δραστηριότητας στην στοιβάδα εξόδου του Α.Δ. με είσοδο είτε ένα παροδικό οπτικό ερέθισμα είτε συνεχή ηλεκτρικό ερεθισμό. Αυτός ο παλμός δίνει την κατάλληλη είσοδο στο προαναφερθέν μοντέλο MSH. Σε παρατεταμένο ηλεκτρικό ερεθισμό, δίνει μια αλληλουχία παλμών στην έξοδο του Α.Δ. με μία καθυστέρηση μεταξύ τους. Η αλληλουχία αυτή δίνει την προαναφερθείσα σκάλα σακκαδικών κινήσεων.
10) Δεν προσομοιώνει το πείραμα της ηλεκτρικής διέγερσης των OPN. Κατά την διάρκεια της υπολειπόμενης σακκαδικής κίνησης μετά την διακοπή της ηλεκτρικής διέγερσης των OPN, δίνει μια υπολειπόμενη δραστηριότητα

στο Α.Δ., η οποία είναι ο ίδιος αμετάβλητος παλμός δραστηριότητας που εκλύεται και για ολόκληρη την σακκαδική κίνηση.

11) Προσομοιώνει τα αποτελέσματα των βλαβών του Α.Δ. μετά από απενεργοποίηση μέρους των μονάδων του. Δίνει μικρότερες (υπομετρικές) οριζόντιες σακκαδικές κινήσεις όταν έχει απενεργοποιηθεί μια περιοχή που αντιστοιχεί σε μεγαλύτερες οριζόντιες σακκαδικές κινήσεις, και μεγαλύτερες (υπερμετρικές) σακκαδικές κινήσεις όταν έχει απενεργοποιηθεί μια περιοχή που αντιστοιχεί σε μικρότερες οριζόντιες σακκαδικές κινήσεις.

Πειραματική αξιολόγηση του μοντέλου μας

Όλες οι παραπάνω παραδοχές και αποτελέσματα υπόκεινται σε πειραματικό έλεγχο. Μερικά πειράματα έχουν ήδη γίνει και είτε αποτελούν το ερμηνευτικό πεδίο του μοντέλου μας είτε μπορούν να χρησιμεύσουν ενδεχομένως για την διάψευσή του. Κάποια πειράματα, τα οποία χρησιμεύουν ως προβλέψεις του μοντέλου, δεν έχουν γίνει ακόμα ή έχουν γίνει από διαφορετικούς ερευνητές με αντιφατικά αποτελέσματα. Ο ακόλουθος πίνακας δείχνει κατά πόσον οι παραδοχές μας και τα αποτελέσματά μας συμφωνούν με τα εμπειρικά δεδομένα.

Επαληθεύσεις	**Προβλέψεις**	**Πιθανές διαψεύσεις**	
(5)Διεγερτικές εσωτερικές συνάψεις **(8)**Μηχανισμός πύλης από την μέλαινα ουσία **(11)**Αμφιβληστροειδικές συντεταγμένες μέσα στο Α.Δ.	**(6)**Εκτεταμένη αναστολή στην κινητική στοιβάδα των TLLB. **(7)**Τοπική αναστολή στο εσωτερικό της στοιβάδας των PV. **(9)**Σύνδεση των νευρώνων RTLLB με ανασταλτικούς νευρώνες PV **(12)**Προσομοίωση της ηλεκτρικής διέγερσης του εν τω βάθει Α.Δ.	**(11)**Το Α.Δ. έξω από τον βρόγχο επανατροφοδότησης	**Παραδοχές**
(2)Αποτέλεσμα του σταθμισμένου μέσου όρου **(4)**Επαναχαρτογράφηση των στόχων στις στοιβάδες PV και QV **(5)**Διαδοχικές σακκαδικές κινήσεις σε δύο στόχους **(6)**Κινήσεις σχεδόν όμοιες κατόπιν ηλεκτρικής διέγερσης με διαφορετική ένταση και συχνότητα. **(7)** Αποτέλεσμα του σταθμισμένου μέσου όρου όταν διεγείρεται ηλεκτρικά σε δύο περιοχές **(8)**'Σκάλα' σακκαδικών κινήσεων σε παρατεταμένο ηλεκτρικό ερεθισμό **(10)**Καταστροφές του Α.Δ.	**(3)**Ένα βουνό δραστηριότητας μετά από διέγερση με δύο ερεθίσματα **(7)**Σταθερός παλμός στην κινητική στοιβάδα εξόδου ανεξαρτήτως τρόπου διέγερσης	**(9)**Σταθερή υπολειπόμενη δραστηριότητα στο Α.Δ. μετά από διακοπή της διέγερσης των νευρώνων OPN	**Αποτελέσματα**

Abbreviations

All bold letters indicate vectors

α_H	The position sensitivity constant.
A_{max}	The maximum activation of a neural network unit. Corresponds to the maximum firing frequency that a particular cell can reach.
BG	Burst generator.
β_H	The amplitude of the saccade that is elicited, when the SC is electrically stimulated and the eye is at the primary position.
BN	Burst neuron. A saccade related neuron giving a burst of activity. Also kind of TLLBs that seizes firing in between saccades.
BUN	Buildup Neuron, motor SC cell which exhibits gradual increase of firing before a saccade inside its movement field.
CBLM	CBLM cerebellum.
CMRF	CMRF central Mesencephalic Reticular Formation
$\mathbf{\Delta E}$	ΔE The amplitude of a saccade.
$\mathbf{\Delta G}$	ΔG Desired gaze displacement
$\mathbf{\Delta H}$	ΔH The horizontal component of a saccade
Δt	Time interval
EBN	Excitatory Burst Neuron. An MLB with excitatory function to the ipsilateral oculomotor nuclei.
$\mathbf{E_A}$	Instantaneous position of the eye.
$\mathbf{E_T}$	Initial eye position measured at the moment of target selection.
FN	Fixation Neuron. Fires only when eyes are still and pauses during movements.
GI(t)	Global inhibition (as a function of time) in Arai's model.
H_1	The initial horizontal position of the eye, before an experiment, as the application of stimulation.
IBN	Inhibitory Burst Neuron. An MLB with inhibitory function to the contralateral MLBs (both EBNs and IBNs)
K	The reciprocal weight, corresponding to the time constant of units in our model.
L-cells	Light responsive visual cells of the superficial tectal layers.
L layer	Layer of visual units simulated in our model.
LIP	Lateral Intra-Parietal area
LLB	Long Lead Burst neuron, and also an element of the MSH burst generator.
M, Me	M (or Me) motor error, the difference between desired final position of the eye and the actual position of the eye.
NRTP	Nucleus Reticularis Tegmenti Pontis.
NI	Neural integrator. Element of the burst generator that integrates the output of the MLB and gives the step response of the Mn.
OPN	Omnipause neuron.
OKR	Optokinetic reflex
PNs	Pause neurons. Contained in raphe interpositus nucleus.
Plant	In cybernetics, the object under control. In this model, it refers to the

	eye.
PPC	Posterior Parietal Cortex:
PPRF	Paramedian Pontine Reticular Formation. A brainstem nucleus.
PV	Predictive Visual cell.
PV layer	Layer of visual units simulated in our model
QV	Quasivisual cell
R	Retinal error, same as **Re**.
Re	Retinal error, the vector representing the position of the visual target relative to the center of the fovea.
riMLF	Rostral interstitial nucleus of the median longitudinal fasciculus.
RIN	Resettable integrator, element of the MSH model of the BG.
SC	Superior colliculus.
S_d	The duration of a saccade.
SNR	Substantia Nigra pars Reticulata.
SNR_1	Cells of the Substantia Nigra pars Reticulata. Also gating units in our model.
SNR_2	Cells of the Substantia Nigra pars Reticulata. Also gating units in our model.
τ	The time constant of units in our model.
T_H	Target position relative to the head
TLLB	Tectal Long Lead Burst neuron
tllb	An inhibitory unit in our model, which has activation function similar with TLLBs
TNs	Tonic neurons
VOR	Vestibuloocular reflex.

Index

P

Q

R

S

T

U

V

A

B

Δ

REFERENCES

Aizawa H., Wurtz R.H. (1998) Reversible inactivation of monkey superior colliculus. I. Curvature of saccadic trajectory. J Neurophysiol 79:2082-2096

Albus J.S.(1971) A theory of cerebellar function. Math Biosci 10:25-61

Andersen R.A., Bracewell R.M., Barash S., Gnadt J.W. and Foggassi L. (1990) Eye position effects on visual, memory and saccade-related activity in areas LIP and7A of macaque. J Neurosci 10:1176-1196

Andersen R.A., Essick G.K. and Siegel R.M. (1985) Encoding of spatial location by posterior parietal neurons. Science 230:456-458

Anderson R.W., Keller E.L., Gandhi N.J., Das S. (1998) Two-dimensional saccade-related population activity in superior colliculus in monkey J Neurophysiol Vol 80:798-817

Anderson ME, Yoshida M (1980) Axonal branching patterns and location of nigrothalamic and nigrocollicular neurons in the cat. J Neurophysiol 43:883-895

Appell PP, Behan M (1990) Sources of subcortical GABAergic projections to the superior colliculus in the cat. J Comp Neurol 302:143-158

Arai K, Keller EL, Edelman JA (1994) Two dimensional neural network model of the primate saccadic system. Neural Networks 7:1115-1135

Araki M, McGeer PL, McGeer ED (1984) Presumptive gamma-aminobutyric acid pathways form the midbrain to the superior colliculus studied by a combined horseradish peroxidase-gamma-aminobutyric acid transaminase pharmacohistochemical method. Neuroscience 13:433-439

Baloh R.W., Sills A.W., Kumley W.E., Hornubia V. (1975) Quantitative measurement of saccade amplitude, duration and velocity. Neurology Vol 25:1065-1070

Bahill A.T., Clark M.R., Stark L. (1975) The main sequence, a tool for studying human eye movements. Math Biosci, 24, 191-204

Behan M., Kime N.M. (1996) Spatial distribution of tectotectal connections in the cat Prog Brain Res 112:131-142

Bergeron A., Guitton D. (2000) Fixation neurons in the superior colliculus encode distance between current and desired gaze positions. Nature Neuroscience Vol 3 No 9:932-939

Birkhoff G., McLane S. (1962) A survey of modern algebra. 11th edition Mc Millan company New York

Büttner-Ennever J.A., Horn A.K.E. (1994) Neuroanatomy of saccadic omnipause neurons in nucleus raphe interpositus. In: Fuchs A.F., Brandt T., Büttner U, Zee D.S., (eds). Contemporatory ocular motor and vestibular research: A tribute to David A. Robinson. Thieme Medical, New York, pp 489-495

Cannon S.C., Robinson A.D. (1987) Loss of the neural integrator of the oculomotor system from brain stem lesions in monkey. J Neurophysiol, Vol 57:1383-1409

Cheron G., Godaux E. (1987) Disabling of the oculomotor neural integrator by kainic acid injections in the prepositus-vestibular complex of the cat. J Physiol, Vol 394:267-290

Contreras-Vidal J.L., Grossberg S., Bullock D. (1997) A neural model of cerebellar learning for arm movement control: cortico-spino-cerebellar dynamics. Learn Mem 3:475-502

Coren S., Hoenig P. (1972) Effect of non-target stimuli upon length of voluntary saccade. Percept Motor Skills 34:499-508

Cowie R.J., Robinson D.L. (1994) Subcortical contributions to head movements in macaques. I. Contrasting effects of electrical stimulation of a medial pontomedullary region and the superior colliculus. J Neurophysiol 72:2648-2664

Dacey D.M., Ulinski P.S. (1986) Optic tectum of the eastern garter snake, *Thamnophis sirtalis*. III. Morphology of intrinsic neurons. J Comp Neurol 245:283-300

Dean P. (1995) Modelling the role of the cerebellar fastigial nuclei in producing accurate saccades: The importance of burst timing. Neuroscience 68:1059-1077

Dean P., Majhew J., Langdon P. (1994) Learning and maintaining saccade accuracy: a model of brainstem-cerebellar interactions. J Cogni Neurosci 6:117-138

Droulez J., Berthoz A. (1991) A neural network model of sensoritopic maps with predictive short-term memory properties. Proc Natl Acad Sci USA 88:9653-9657

Edelman J.A., Keller E.L. (1998) Dependence on target configuration of express saccade-related activity in the primate superior colliculus. J Neurophysiol 80:1407-1426

Edwards S.B. (1977) The commisural projection of the superior colliculus in the cat. J Comp Neurol 173:23-40

Evinger C., Fuchs A.F. (1978) Saccadic, smooth pursuit, and optokinetic eye movements of the trained cat. J Physiol [Lond] 285:209-229

Ficalora A.S., Mize R.R. (1989) The neurons of the substantia nigra and zona incerta which project to the cat superior colliculus are GABA immunoreactive: a double-label study using GABA immunocytochemistry and lectin retrograde transport. Neuroscience 29:567-581

Findlay J.M. (1982) Global visual processing for saccadic eye movements. Vision Res 22:1033-1045

Fujita M (1989) Network models for eye movement control. In: Ito M. (ed) Neural programming. Japan Scientific Societies Press, Tokyo, pp 165-172

Glimcher P.W., Sparks D.L. (1993) Representation of averaging saccades in the superior colliculus of the monkey. Exp Brain Res 95:429-435

Goldberg M.E., Bruce C.J. (1990) Primate frontal eye fields. III. Maintenance of a spatially accurate saccade signal. J. Neurophysiol 64:489-508

Goosens H.H.L.M., Van Opstal A.J. (2000a) Blink-perturbed saccades in monkey. I. Behavioural analysis. J Neurophysiol 83:3411-3429

Goosens H.H.L.M., Van Opstal A.J. (2000b) Blink-perturbed saccades in monkey. II. Superior colliculus activity. J Neurophysiol 83:3430-3452

Grantyn A., Berthoz A. (1985) Burst activity of identified tectoreticulo-spinal neurons in the alert cat. Exp Brain Res 57:417-421

Grantyn a., Brandi A.M., Dubayle D., Graf W., Ugolini G., Hadjidimitrakis K., Moschovakis A. (2002) Density gradients of trans-synaptically labelled collicular neurons after injections of rabies virus in the lateral rectus muscle of the rhesus monkey. J Comp Neurol Sep 30; 451(4):346-361

Grantyn A., Olivier E, Kitama T. (1993) Tracing premotor brain stem networks of orienting movements. Curr Opin Neurobiol 3:973-981

Grantyn A.A., Dalezios Y., Kitama T., Moschovakis A.K. (1996) Neuronal mechanisms of two-dimensional orienting movements in the cat. I. A quantitative study of saccades and slow drifts produced in response to the electrical stimulation of the superior colliculus. Brain Res Bull 41:65-82

Grantyn A , Dalezios Y, Kitama T, Moschovakis A.K. (1997) Neuronal mechanisms of two-dimensional orienting movements in the cat: An anatomical basis for the spatio-temporal transformation. Proc Soc Neurosci 23:1295

Groh J.M (2001) Converting neural signals form place codes to rate codes. Biol. Cyben 85:159-165

Groh J.M., Sparks D.L. (1992) Two models for transforming auditory signals from head-centered to eye-centered coordinates. Biol Cybern 67:291-302

Grossberg S., Kuperstein M. (1989) Neural dynamics of adaptive sensory-motor control. New York: Pergamon Press

Grossberg S., Roberts K., Aguilar M., Bullock D. (1997) A neural model of multimodal adaptive saccadic eye movement control by superior colliculus. J Neurosci Dec 15, 17(24):9706-9725

Hallett P.E., Lightstone A.D. (1976a) Saccadic eye movements to flashed targets. Vision Res 16:107-114

Hallett P.E., Lightstone A.D. (1976b) Saccadic eye movements toward stimuli triggered by prior saccades. Vision Res, 16:99-106

Harris L.R. (1980) The superior colliculus and movements of the head and eyes in cats. J Physiol 300:367-391

Harting J.K. (1977) Descending pathways from the superior colliculus: an autoradiographic analysis in the rhesus monkey (*Macaca mulatta*). J Comp Neurol 173:583-612

Harting J.K., Lieshout D.P. van (1991) Spatial relationships of axons arising from the substantia nigra, spinal trigeminal nucleus, and pedunculopontine tegmental nucleus within the intermediate gray of the cat superior colliculus. J Comp Neurol 305:543-558

Harting J.K., Huerta M.F., Frankfurter A.J., Strominger N.L., Royce J.G. (1980) Ascending pathways from the monkey superior colliculus: an autoradiographic analysis. J Comp Neurol 192:852-882

Harting J.K., Huerta M.F., Hashikawa T., Weber J.T., Lieshout D.P. van (1988) Neuroanatomical studies of the nigrotectal projection in the cat. . J Comp Neurol 278:615-631

Hartwich-Young R., Nelson J.S., Sparks D.L. (1990) The perihypoglossal projection to the superior colliculus in the rhesus monkey. Visual Neurosci 4:29-42

Henn V., Cohen B (1973) Quantitative analysis of activity in eye muscle motoneurons during saccadic eye movements and positions of fixation. J. Neurophysiol 36: 115-126

Hepp K., Henn V. (1983) Spatio-temporal recording of rapid eye movement signals in the monkey paramedian pontine reticular formation (PPRF). Exp Brain Res Vol 52:105-120

Hepp K., van Opstal A.J., Straumann D., Hess B.J.M., Henn V. (1993) Monkey superior colliculus represents rapid eye movements in a two-dimensional motor map. J Neurophysiol Vol 69,3:965-979

Hess W.R., Burgi S., Bucher V. (1946) Motorische Funktion des Tectal- und Tegmentalgebietes. Minatschr Psychiatr Neurol 112:1-52

Hikosaka O., Wurtz R.H. (1983a) Visual and oculomotor functions of the monkey substantia nigra pars reticulata. I. Relation of visual and auditory responses to saccades. J. Neurophysiol 49:1230-1253

Hikosaka O., Wurtz R.H. (1983b) Visual and oculomotor functions of the monkey substantia nigra pars reticulata. III. Memory-contingent visual and saccade responses. J. Neurophysiol 49:1268-1284

Hikosaka O., Wurtz R.H. (1983c) Visual and oculomotor functions of the monkey substantia nigra pars reticulata. IV. Relation of substantia nigra to superior colliculus. J. Neurophysiol 49:1285-1301

Hikosaka O., Wurtz R.H. (1985) Modification of saccadic eye movements by GABA-related substances. I. Effect of muscimol and bicuculline in monkey superior colliculus. J. Neurophysiol 53:266-291

Hikosaka O., Wurtz R.H. (1986) Saccadic eye movements following injection of lidocaine into the superior colliculus. Exp Brain Res 61:531-539

Huerta M.F., Harting J.K. (1984) The mammalian superior colliculus: studies of its morphology and connections. In: Vanegas H (ed) Comparative neurology of the optic tectum. Plenum Press, New York, pp 687-773

Infante C., Leiva J (1986) Simultaneous unitary neuronal activity in both superior colliculi and its relation to eye movements in the cat. Brain Res 381:390-392

Isa T. and Saito Y. (2001) The direct visuo-motor pathway in mammalian superior colliculus; novel perspective on the interlaminar connection Neuroscience Research 41:107-113

Jay M.F., Sparks D.L. (1987) Sensorimotor integration in the primate superior colliculus. II. Coordinates of auditory signals. J Neurophysiol 57:35-55

Jayaraman A, Batton R.R.I., Carpenter M.B. (1997) Nigrotectal projections in the monkey: an autoradiographic study. Brain Res 135:147-152

Karabelas A.B., Moschovakis A.K. (1985) Nigral inhibitory termination of efferent neurons of the superior colliculus. An intracellular horseradish peroxidase study in the cat. J Comp Neurol 239:309-329

Kawamura K., Hashikawa T. (1978) Cell bodies of origin of reticular projections from the superior colliculus in the cat: an experimental study with the use of horseradish peroxidase as a tracer. J Comp Neurol 182: 1-16

Keller E.L., Edelman J.A. (1994) Use of interrupted saccade paradigm to study spatial and temporal dynamics of saccade burst cells in superior colliculus in monkey. J. Neurophysiol 72: 2754-2770

Krommenhoek K.P., Wiegerinck W.A.J.J. (1998) A neural network study of precollicular saccade averaging. Biol Cybern 78:465-477

Lee C., Rohrer W.H., Sparks D.L. (1988) Population coding of saccadic eye movements by neurons in the superior colliculus. Nature 332:357-360

Lefèvre P., Galiana H.L. (1992) Dynamic feedback to the superior colliculus in a neural network model of the gaze control system. Neural Networks 5:871-900

Lefèvre P., Quaia C., Optican L.M. (1998) Distributed model of control of saccades by superior colliculus and cerebellum. Neural Networks 11:1175-1190

Ma T.P., Porter J.D., May P.J. (1991) Reciprocal connections between the zona incerta and superior colliculus in the macaque. Invest Ophthalmol Vis Sci 32:897

Massone L.L.E., Khoshaba T. (1995) Local dynamic interactions in the collicular motor map: a neural network model. Network 6:1-18

Mays L.E., Sparks D.L. (1980) Dissociation of visual and saccade-related responses in superior colliculus neurons. J. Neurophysiol 43:207-232

Mc Ilwain J.T. (1976) Large receptive fields and spatial transformations in the visual system. In Neurophysiology II. (ed. Porter R.), Vol 10, pp 223-248. Univ. Park Press, Baltimore.

McIlwain J.T. (1982) Lateral spread of neural excitation during microstimulation in intermediate gray layer of cat's superior colliculus. J Neurophysiol 47:167-178

McIlwain J.T. (1991) Distributed spatial coding in the superior colliculus: a review. Vis Neurosci 6:3-13

Meredith M.A., Stein B.E. (1985) Descending efferents from the superior colliculus relay integrated multisensory information. Science 227:657-659

Meredith M.A., Nemitz J.W., Stein B.E. (1987) Determinants of multisensory integration in superior colliculus neurons. I. Temporal factors. J Neurosci 7:3215-3229

Mooney R.D., Bennet-Clarke C.A., King T.D., Rhoades R.W. (1990) Tectospinal neurons in hamster contain glutamate-like immunoreactivity. Brain Res 537:375-380

Mooney R.D., Nikoletseas M.M., Hess P.R., Allen Z., Lewin A.C., Rhoades R.W. (1988) The projection from the superficial to the deep layers of the superior colliculus: An intracellular horseradish peroxidase injection study in the hamster. J Neurosci 8, 1384-1399

Moschovakis A.K. (1987) Observations on the appearance and function of neurons in the primate superior colliculus. An intracellular HRP study. Washington University, Washington

Moschovakis A.K. (1994) Neural network simulations of the primate oculomotor system. I. The vertical saccadic burst generator. Biol Cybern 70:291-302

Moschovakis A.K. (1996a) Neural network simulations of the primate oculomotor system. II. Frames of reference. Brain Res Bull 40:337-345

Moschovakis A.K. (1996b) The superior colliculus and eye movement control. Curr Opin Neurobiol 6:811-816

Moschovakis A.K., Gregoriou G.G., Savaki H.E. (2001) Functional imaging of the primate superior colliculus during saccades to visual targets. Nature Neuroscience Vol 4,10:1026-1031

Moschovakis A.K., Karabelas A.B. (1985) Observations on the somatodendritic morphology and axonal trajectory of intracellularly HRP-labelled efferent neurons located in the deeper layers of the superior colliculus of the cat. J Comp Neurol 239:276-308

Moschovakis A.K., Karabelas A.B., Highstein S.M. (1988a). Structure-function relationships in the primate superior colliculus. I. Morphological classification of efferent neurons. J Neurophysiol 60:232-262

Moschovakis A.K ,Karabelas A.B., Highstein S.M. (1988b). Structure-function relationships in the primate superior colliculus. II. Morphological identity of presaccadic neurons. J Neurophysiol 60:263-302

Moschovakis A.K., Scudder C.A., Highstein S.M. (1991a) Structure of the primate burst generator. I. Medium-lead burst neurons with upward on-directions. J Neurophysiol 65:203-217

Moschovakis A.K. , Scudder C.A., Highstein S.M , Warren J.D.. (1991b) Structure of the primate burst generator. II. Medium-lead burst neurons with downward on-directions. J Neurophysiol 65:218-229

Moschovakis A.K. , Scudder C.A., Highstein S.M. (1996) The microscopic anatomy and physiology of the mammalian saccadic system. Prog Neurobiol 50:133-254

Moschovakis A.K., Kitama T., Dalezios Y., Petit J., Brandi A.M., and Grantyn A.A. (1998b) An anatomical substrate for the spatiotemporal transformation. J Neurosci Dec 1, 18(23): 10219-10229

Moschovakis A.K., Dalezios Y., Petit J. and Grantyn A.A. (1998a) New mechanism that accounts for position sensitivity of saccades evoked in response to electrical stimulation of superior colliculus. J Neurophysiol 80:3373-3379

Munoz D.P., Wurtz R.H. (1993) Fixation cells in monkey superior colliculus. I. Characteristics of cell discharge. J Neurophysiol 70:559-575

Munoz D.P., Wurtz R.H. (1995) Saccade-related activity in monkey superior colliculus. II. Spread of activity during saccades. J Neurophysiol 73:2334-2348

Munoz D.P., Guitton D., Pelisson D. (1991a). Control of orienting gaze shifts by the tectoreticulospinal system in the head-free cat. III. Spatiotemporal characteristics of phasic motor discharges. J. Neurophysiol 66:1642-1666

Munoz D.P., Pelisson D., Guitton D. (1991b) Movement of neural activity on the superior colliculus motor map during gaze shifts. Science 251:1358-1360

Munoz D.P., Waitzman D.M., Wurtz R.H. (1996) Activity of neurons in monkey superior colliculus during interrupted saccades. J Neurophysiol 75:2562-2580

Nichols M.J., Sparks D.L. (1995) Nonstationaty properties of the saccadic system: new constraints on models of saccadic control. J Neurophysiol 73:431-435

Nichols M.J., Sparks D.L. (1996) Independent feedback control of horizontal and vertical amplitude during oblique saccades evoked by electrical stimulation of the superior colliculus. J Neurophysiol 76:4080-4093

Olivier E., Chat M., Grantyn A. (1991) Rostrocaudal and lateromedial density distributions of superior colliculus neurons projecting in the predorsal bundle and to the spinal cord: a retrograde HRP study in the cat. Exp Brain Res 87:268-282

Olivier E., Porter J.D., May P.J. (1998) Comparison of the distribution and somatodendritic morphology of tectotectal neurons in the cat and monkey. Vis Neurosci 15:903-922

Optican L.M. (1995) A field theory of saccade generation: temporal-to-spatial transform in the superior colliculus. Vision Res 35:3313-3320

Optican L.M., Miles F.A. (1985) Visually induced adaptive changes in primate saccadic oculomotor control signals. J Neurophysiol 54:940-958

Özen G., Augustine G.J., Hall W.C. (2000) Contribution of superficial layer neurons to premotor bursts in the superior colliculus. J Neurophysiol Jul; 84(1) 460-471

Peck C.K. (1986) Eye position signals in cat superior colliculus. Exp Brain Res 61:447-450

Peck C.K.(1990) Neuronal activity related to head and eye movements in cat superior colliculus. J Physiol 421:79-104

Quaia C., Aizawa H., Optican L.M., Wurtz R.H. (1998) Reversible inactivation of monkey superior colliculus. II. Maps of saccadic deficits. J Neurophysiol 79:2097-2110

Quaia C., Lefèvre P., Optican L.M. (1999) Model of the control of saccades by superior colliculus and cerebellum. J Neurophysiol 82:999-1018

Ricardo J.A.(1981) Efferent connections of the subthalamic region in the rat. The zona incerta. Brain Res 214:43-60

Robinson D.A. (1972) Eye movements evoked by collicular stimulation in the alert monkey. Vision Res 12:1795-1808

Robinson D.A. (1975) Oculomotor control signals. In G. Lennerstrand and P. Bach-y-Rita (Eds), Basic mechanisms of ocular motility and their clinical implications (p. 337-374). Oxford, England: Pergamon Press

Robinson F.R. (1995) Role of the cerebellum in movement control and adaptation. Curr. Opin. Neurobiol. 5:755-762

Robinson F.R., Straube A., Fuchs A.F. (1993) Role of the caudal fastigial nucleus in saccade generation. II. Effects of muscimol inactivation. J Neurophysiol 70:1741-1758

Robinson D.A., Fuchs A.F. (1969) Eye movements evoked by stimulation of frontal eye fields. J Neurophysiol 32:637-648

Robinson F.R., Straube A., Fuchs A.F. (1993) Role of the caudal fastigial nucleus in saccade generation. II. Effects of muscimol inactivation. J Neurophysiol 70:1741-1758

Roucoux A., Guitton D., Crommelinck M. (1980) Stimulation of the superior colliculus in the alert cat. II. Eye and head movements evoked when the head is unrestrained. Exp Brain Res 39:75-85

Rumelhart D., Hinton G., Williams R. (1986) Learning internal representations by error backpropagation. In: Rumelhart D., McClelland J., and the PDP research group (eds) Parallel distributed processing. MIT Press, Cambridge, Mass., 318-363

Schiller P.H., Koerner F. (1971) Discharge characteristics of single units in the superior colliculus of the alert rhesus monkey. J Neurophysiol 34:920-93

Schiller P.H., Stryker M. (1972) Single-unit recording and stimulation in superior colliculus of the alert rhesus monkey. J Neurophysiol 35:915-924

Schiller P.H., True S.D., Conway J.L. (1980) Deficits in eye movements following frontal eye field and superior colliculus ablations. J Neurophysiol 44:1175-1189

Schlag J., Schlag-Rey M.(1995) Illusory localisation of stimuli flashed in the dark before saccades. Vision Res 35:2347-2357

Schlag J., Schlag-Rey M., Dassonville P. (1990) Saccades can be aimed at the spatial location of targets flashed during pursuit. J Neurophysiol 64:575-581

Schultz W. (1998) Predictive reward signal of dopamine neurons. J Neurophysiol 80:1,1-27

Scudder C.A. (1988) A new local feedback model of the saccadic burst generator. J Neurophysiol 59:1455-1475

Scudder C.A. (1997) Reduction of excitatory burst neuron (EBN) discharges reduces saccade size; implications for models of saccade generation. Proc Soc Neurosci 23:2368 (Abstract)

Scudder C.A., Moschovakis A.K., Karabelas A.B., Highstein S.M. (1996a) Anatomy and physiology of saccadic long-lead burst neurons recorded in the alert squirrel monkey. I. Descending projections from the mesencephalon. J. Neurophysiol 76:332-352

Scudder C.A., Moschovakis A.K., Karabelas A.B., Highstein S.M. (1996b) Anatomy and physiology of saccadic long-lead burst neurons recorded in the alert squirrel monkey. II. Pontine neurons. J. Neurophysiol 76:353-370

Soetedjo R., Kaneko C.R.S., Fuchs A.F. (2002) Evidence against a moving hill in the superior colliculus during saccadic eye movements in the monkey. J Neurophysiol 87:2778-2789

Sparks D.L. (1986) Translation of sensory signals into commands for control of saccadic eye movements: role of primate superior colliculus. Physiol Rev 66:118-171

Sparks D.L., Mays L.E. (1982) Role of the monkey superior colliculus in the spatial localization of saccade targets. In: Hein A., Jeannerod M. (eds) Spatially oriented behaviour. C.C. Springer, New York, pp 63-85

Sparks D.L., Holland R, Guthrie B.L. (1976) Size and distribution of movement fields in the monkey superior colliculus. Brain Res 113:21-34

Stanton GB, Greene RW (1981) Brain stem afferents to the periabducens reticular formation (PARF) in the cat. An HRP study. Exp Brain Res 44: 419-426

Straschill M., Hoffmann K.P. (1970) Activity of movement sensitive neurons of the cat's tectum opticum during spontaneous eye movements. Exp Brain Res 11:318-326

Straschill M., Rieger P. (1973) Eye movements evoked by focal stimulation of the cat's superior colliculus. Brain Res 59:211-227

Straschill M., Schick F. (1977) Discharges of superior colliculus neurons during head and eye movements of the alert cat. Exp Brain Res 27:131-141

Tardif E. and Clarke S. (2002) Commisural connections of human superior colliculus. Neuroscience Vol. 111, No.2:363-372

Tweed D., Villis T. (1990) The superior colliculus and spatiotemporal translation in the saccadic system. Neural Networks 3:75-86

Tweed D., Villis T. (1985) A two-dimensional model for saccade generation. Biol Cybern 52:219-227

Van Gisbergen J.A.M., Robinson D.A., Gielen S. (1981) A quantitative analysis of generation of saccadic eye movements by burst neurons. J Neurophysiol 45:417-442

Van Opstal A.J., Van Gisbergen J.A.M. (1989) A non-linear model for collicular spatial interactions underlying the metrical properties of electrically elicited saccades. Biol Cybern 60:171-183

Van Opstal A.J. and Hepp K. (1995) A novel interpretation for the collicular role in saccade generation. Biol Cybern 73:431-445

Van Opstal A.J., Hepp K., Suzuki Y. and Henn V. (1995) Influence of eye position on activity in monkey superior colliculus. J Neurophysiol Oct 74(4):1593-1610

Van Opstal A.J., Hepp K., Hess B.J.M., Straumann D., and Henn V. (1991) Two-rather than three-dimensional representation of saccades in monkey superior colliculus. Science 252:1313-1315

Van Opstal A.J., Van Gisbergen J.A.M., Smit A.C. (1990) Comparison of saccades evoked by visual stimulation and collicular electrical stimulation in the alert monkey. Exp Brain Res 79:299-312

Van Opstal A.J., Van Gisbergen J.A.M. (1990) Role of monkey superior colliculus in saccade averaging. Exp Brain Res 79:143-149

Waitzman D.M., Ma T.P., Optican L.M.. Wurtz R.H. (1991) Superior colliculus neurons mediate the dynamic characteristics of saccades J Neurophysiol Vol 66:1716-1737

Walker M.F., Fitzgibbon E.J., Goldberg M.E. (1995) Neurons in the monkey superior colliculus predict the visual result of impeding saccadic eye movements. J Neurophysiol 73:1988-2003

Wallace M.T., Stein B.E. (1994) Cross-modal synthesis in the midbrain depends on input from cortex. J Neurophysiol 71:429-432

Yarbus A.L. (1967) Eye movements and vision. Plenum Press, New York